Characterization of a Biphenyl Isoxazole, KRIBB3, as an Anti-Migratory and Anti-Mitotic Compound in Cancer Cell

Ki Deok Shin

The Graduate School

Yonsei University

Department of Biochemistry

Characterization of a Biphenyl Isoxazole, KRIBB3, as an Anti-Migratory and Anti-Mitotic Compound in Cancer Cell

A Dissertation
Submitted to the Department of Biochemistry
and the Graduate School of Yonsei University
in partial fulfillment of the
requirements for the degree of
Doctor of Philosophy

Ki Deok Shin

August 2008

This certifies that the dissertation

of Ki Deok Shin is approved.

_____

Thesis Supervisor: Dr. Young-Ki Paik

_____

Dr. Jong-Bok Yoon

_____

Dr. Dae-Won Kim

_____

Dr. Byoung-Mog Kwon

_____

Dr. Dong Cho Han

The Graduate School

Yonsei University

June 2008

Acknowledgement

실험결과에 기뻐하며 때론 좌절에 빠져 내일을 기약하며 생활하다 보니 어느덧 4 년 반이라는 세월이 지나 박사학위를 받게 되었습니다. 학·연 과정 동안 서울로 기차를 타고 수업을 들으러 오가는 것이 힘들 때도 있었지만, 한편으론 실험에 대한 생각과 삶에 대한 생각을 할 수 있었기에 저에게는 소중한 시간이었습니다. 지난 세월을 되돌아 보며 지금까지 도움을 주셨던 많은 분들에게 부족하나마 지면으로 그 고마움을 전하고자 합니다.

자주는 못 뵙지만 언제나 반갑게 맞아주시고 많은 가르침을 주신 백융기 교수님, 옆에서 많은 조언과 실험실 생활에 많은 도움을 주신 권병목 박사님, 프로젝트를 진행하면서 많은 고민을 해결해 주시고 문제해결의 부족한 점을 채워주신 한동초 박사님께 감사의 마음을 전하고 싶습니다. 그리고, 바쁘신 와중에 본 논문을 심사해주신 윤종복 교수님과 김대원 교수님께 진심으로 감사 드립니다. 또한, 정겹게 웃어주시고 재치 있는 말로 저희들을 즐겁게 해주시는 손광희 박사님과 같은 층에 계시는 박호용 박사님, 김성욱 박사님 및 정태숙 박사님에게도 감사의 인사를 전합니다.

주말을 제외한 대부분의 시간을 같이 보내며 기쁨과 슬픔을 함께 나눌 수 있었던 실험실 요원들이 있었기에 이 자리에 설수 있었던 것 같습니다. 밤낮으로 열심히 실험하면서 실험실을 지키는 신대섭 박사, 자기 일에 열심히 일하며 이제는 아기아빠가 된 종석씨, 한 가정의 가장이 된 새신랑 지훈, 큰 웃음으로 연예계 소식을 전하는 진아, 날카로운 눈빛으로 실험실을 이끄는 일꾼 소영, 일에 욕심 많은 혜난, 어려움이 있어도 오뚝이처럼 잘 일어서는 영주, 뒷자리에 앉아서 엉뚱함으로 웃음을 주는 영림, 묵묵하게 자기일에 열심인 영란, 밝게 웃으며

백곰이라는 별명이 잘 어울리는 은진, 매사에 적극적인 사내대장부 같은 란희, 그리고 항상 너털웃음 짓는 영민에게 고마움과 감사의 마음을 전합니다.

학위과정 동안 함께 일하며 도움을 준 많은 분들이 각자 자기의 일을 찾아 떠났습니다. 실험실 생활하는 동안 많은 도움을 주신 김정민 박사님과 강현미 박사님께 감사 드립니다. 처음 들어와 적응하는데 많은 도움을 주었고 실험파트너였던 순복이, 큰 웃음이 매력인 미영이, 짧았지만 많은 힘이 되었던 종환이와 성규에게도 진심으로 감사합니다.

처음 학위 시작할 때 어색할 수 있는 학교실험실에서 마음 편히 쉴 수 있게 공간을 마련해 주고 먼저 다가와 맞이해준 학교 실험실 식구들께 고마운 마음을 전합니다. 낯선 환경에 잘 적응할 수 있도록 도움을 준 지금은 미국계신 김기영 박사님과 신유경 박사, 실험에 열정적이었던 정판영 박사님, 다정다감했던 조상연박사님, 언제나 편안하게 대해주시는 이은영 박사님, 궂은 심부름과 어려운 부탁에도 열심히 도와준 효진, 항상 웃으며 맞아 주었던 미정과 정의, 중국에서 낯선 한국으로 와서 열심히 노력하는 영수씨와 허말, 그리고 이외에 실험실 식구들에게도 모두 감사 드립니다.

늦은 나이까지 공부하는 아들을 위해 많은 도움을 주시고, 멀리서 항상 사랑으로 건강과 앞날을 기원해 주셨던 아버님, 어머님, 그리고 자식의 일처럼 기뻐해 주셨던 장모님께 진심으로 감사의 인사를 올립니다. 항상 곁에서 공부와 실험에 매진 할 수 있도록 내조를 잘해준 아내와 존재만으로도 힘과 용기를 주는 딸 현송이와 아들 우진이에게 사랑한다는 말을 전하고자 합니다.

2008 년 7 월

신기덕 올림

CONTENTS

List of figures

List of Table

Abbreviations

APC/C	Anaphase-promoting complex/cyclosome
ATCC	American Type Culture Correction
CDC20	Cell-division-cycle 20 homologue
CHAPS	3-[(3-cholamidoprophyl) dimethylammonio]-1-propansulfonate
DAPI	4', 6-diamidino-2-phenylindole
DMSO	Dimethyl Sulfoxide
EDTA	Ethylenediaminetetraacetic acid
EGTA	Ethylene glycol tetraacetic acid
FACS	Fluorescence activating cell sorting
FAK	Focal adhesion kinase
FBS	Fetal bovine serum
HEPES	4-(2-hydroxyethyl)-1-piperazineethanesulfonic acid
KRIBB2	4-ethyl-5-methoxy-2(3-methyl-4-phenylisoxazole-5-yl) phenol
KRIBB3	5-(5-ethyl-2-hydroxy-4-methoxyphenyl)-4-(4-methoxyphenyl) isoxazole
MAPKAPK	Mitogen-activated protein kinase-activated protein kinase
MDR	Multidrug resistance

MEK	Mitogen-activated protein kinase/extracellular signal-regulated kinase
PAGE	Polyacrylamide Gel Electrophoresis
PARP	Poly (ADP-Ribose) Polymerase
PBS	Phosphate-Buffered Saline
PI	Propidium Iodide
PI3K	Phosphatidylinositol 3-kinase
PIPES	Piperazine-N, N′-bis (2-ethanesulfonic acid)
PKC	Protein kinase C
PMA	Phorbol 12-myristate 13-acetate
PMSF	Phenyl-Methyl-Sulfonyl Fluoride
PVDF	Poly Vinylidene DiFluoride
RPMI 1640	Rosewell Park Memorial Institute 1640
SDS	Sodium Dodesyl Sulfate
siRNA	Small interfering RNA
TBS	Tris-Buffered Saline
TEMED	N, N, N', N'-Tetramethylethylenediamine
WST-1	Tetrazolium salt, 4-[3-(4-Iodophenyl)-2-(4-nitrophenyl)-2H-5-tetrazolio]-1, 3-benzene disulfonate

Abstract

Characterization of a biphenyl isoxazole, KRIBB3, as an anti-migratory and anti-mitotic compound in Cancer Cell

Ki Deok Shin

Department of Biochemistry

The Graduate School

Yonsei University

Cell migration is a prerequisite for cancer invasion and metastasis, suggesting cell motility as a potential therapeutic target for cancer treatment. A synthetic library was screened to identify inhibitors of tumor cell migration. From this, I discovered CAC-1098 (aurintricarboxylic acid) and CBI-0997 (5-(2, 4-dimethoxy-5-ethylphenyl)-4-(4-Bromophenyl) isoxazole) that inhibited migration of

MDA-MB-231 with an IC_{50} of 5 nM and 50 nM, respectively. I synthesized KRIBB3 (5-(5-ethyl-2-hydroxy-4-methoxyphenyl)-4-(4-methoxyphenyl) isoxazole) by replacing bromide group of CBI-0997 with methoxyl group. Like CBI-0997, KRIBB3 has anti-migratory and anti-invasive activity for MDA-MB-231. Because KRIBB3 has better drug-like structure, I focused my effort to understand its anti-migratory mechanism further. Biotinyl-KRIBB3 was synthesized as an affinity probe for identification of KRIBB3-binding proteins. Using affinity chromatography, Hsp27 was identified as a target protein of KRIBB3 *in vitro*. Treatment of MDA-MB-231 with PMA induced PKC-dependent phosphorylation of Hsp27 and tumor cell migration. In contrast, treatment of MDA-MB-231 with KRIBB3 blocked PMA-induced phosphorylation of Hsp27 and tumor cell migration. Furthermore, overexpression of Hsp27 could antagonize inhibitory effect of KRIBB3 on tumor cell invasion and knockdown of Hsp27 using siRNA inhibited tumor cell migration. Overall, my results demonstrated that KRIBB3 inhibits tumor cell migration and invasion by blocking PKC-dependent phosphorylation of Hsp27 through its direct binding to Hsp27.

During the test of anticancer effects by KRIBB3, I found that KRIBB3 inhibited cell proliferation in several cancer cells. Especially, HCT-116 cells were inhibited cell growth with a GI_{50} of 0.35 μM. Flow cytometry study showed that KRIBB3 caused cell cycle arrest at G_2/M phase and apoptosis. This was confirmed by detecting accumulation of Cyclin B1 and cleavage of poly (ADP-ribose) polymerase (PARP). While transient inhibition by KRIBB3 leaded to reversible mitotic arrest, prolonged exposure to the KRIBB3 induced apoptosis. Co-

immunoprecipitation assay showed that KRIBB3 initially induced association of inhibitory Mad2 with p55CDC (mammalian homologue of CDC20), activator of APC/C (anaphase-promoting complex/cyclosome), suggesting that mitotic spindle checkpoint was activated by KRIBB3. However, this inhibitory complex of Mad2 with p55CDC was gradually decreased 24 h after KRIBB3 treatment and was hardly detectable after 48 h, indicating slippage of mitotic checkpoint. Consistent with these observations, KRIBB3 activated the mitotic spindle checkpoint by disrupting microtubule cytoskeleton. KRIBB3 was proven to be a tubulin inhibitor using *in vitro* polymerization assays and *in vivo* indirect immunofluorescence staining. The temporal pattern of Bax activation by KRIBB3 was similar to PARP cleavage, suggesting that Bax is a mediator of KRIBB3-dependent apoptosis. Furthermore, when KRIBB3 was administered intraperitoneally into nude mice at 50 mg/kg or 100 mg/kg, it inhibited 49.5% or 70.3% of tumor growth, respectively. These results suggest that KRIBB3 is a good drug candidate for cancer therapy.

Keywords: migration, metastasis, Hsp27, chemical genetics, isoxazole, microtubule inhibitor, mitotic arrest, apoptosis, Bax activation, and cancer therapy

Overview

Metastasis is the most dangerous phenomenon causing decease of cancer patient. In metastasis, migration performs pivotal roles. The primary tumor cells move into blood vessels (intravasation) or the circulatory tumor cells invade into secondary organ tissue (extravasate). In addition, migration is participating in diseases processes, comprising vascular disease, osteoporosis, chronic inflammatory diseases, and mental retardation. More comprehensively understanding of cell migration mechanisms proffer us lots of advantage of therapeutic approaches for treating disease related with cell migration.

Mechanism of Migration

Cell migration cycles consist of sensing chemoattractant, cell polarity, protrusion, focal adhesion, and rear retraction. Moving cells have to sense gradient of chemoattractant, such as chemokines or growth factors. Cell membrane receptors such as G protein coupled receptors (GPCRs) and receptor tyrosine kinases (RTKs) specifically recognize their chemokine ligands and growth factors. As a result, activated signaling pathways are remodeling of cytoskeleton and controlling cell migration. Recently, some ligands and receptors are reported to be involved in cell motility, such as CXCL12 (also known as SDF-1)/CXCR4, epidermal growth factor (EGF) or heregulin (HRG)/ErbB family, and hepatocyte growth factor (HGF)/Met (Kedrin et al., 2007).

The polarized morphology is observed in the migrating cells. The microtubule

reorganization and arrangement of nucleus, microtubule organization center (MTOC), and Golgi are important to organize polarity, which is controlled by Cdc42. Unrevealed signaling pathway of linking integrins activate Cdc42. This affects the mPar6-atypical PKC (aPKC) complex, which inactivates GSK3 (Hall, 2005). The microtubule polarization and centrosome reorientation mechanism was not well understood, but recent evidence suggests that adenomatous polyposis coli (APC), CLIP170, IQGAP, and/or dynein/dynactin motor protein complex could be involved in microtubules local capture (Etienne-Manneville and Hall, 2003).

After the complete of cell polarization, migration begins to produce the formation of protrusion in the moving direction. Activated GPCR and RTK stimulate phosphoinositide-3 kinase (PI3K) signaling pathway. The gradient sensing of chemoattractant brings about the localized accumulation of phosphoinosites (PIPs) on the leading edge, side, and rear. One of the PIP_3 is produced at leading edge that is activated by PI3K. PIP_3 activates guanine-nucleotide exchange factors (GEFs) that control the Rho GTPases activity, such as Rac, Cdc42, and Rho (Charest and Firtel, 2007; Kedrin et al., 2007; Pullikuth and Catling, 2007). However, RhoA/ROCK signaling pathway phosphorylates PTEN known as PIP_3 phosphatase that covert PIP_3 into PIP_2. The phospho-PTEN moves to the side and rear so that PIP_2 exists there and blocks the protrusion. The reason of protrusion occurred in leading edge is because of PTEN and Myosin II. The Arp2/3 (actin related protein 2/3) complex induces actin polymerization, which binds to the Wiscott-Aldrich Syndrome (WASP) and WAVE (WASP family verprolin homology) through a VCA region (verprolin homology domain, cofilin homology

domain, and acidic region). The local activation of Rac controls WAVE protein that leads to lamellipodia formation. WASP, the downstream target of Cdc42, regulates filopodia formation in the direction of migration (Sasaki and Firtel, 2006). Unlike Arp2/3 complex, formins are another actin polymerization factors that relate with ruffle dynamic at the leading edge of moving cell. The formin-nucleated filament elongation is regulated by profilin, which is associated with the FH1 domain of formin. ADF/cofilin severs and depolymerizes ADP-filament, which is converted for ATP-actin by profilin (Chhabra and Higgs, 2007).

Cell movement toward leading edge requires new focal adhesion that is mediated by integrins; these heterodimeric transmembrane receptor consisting with α and β subunit, contact with ECM ligands. Clustered integrins bind α-actinin, talin, focal adhesion kinase (FAK), and tensin. These proteins interact with actin-binding proteins, such as vinculin and paxillin. Vinculin provides a connection between the actin/Arp2/3 complex and emerging focal contacts. FAK controls the cycle of assembly and disassembly of focal adhesion; FAK-PI3K signaling activates Rac through Rac GEF and FAK-$p130^{Cas}$-Crk-DOCK180 complex also activate Rac. Furthermore, Rac activation is required for down-regulation of Rho by FAK-Src phosphorylation of p190RhoGAP and FAK binding p190RhoGEF (Moissoglu and Schwartz, 2006).

The cell motility cycle is completely done by rear retraction. The rear retraction consists of actin contraction and focal contact disassembly. Cell contraction is induced by actin filament (actomyosin) which is activated by Myosin II. Myosin II is activated by Ca^{2+}- and calmodulin-dependent myosin light-chain

kinase (MLCK) pathway or deactivated by dephosphorylation via the MLC phosphatase (MLCPtase) which is regulated by Rho-associated serine/threonine kinase (ROCK) via Rho GTPase pathway (Clark et al., 2007). In focal contact disassembly, calpain protease and calcineurin phosphatase are important calcium activated target protein that cleave focal contact proteins. In addition, FAK activates ERK2, which promotes Calpain-2-mediated cleavage of focal-adhesion proteins (Carragher et al., 2003; Franco et al., 2004). After rear adhesion disassemble is completed, main cell body is slowly glide forward. (Fig.1.). All the proteins discussed above can be target molecules of searching migration inhibitors.

Migration inhibitors

Migrastatin is a macrolide natural product first isolated from a culture broth of a *Streptomyces*. Migrastatin inhibits several types of tumor cell migration (IC_{50} =29 μM) *in vitro*, but has no effect on the biosyntheses of DNA, RNA, and protein in theses cells (Nakae et al., 2000). Recently, more potent synthetic analogs of migrastatin have been reported to inhibit tumor cell migration with sub-micromolar IC_{50} values (Metaferia et al., 2007; Njardarson et al., 2004; Shan et al., 2005). Migrastatin inhibits lamellipodium formation at the leading edge of cells by inhibiting Rac activation.

Rockout is a 3-4(-pyridyl)indole compound that inhibits cell migration (Yarrow et al., 2005). Yarrow and his colleagues performed a visual screening based on classical wound healing assays in a high-throughput format. They screened inhibitors from library of 16,000 chemicals and identified a new Rho-kinase

inhibitor. Rho-kinase is important target of small molecule because it contributes to control actin contraction and rear retraction.

Locostatin (UIC-1005) is an oxazolidinone derivative compound that inhibits cell locomotion in multiple systems (Zhu et al., 2005). The biological activity of locostatin was discovered by an epithelial wound closure assay system (Mc Henry et al., 2002). The target of locostatin is Raf kinase inhibitor protein (RKIP). It disrupts a protein-protein interaction between RKIP and Raf-1 kinase. RKIP plays a critical role in epithelial cell migration (Zhu et al., 2005).

DX-52-1 is an analog of quinocarmycin. It was discovered from wound-healing assay with epithelial cell. By using pulldown assay, radixin was identified as a relevant molecular target of DX-52-1 (Kahsai et al., 2006). Radixin is one of the members of ezrin/radixin/moesin (ERM) protein family, which functions as membrane-cytoskeleton linkers. Radixin, membrane-associated and actin-binding protein, is important for organization of the membrane-associated cortical actin cytoskeleton, cell migration, adhesion, and proliferation (Hoeflich and Ikura, 2004).

Furan-2-ylmethylene thiazolidinediones (AS-252424) is a specific ATP-competitive PI3Kγ (p110γ) inhibitor (Pomel et al., 2006). PI3Kγ inhibitors were achieved using a proprietary substructure analysis method. Thus, a set of selected 59,000 compounds was tested with PI3Kγ enzyme inhibition assay. The PI3K pathway promotes proliferation and survival in many different cell types. Therefore, PI3Kγ knockout (KO) mice revealed reduced neutrophil migration to infection sites induced by chemoattractant and respiratory burst (Condliffe et al., 2005; Hirsch et al., 2000; Li et al., 2000; Sasaki et al., 2000). PI3Kγ is thought to be important role

in mediating leukocyte chemotaxis as well as mast cell degranulation. Thus, PI3Kγ may be an attractive target for autoimmune and inflammatory diseases (Camps et al., 2005; Wymann et al., 2003).

Two classes of small molecular suppressor have been developed using a target of Integrin $\alpha_L\beta_2$ (lymphocyte function associated antigen-1 (LFA-1)) which is related with inflammatory diseases. One group of antagonist is LFA703 and BIRT377, which bind the hydrophobic pocket underneath the Integrin α7 helix of the α_L I domain (Weitz-Schmidt et al., 2001; Wu et al., 2004). These antagonists are called as an α I allosteric inhibitors (Yang et al., 2006). The other group of antagonists bind to the metal ion-dependent adhesion site (MIDAS) of the β_2 I-like domain, as well as to a region of the α_L subunit that does not include the I domain (Shimaoka et al., 2003; Welzenbach et al., 2002). This antagonist, such as XVA143, is called as an α/β I-like allosteric inhibitor (Salas et al., 2004; Yang et al., 2006). Controlling of $\alpha_L\beta_2$ activation is critical for regulating leukocyte movement and immune reactions. Thus, $\alpha_L\beta_2$ is a good target for treating autoimmune and inflammatory diseases (Gottlieb and Bos, 2002; Yusuf-Makagiansar et al., 2002).

Recently, Slack-Davis and colleagues discovered inhibitor of FAK, PF-228 (Slack-Davis et al., 2007). PF-228, (6-[(4-((3-(methanesulfonyl)benzyl)amino)-5-trifluoromethylpyrimidin-2-yl)amino]-3,4-dihydro-1H-quinolin-2-one) is a competitive inhibitor of ATP with specificity for FAK family protein-tyrosine kinases. This inhibitor was screened using commercially available recombinant enzymes. Several studies show that FAK expression and/or activity is related with cell growth and migration by adhesion dependent signaling pathway. Interestingly,

PF-228 specifically regulates cell migration, but it does not inhibit cell growth nor induce apoptosis *in vitro*. Thus, PF-228 provides an useful tool to in-depth study of FAK related signaling in cell adhesion dynamic.

Perspective

Migration inhibitors discussed above have been identified using enzyme-based assay or phenotype-based assay. In decades, many researchers have been studying the cell migration in different cells and diseases. Therefore, they disclosed important molecules and signaling pathways in cell motility procedures, such as chemoattractant sensing, cell polarity formation, protrusion, integrin, adhesion formation, and retraction, which become attractive therapeutic targets in drug discovery. However, unrevealed mechanisms of cell migration are remaining in these fields. In recent years, Yarrow and his colleagues developed a cell image-based screening system by wound healing assay. This kind of phenotypic screening method has been useful tools for screening of small molecules, siRNA, and protein libraries. Additionally, phenotypic screening method may be provided with solution of many unrevealed proteins or diverse migration-related pathways in cell migration. In spite of many endeavors to understanding of cell migration, our *in vitro* studying tools are not a mimic the microenvironment. Therefore, we do not exactly understand a mechanism of cell migration *in vivo*. In the future, we have to overcome these issues and effort to discover the tools of mimic the microenvironment and develop the equipment of detecting or monitoring the single cell movement in that microenvironment.

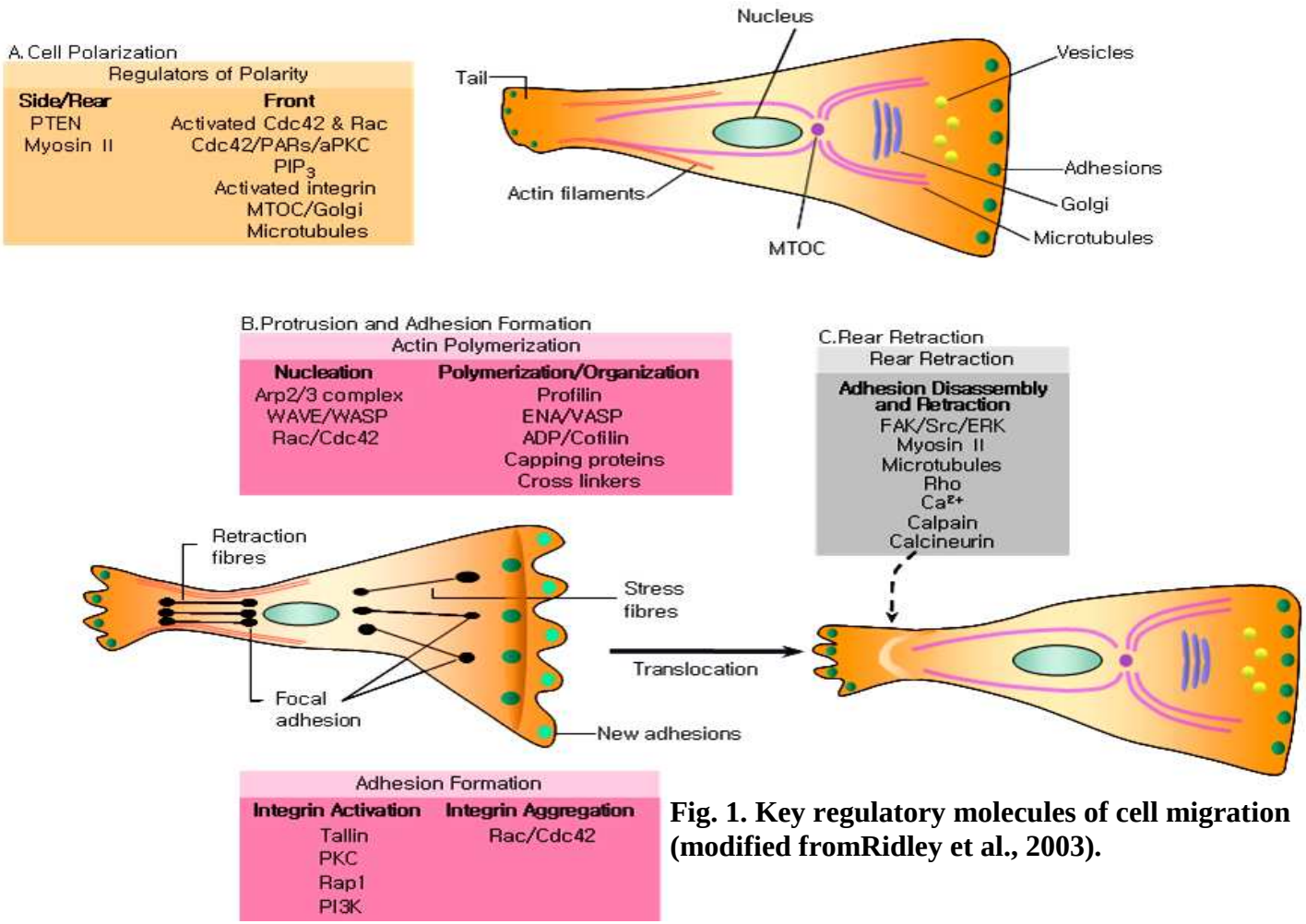

Fig. 1. Key regulatory molecules of cell migration (modified fromRidley et al., 2003).

Table 1. Structure of inhibitor of cell migration.

Name	Structure	Screen Method/Mode of Action
Migrastatin	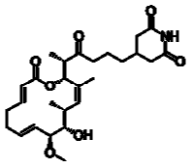	Inhibit Rac activation
Rockout	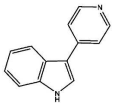	Wound healing assay/Rho kinase inhibitor
Locostatin (UIC-1005)	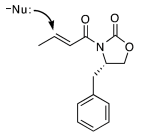	Wound closure assay/RKIP
DX-52-1	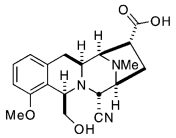	Wound healing assay/Radixin
AS-252424	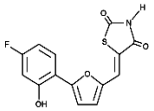	Enzyme based assay/PI3Kγ inhibitor
LFA703	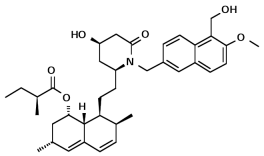	lovastatin-based series of designed compounds/LFA-1 (α I allosteric) inhibitor
BIRT377	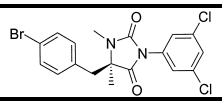	LFA-1/ICAM-1 binding assay/LFA-1 (α I allosteric) inhibitor
XVA143	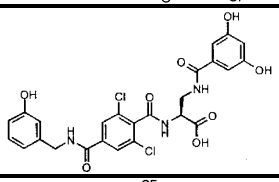	LFA-1-ICAM-1 ELISA-type binding assay/LFA-1 (α/β I-like allosteric) inhibitor
PF-228	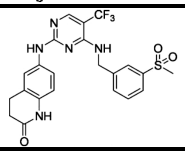	Enzyme based assay/FAK inhibitor
KRIBB3	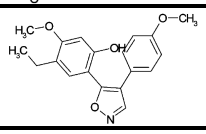	Boyden chamber assay/Hsp27 inhibitor

Part Ⅰ.

Blocking tumor cell migration and invasion with biphenyl isoxazole derivative KRIBB3, a synthetic molecule that inhibits Hsp27 phosphorylation

Abstract

Cell migration is a prerequisite for cancer invasion and metastasis, suggesting cell motility as a potential therapeutic target for cancer treatment. A synthetic library was screened to identify inhibitors of tumor cell migration. From this, I discovered CAC-1098 (aurintricarboxylic acid) and CBI-0997 (5-(2, 4-dimethoxy-5-ethylphenyl)-4-(4-Bromophenyl) isoxazole) that inhibited migration of MDA-MB-231 with an IC_{50} of 5 nM and 50 nM, respectively. I synthesized KRIBB3 (5-(5-ethyl-2-hydroxy-4-methoxyphenyl)-4-(4-methoxyphenyl) isoxazole) by replacing bromide group of CBI-0997 with methoxyl group. Like CBI-0997, KRIBB3 has anti-migratory and anti-invasive activity for MDA-MB-231. Because KRIBB3 has better drug-like structure, I focused my effort to understand its anti-migratory mechanism further. Biotinyl-KRIBB3 was synthesized as an affinity probe for identification of KRIBB3-binding proteins. Using affinity chromatography, Hsp27 was identified as a target protein of KRIBB3 *in vitro*. Treatment of MDA-MB-231 with PMA induced PKC-dependent phosphorylation of Hsp27 and tumor cell migration. In contrast, treatment of MDA-MB-231 with KRIBB3 blocked PMA-induced phosphorylation of Hsp27 and tumor cell migration. Furthermore, overexpression of Hsp27 could antagonize inhibitory effect of KRIBB3 on tumor cell invasion and knockdown of Hsp27 using siRNA inhibited tumor cell migration. Overall, my results demonstrated that KRIBB3 inhibits tumor cell migration and invasion by blocking PKC-dependent phosphorylation of Hsp27 through its direct binding to Hsp27.

Keywords: migration, metastasis, Hsp27, inhibitor, and chemical genetics

1. Introduction

Traditionally, genetic mutagenesis has proven to be a useful tool in solving the function of wide range of genes in biological process. Recently, chemical genetic approach has been developed to elucidate the principles of a wide range of biological processes (for review, (Mayer, 2003; Schreiber, 1998; Stockwell, 2004)).

Metastasis plays a major role in morbidity and mortality from breast cancer (Mundy, 2002). Potential of metastasis of cancer cell is related with ability to digest the extracellular matrix, migrate, cross blood vessel walls, and reach the blood circulation (for review, (Chambers et al., 2002; Friedl and Wolf, 2003; Hood and Cheresh, 2002; Pantel and Brakenhoff, 2004)). Cell movement is a complex process involving a number of steps, including the disruption of cell-cell junctions, cytoskeletal rearrangements, and the constant remodeling of adhesive contacts with the extracellular matrix (for review, (Franz et al., 2002; Lauffenburger and Horwitz, 1996; Ridley et al., 2003)). Cell migration contributes to several other important pathological processes, including vascular disease, osteoporosis, chronic inflammatory disease such as rheumatoid arthritis and multiple sclerosis, cancer, and mental retardation.

Anticancer drug development strategy has traditionally focused on inhibitor of cancer cell growth. However, other processes in the tumor progression can be potential targets for cancer treatment. Among these, migration is one of interesting processes for tumor progression. Expression of different growth factor receptors in

malignant cells was reported and could participate not only in transducing growth signals but also contribute to the motile properties of malignant cancer cell. Multiple growth factors and their receptors are involved in the malignant progression (van der Valk et al., 1997). The number of cells expressing multiple growth factors and their receptors tends to increase with increasing malignancy grade. High metastatic cells exhibit higher spontaneous rate of migration as compared with their low-metastatic counterparts (Clark et al., 2000; Volk et al., 1984).

Hsp27 (heat shock protein of 27 kDa) belongs to a family of abundant and ubiquitous stress proteins which are detectable in virtually all organisms from prokaryotes to mammals (Concannon et al., 2003). In unstressed cells, Hsp27 levels are generally low, and it exists predominantly as a large oligomeric unit of up to 800 kDa. The size of this oligomeric unit is dependent on a number of parameters, including temperature and degree of phosphorylation of Hsp27 (Lavoie et al., 1995; Zantema et al., 1992). During the stress condition, an increase in the level of Hsp27 expression is preceded by a phosphorylation-induced reorganization of the multimeric status of the Hsp27. Phosphorylation occurs on four different residues, Ser-15, Ser-78, Ser-82, and Thr-143 and this induces redistribution of the large oligomers to small tetrameric units (Lavoie et al., 1995; Zantema et al., 1992). Phosphorylation of Hsp27 catalyzed by MAKPAP kinase 2 and 3 (Landry et al., 1992; Ludwig et al., 1996; Stokoe et al., 1992), PKC (Maizels et al., 1998), cGMP-dependent protein kinase (Butt et al., 2001), and PKD (Doppler et al., 2005). The increased phosphorylation of Hsp27 is detectable several minutes after exposure to stress and subsequent increase in the expression level of the protein is detectable

within several hours (Landry et al., 1991). Hsp27 has been recognized as a potent regulator of cytoskeleton dynamics, actin microfilaments. Actin cytoskeleton is modulated by both the spatial arrangement as well as the polymerization dynamics of its different elements (Liang and MacRae, 1997). Overexpression of Hsp27 increases the stability of F-actin microfilaments during exposure to stress (Guay et al., 1997; Huot et al., 1995; Lavoie et al., 1993). The exact mechanism by which Hsp27 stabilizes F-actin is poorly characterized. Actin microfilaments are not the only components of the cytoskeleton that have been reported to interact with Hsp27. Hsp27 colocalizes with tubulin/microtubles (Hino et al., 2000). Higher levels of Hsp27 expression are commonly detected in variety different cancers including breast (Love and King, 1994; Oesterreich et al., 1993), prostate (Cornford et al., 2000), gastric (Chen et al., 2004; Ehrenfried et al., 1995), and ovarian (Langdon et al., 1995) cancer. Several studies point to the ability of Hsp27 to increase the metastatic potential of tumor cells in nude mice as well as enhancing their resistance to therapy (Blackburn et al., 1997; Katoh et al., 2000).

I now report that I have identified anti-migratory compounds by chemical library screening. One of inhibitors, KRIBB3, inhibited both tumor cell migration and invasion. In addition, I found that KRIBB3 bound to Hsp27 and inhibited cell migration by blocking PKC-dependent Hsp27 phosphorylation.

2. Materials and Methods

2.1. Materials

Monoclonal anti-phospho-Hsp27 (ser 78) antibody was purchased from Upstate Biotechnology. Antibodies against Hsp27, AKT, phospho-AKT, phospho-PKCμ(mu), and phospho-PLCβ3 were purchased from Cell Signaling. Antibodies against FAK, p130^{Cas}, and PY-20 were purchased from transduction laboratories (Lexington, KY). Chemicals used in these experiments were purchased from Sigma Chemical (St. Louis, MO) and Calbiochem (San Diego, CA). CAC-1098 (aurintricarboxylic acid) was purchased from Sigma Chemicals (St. Louis, MO) and CBI-1098 (5-(2, 4-dimethoxy-5-ethylphenyl)-4-(4-Bromophenyl) isoxazole) and KRIBB3 (5-(5-ethyl-2-hydroxy-4-methoxyphenyl)-4-(4-methoxyphenyl) isoxazole) were synthesized in my laboratory.

2.2. Cell culture

The cell lines used were obtained originally from ATCC. MDA-MB-231 (human breast cancer cell line) was maintained in RPMI 1640 (Gibco/BRL) supplement with 10% heat inactivated FBS (Gibco/BRL) and 25 mM Hepes. Cell cultures were maintained at 37℃ under a humidified atmosphere of 5% CO_2 in an incubator.

2.3. Construction of Hsp27 overexpressing MDA-MB-231 cell line

Full length Hsp27 was obtained by PCR using sense (5'-CGCGGATCCATGACCGAGCGCCGCGTCC-3') and antisense (5'-GGAATTCGTGGGCATCCGGGCTAAGG-3') oligonucleotides with an expressed sequence tag clone containing Hsp27 (Korea UniGene Clone ID hMU001508, cDNA clone MGC: 21487) as a template. The PCR product was digested with BamHI and EcoRI, and then inserted into a mammalian expression vector pcDNA3.1 that had been digested with BamHI and EcoRI. To generate cells stably expressing Hsp27, MDA-MB-231 cells were transfected using Lipofectamine and 1 μg of pcDNA3.1-Hsp27. Clones were selected in growth medium containing 0.8 mg/ml G418 for 21 days. In order to avoid colony-specific variation, I used whole population of selected colonies for further study.

2.4. Knockdown of Hsp27 protein by using Hsp27 siRNA

The Hsp27 siRNA and control siRNA were purchased from Cell Signaling (Beverly, MA). Cells plated at a density of 8×10^4 cells per well in six-well plates were transfected with 100 nM of Hsp27 specific and control small interfering RNA (siRNA) oligoduplexes after a preincubation for 20 min with oligofectamine in serum free OPTI-MEM (Invitrogen-Life Technologies, Inc.). Four hours after the beginning of the incubation, the medium was added with the RPMI 1640 containing

3X the normal concentration of serum (without antibiotics). 48 hours after transfection, cells were collected and used for migration assay or for preparation of whole cell lysates.

2.5. Cell proliferation assays

Proliferation assay was done, as described previously (Han et al., 2004). Briefly, cells (5,000 cells) were seeded into 96 well plates in RPMI 1640 containing 10% FBS. After 20-24 h, cells were replenished with fresh complete medium containing either a test compound or 0.1% DMSO. After incubation for 48 h, cell proliferation reagent WST-1 (Roche Applied Science) was added to each well. The amount of WST-1 formazan produced was measured at 450 nm using an ELISA Reader (Bio-Rad, CA).

2.6. Cell migration assays

Migration was measured using a 48-well Boyden chamber (Neuroprobe Inc., Gaithersburg, MD). Various concentrations of chemicals in RPMI 1640 medium with 10% FBS were placed into the base wells separated from the top wells by polycarbonate filters (Neuroprobe Inc., 8 μm pore size, 25×80 mm, PVP-free). Cells were harvested by trypsinization, washed once with serum-free RPMI 1640 medium containing 0.5 mg/ml soybean trypsin inhibitor (Sigma, St Louis, MO), and then washed twice with serum-free RPMI 1640 medium. Cells were resuspended in

serum-free RPMI 1640 medium and added to the upper chamber at 8×10^3 cells per well. Cells were incubated for 16 h at 37℃ in 5% CO_2 humidified incubator. At the end of experiment, cells were fixed with methanol for 10 min and stained with modified Giemsa stain (Sigma, St Louis, MO) for 1 hr. Cells on the upper side of the membrane were then removed by cotton swab. The migrated cells were counted under light microscope at 100 × magnifications.

Several known inhibitors of kinase were used at concentration indicated; Rottlerin (PKC-δ inhibitor, 5 μM):, PD98059 (MEK inhibitor, 40 μM):, Bisindolylmaleimide I (broad PKC inhibitor, 5 μM):, Y-27632 (ROCK inhibitor, 10 μM):, Wortmanin (PI3 kinase inhibitor, 10 μM):, SB203580 (p38 MAPK inhibitor, 10 μM):, AG1478 (EGFR inhibitor, 10 uM):, and PP2 (Src inhibitor, 50 uM).

2.7. Cell invasion assay

MDA-MB-231 cells were starved for overnight in serum-free RPMI 1640 medium. Thawed Matrigel (BD Bioscience, MA) was diluted 1:20 with 1 × RPMI and 100 μl was used to coat each invasion chamber (Transwell, BD Bioscience, MA) equipped with an 8 μm pore size micropore filter. After the chambers were incubated at 37℃ for 1 hr, unbound matrigel was aspirated and rinsed gently using serum-free RPMI 1640 medium. Matrigel barrier was reconstituted with 100 μl serum-free medium for 2 h at 37℃. In the meantime, MDA-MB-231 cells were harvested after trypsinization, washed once with serum-free RPMI 1640 medium containing 0.5 mg/ml soybean trypsin inhibitor (Sigma, St Louis, MO), and then

washed twice with serum-free RPMI 1640 medium. Cells were diluted to 1×10^5 cells/ml and 200 μl was inoculated into upper chamber. 10% FBS as chemoattractant was added to the 24 well culture dishes. After incubation at 37℃ for 24 h, the Matrigel on the filter was removed with a cotton swab. The filter was then stained with crystal violet (300 ㎕ of 5 mg/ml crystal violet dissolved in 20% Methanol) and incubated for 30 min. The membrane was washed several times with 1×PBS and the cells that had penetrated the filter were counted under a microscope.

2.8. Western Blotting and immunoprecipitation

Lysates were prepared using RIPA buffer, as described previously (Han et al., 2004). A 40 μg protein was resolved by 7.5% or 10% SDS-PAGE and transferred to PVDF membrane (Roche, Germany). Membrane was blocked with 1% Western Blocking Reagent (Roche, Germany) in TBS-T (50 mM Tris-HCl, pH 7.4, 150 mM NaCl, 0.05% Tween 20). The primary antibodies were used as recommended by the manufactures. The secondary antibodies used were horseradish peroxidase-conjugated goat anti-rabbit or anti-mouse IgG (Jackson ImmunoResearch Laboratories, Inc.). The membrane was incubated with primary antibody for 2 h at room temperature, washed 3 times with TBS-T, and visualized with chemiluminescent β-peroxidase reagents (Roche, Germany). For immunoprecipitation, 400 μg of lysates were incubated with primary antibody for 2 h at 4℃ in rotary shaker and then, 40 μl of protein G-agarose beads were added. After 1 hr, beads containing lysates were centrifuged and washed 3 times with lysis

buffer. Beads-bound proteins were resolved by SDS-PAGE and immunoblotted using specific antibody.

2.9. Detection of KRIBB3-binding proteins

MDA-MB-231 cells were washed with PBS and then homogenized with a 27G syringe in binding buffer (10 mM Tris-HCl pH 7.4, 50 mM KCl, 5 mM $MgCl_2$, 1 mM EDTA, and 0.1 mM Na_3VO_4). The cell lysate was centrifuged at 13,000 rpm for 30 min at 4℃, and the supernatant was collected. After the supernatant of MDA-MB-231 cells had been precleared by incubating with immobilized streptavidin (Sigma Chemical Co., St. Louis, MO) for 60 min at 4℃ followed by centrifugation at 500 × g for 5 min, the cleared supernatants were incubated with biotinyl-KRIBB3 compound. After incubation for 2 h at 4℃, proteins associated with the biotinyl-KRIBB3 compound were precipitated with UltraLink-Immobilized NeutrAvidin-agarose (PIERCE Biotechnology, Rockford, IL). Precipitated samples were applied to the column. Samples were washed with 10 bed volumes of washing buffer containing 50 mM HEPES pH 7.5, 30 mM NaCl, 1 mM EDTA, 2.5 mM EGTA, 0.1% Tween 20, 10% (v/v) glycerol, 1 mM NaF, 0.1 mM Na_3VO_4, and Protease Inhibitor Cocktail Tablets (1 tablets/10 ml; Roche, Germany). Samples were eluted from the column with 5 bed volumes of the elution buffer (0.1 M glycine•HCl pH 2.8). Samples were boiled in SDS-PAGE sample buffer, separated by 10% polyacrylamide gel, and visualized by Coomassie Briliant Blue stainging.

2.10. Peptide analysis of the KRIBB3-binding protein

Specific KRIBB3-binding protein in gel was cut out and sent to Korea Basic Science Institute (Daejeon, Korea) for peptide analysis. Sample was digested with trypsin. Peptide tandem mass spectrometry analysis of the digested peptides was performed using an electrospray ionization quadrupole time-of-flight mass spectrometer as described previously (Nam et al., 2003).

3. Results

3.1. Screening of anti-migratory chemicals

I sought anti-migratory compounds by using cell-based screening. Whole cell based assay was preferred because of its ability to simultaneously assess multiple targets. In addition, this approach can avoid problems with drug permeability by identifying active compounds that freely enter the cell. The effect of chemicals on the cell migration of MDA-MB-231 cells was measured by using modified Boyden Chamber assay (Fig. 2). Cell migration was performed in the presence of 10 μM of chemical and 10% FBS was used as a chemoattractant. The components provided by serum are certain highly specific proteins called growth factors. Serum containing growth factors are IGF-1 (insulin-like growth factor 1), EGF (epidermal growth factor), and PDGF (platelet-derived growth factor).

In screening ~12,000 synthetic chemicals for compounds, "cell stoppers", that inhibit migration of human breast cancer cell line MDA-MB-231, I identified CAC-1098 (aurintricarboxylic acid) and CBI-0997 (5-(2, 4-dimethoxy-5-ethylphenyl)-4-(4-Bromophenyl) isoxazole) (Fig. 3). The CAC-1098 and CBI-0997 inhibited migration of MDA-MB-231 with an IC_{50} of 5 nM and 50 nM, respectively (Fig. 4A).

To clarify whether the inhibitory action on motile functions could be due to a cytotoxic effect, the cell stoppers were tested for its effect on MDA-MB-231 cell

proliferation. The cell stopper, CAC-1098 and CBI-0997 inhibited proliferation of MDA-MB-231 with a GI_{50} of > 100 μM and 25 μM, respectively (Fig. 4B). These results indicate that the cell stoppers significantly inhibit cell migration at 0.1-1 μM without cytotoxic problem.

I synthesized several CBI-0997 derivatives and analyzed their anti-migratory activities (unpublished data). From this study, I found that replacement of bromide with methoxyl group did not change its anti-migratory activity and I decided to study methoxyl derivative further. I called methoxyl derivative, (5-(5-ethyl-2-hydroxy-4-methoxyphenyl)-4-(4-methoxyphenyl) isoxazole) as "KRIBB3" (Fig. 3). KRIBB2 (4-ethyl-5-methoxy-2(3-methyl-4-phenylisoxazole-5-yl) phenol) was an inactive analogue of KRIBB3 and used as a negative control.

CAC-1098 (aurintricarboxylic acid; ATA), another identified cell stopper, is a polymeric carboxylated triphenylmethane derivative (Fig. 3). Aurintricarboxylic acid was reported as an angiogenesis inhibitor (Gagliardi and Collins, 1993). It has been reported to have antiproliferative activity to vascular smooth muscle cells (Benezra et al., 1994). However, when MDA-MB-231 cells were treated with ATA, more than 80% of cell migration was inhibited by 0.01 μM of ATA. In addition, I could not detect any antiproliferative activity of ATA up to 10 μM (Fig. 4A and B). This result implies the possibility that ATA may inhibit angiogenesis by inhibiting migration of vascular endothelial cells. It will be interesting to test this possibility. Successful identification of previously known anti-angiogenesis compound validated my approach to identify novel compound that may inhibit cell migration.

3.2. Inhibition of tumor invasion by cell stopper

Invasive behavior of cancer cell is accompanied with increased cell movement. This suggests that cell stopper can block invasion of tumor. The effect of cell stoppers on the MDA-MB-231 cells to invade through Matrigel-coated porous filters in response to a chemotactic stimulus was examined in an 8 μm pore size invasion chamber assay. Cells were treated with cell stoppers at different concentration (0-100 μM) for 24 h, and I used 10% FBS as a chemoattractant. CAC-1098 and KRIBB3 inhibited invasion of MDA-MB-231 cell in a dose dependent manner, with half maximal inhibition at 2.8 μM and 0.15 μM, respectively (Fig. 5A and B). Especially, invasion was almost completely blocked by 1 μM concentration of KRIBB3 (by ~90%).

3.3 Analysis of phosphorylation of FAK, p130^{Cas}, and AKT

When cells were treated with KRIBB3, they became round in morphology within 5 min (Fig. 6A). Cells treated with vehicle, DMSO, did not induce any detectable morphological changes (data not shown). Spreading of cell is regulated by integrin receptors and its ligands, ECM. Activation of integrins induces phosphorylation of many focal adhesion proteins, including FAK (Guan and Shalloway, 1992) and p130^{Cas} (Vuori and Ruoslahti, 1995). Cells lacking the

tyrosine kinase FAK or Src have more and larger adhesions and migrate poorly (Alahari et al., 2002; Webb et al., 2002). The interaction of FAK with Src and the adaptor proteins $p130^{Cas}$ and Crk appears to regulate adhesion turnover. Therefore, I analyzed tyrosine phosphorylation of whole cell lysates or specific focal adhesion proteins after immunoprecipitation. In general, tyrosine phosphorylation of whole cell lysate increased after KRIBB3 treatment and reached maximum 3 h after the treatment and then, gradually decreased (Fig. 6B). However, profile of tyrosine phosphorylation of whole cell lysate was not altered by treatment with DMSO. In order to test whether FAK was tyrosine phosphorylated by KRIBB3, FAK was immunoprecipitated with anti-FAK antibody and blotted with phosphotyrosine-specific antibody. As shown in Fig. 7A, I could not detect any decrease of FAK phosphorylation. In contrast, I could see significant increase of FAK phosphorylation 3 h after KRIBB3 treatment. Similarly, $p130^{Cas}$ was immunoprecipitated with anti-$p130^{Cas}$ antibody and analyzed with phosphotyrosine-specific antibody. However, I could not detect any decrease of $p130^{Cas}$ phosphorylation (Fig. 7B). These suggest that FAK or $p130^{Cas}$ are not involved in KRIBB3-induced anti-migratory activity.

Directed cell migration toward a soluble growth factor is a general phenotype of motile cells and requires highly polarized intracellular signaling events promoting the recruiting of the PH-domain containing proteins to the leading edge (Firtel and Chung, 2000; Parent and Devreotes, 1999). This localized increase of phosphatidylinositol-3-phosphates is the result of spatial activation of PI-3-kinase (Funamoto et al., 2002). Therefore, I examined PI-3-kinase activity by measuring

amount of phosphorylated AKT, effector of PI-3-kinase. In this case, I found small increase of AKT phosphorylation 1 hr after KRIBB3 treatment and I could not see any inhibition of PI-3-kinase activity (Fig. 7C). This result suggested that KRIBB3 did inhibit cell migration not via PI-3-kinase, neither. When cells were treated with DMSO, phosphorylation of FAK, $p130^{Cas}$, or AKT was not changed (data not shown).

3.4. Target identification of KRIBB3

Target identification represents a major challenge for all forward-chemical genetic screening. Biochemical purification has been the method of choice for target identification. The generally used method is to immobilize the compound via a chemical linker on a solid phase support, followed by affinity purification of the cellular target. Therefore, I synthesized biotin-linked KRIBB3. For this, hydroxyl group of KRIBB3 was covalently attached to butyl-biotin moiety. The synthesized biotinyl-KRIBB3 has acceptable anti-migratory activity (IC_{50} is 0.2 μM). KRIBB2 is a KRIBB3 analogue lacking biological activity and biotinyl-KRIBB2 was synthesized for negative control.

Cell extracts of MDA-MB-231 cells were incubated with biotinyl-KRIBB3 or biotinyl-KRIBB2 or biotin. The bound proteins were precipitated with NeutrAvidin beads and bound proteins were detected by using Coomassie Brilliant Blue staining. A 30 kDa protein was detected as a biotinyl-KRIBB3 binding protein. This band was analyzed by ESI-Q-TOF mass spectrometer in Korea Basic Science

Institute and was identified as an Hsp27 protein (Fig. 8A and B). I wanted to confirm the 30-kDa protein as an Hsp27 by using Hsp27-specific antibody. The proteins bound to biotin- NeutrAvidin, biotinyl-KRIBB2- NeutrAvidin beads, or biotinyl-KRIBB3- NeutrAvidin beads were resolved using SDS-PAGE and separated bands were transferred onto a membrane. Then, Hsp27 band was visualized by using an anti-Hsp27 antibody. As shown in Fig. 8C, the Hsp27 band was only detected from biotinyl-KRIBB3 lane. In addition, when interaction between Hsp27 and biotinyl-KRIBB3 was challenged by excess of KRIBB3, the interaction between Hsp27 and biotinyl-KRIBB3 was decreased (Fig. 8D). These results support strongly that Hsp27 is a target protein for KRIBB3.

3.5. Overexpression of HSP27 relieved cells from KRIBB3 inhibition

It is important to prove not only that Hsp27 physically interacts with KRIBB3 but also that Hsp27 is functionally involved in KRIBB3–dependent inhibition of cell migration and invasion. To address the functional role of Hsp27 during the KRIBB3-dependent inhibition, I tested whether overexpression of Hsp27 could overcome KRIBB3-dependent inhibition of tumor invasion. For this, I constructed Hsp27-overexpressing MDA-MB-231 cell line by transfecting expression vector pcDNA3-Hsp27 to MDA-MB-231 cells. Hsp27 expressing stable cell lines were selected with G418 for 21 days, as described in Materials and Methods. Fig. 9A showed expression level of Hsp27 from vector or Hsp27 transfected cell lines. Tumor invasion assay was performed in the presence or

absence of KRIBB3. When Hsp27 was overexpressed, KRIBB3-induced inhibition of invasion was significantly overcome (Fig. 9B). This result further supported that Hsp27 is a target protein of KRIBB3 *in vivo*. Fig. 9C is a representative membrane images after staining of migrated cells during the invasion assay.

3.6. Knockdown of Hsp27 protein by using siRNA inhibited cell migration

To determine whether down expression of Hsp27 affect cell migration, I introduced Hsp27 siRNA into MDA-MB-231 cells. As shown in Fig. 10A, expression of Hsp27 was significantly eliminated from MDA-MB-231 cells after transfection of Hsp27 siRNA, indicating that my siRNA for MDA-MB-231 can target Hsp27 mRNA efficiently. Then, I analyzed migration of MDA-MB-231 cells after cells were treated with control siRNA, Hsp27 siRNA, or H_2O. As expected, migration of MDA-MB-231 cells was inhibited by 60% when Hsp27 expression was abolished (Fig. 10B). More than 95% of MDA-MB-231 cells were transfected by control siRNA when fluorescence-tagged siRNA was used as a control (data not shown). The expression of actin was not affected by control siRNA or Hsp27 siRNA.

3.7. PKC, Src, and PI-3-kinase are important for MDA-MB-231 cell migration

In order to figure out what kinds of cellular signal pathways are involved in my assay system, I tested several known kinase inhibitors such as AG1478 for EGFR, wortmannin for PI-3-kinase, Y27632 for ROCK, PD98059 for MEK1, SB203580 for p38, rottlerin for PKC δ, or Bisindolylmaleimide I for PKC α, β, γ, δ.

As shown in Fig. 11**,** inhibitors of MEK, EGFR, p38 kinase, or ROCK did not inhibit migration of MDA-MBV-231 cells in my assay system. However, inhibitors of PKC, Src, and PI-3-kinase could block migration of MDA-MB-231 cells. This result implies that signaling of PKC, Src, and PI-3-kinase is important for MDA-MB-231 cells to migrate toward serum and any inhibitor of these pathways should be detectable by my assay system. Among the candidate kinases, PKC has been known to phosphorylate Hsp27, an identified KRIBB3 binding protein. This leads us to explore the role of PKC during the cell migration.

3.8. Treatment with PMA antagonizes KRIBB3-induced inhibition of migration

Because PKC has been known to phosphorylate Hsp27 and its phosphorylation is involved in Hsp27-dependent actin dynamics, I analyzed effect of PKC activation on the cell migration in the presence or absence of KRIBB3. As shown in Fig. 12A, treatment with KRIBB3 inhibited migration of MDA-MB-231 cells. However, co-treatment of PMA with KRIBB3 could relieve KRIBB3-dependent inhibition of migration. This result suggested that activation of PKC could reverse KRIBB3 effects. Fig. 12B showed typical pictures of migrated cells in the membrane after staining during the migration assay. In order to see the correlation between cell migration and phosphorylation of Hsp27, I analyzed phosphorylation of Hsp27 (Ser-78) by using a phospho-specific antibody for Hsp27. Consistent with previous report, phosphorylation of Hsp27 was significantly increased by PMA treatment (Fig. 12C). However, when cells were treated with

KRIBB3, PMA-induced Hsp27 phosphorylation was significantly decreased. These data indicated that KRIBB3 inhibited migration of MDA-MB-231 cells via blocking phosphorylation of Hsp27. In order to test specificity of KRIBB3 on Hsp27, I analyzed phosphorylation of other PKC substrate in the presence of KRIBB3. PLCβ3 is known substrate of PKC (Strassheim and Williams, 2000). If KRIBB3 blocked phosphorylation of Hsp27 by direct binding to Hsp27 itself, KRIBB3 may not block phosphorylation of PLCβ3. As expected, KRIBB3 could not block PMA-induced phosphorylation of PLCβ3, supporting that direct binding of KRIBB3 to Hsp27 is responsible for inhibition of phosphorylation of Hsp27.

4. Discussion

My first aim was identification of migration-specific genes that are involved in the regulation of cell migration. In order to identify migratory gene, I sought anti-migratory compounds by using cell-based screening. I excluded chemicals which showed growth inhibition. Whole cell based assay was preferred because of its ability to simultaneously assess multiple targets. From this, I identified “cell stoppers”, CAC-1098 and CBI-0997. These compounds can block cell migration without cytotoxicity. Among the identified chemicals, CBI-0997 has better drug-like structure and I decided to characterize it further. As a derivative of CBI-0997, KRIBB3 was synthesized by replacing bromide with methoxyl group. KRIBB3 has similar anti-migratory and anti-invasive activity as CBI-0997.

One of the characteristic features of KRIBB3 treated cells was rounding of cell morphology in the early time point (within 5 min). This implies that KRIBB3 may affect cytoskeleton. Because integrin is an important regulator for cytoskeleton and cell migration and FAK is a major downstream effector of integrin signaling, I examined whether FAK is inhibited by KRIBB3 or not. As shown in Fig. 7A, amount of phosphorylation of FAK was increased 1 hr after KRIBB3 treatment and reached maximum 3 h after the treatment. Then, its phosphorylation was gradually decreased and reached basal level 24 h after the treatment. Therefore, it is unlikely that KRIBB3 inhibited cell migration through FAK inhibition.

In order to know general properties of my migration assay system, I analyzed several inhibitors of kinases known to be involved in cell migration. From

this, I noticed that Src, PI-3-kinase, and PKC are important signaling kinases for migration of MDA-MB-231 cells (Fig. 11). Because $p130^{Cas}$ is a major substrate of Src (Sakai et al., 1994) and localized at focal adhesion, I tested whether KRIBB3 inhibited phosphorylation of $p130^{Cas}$. However, I could not detect any inhibition of $p130^{Cas}$ phosphorylation by KRIBB3 (Fig. 6B), suggesting that KRIBB3 did not inhibit Src kinase. Next, I analyzed PI-3-kinase activity by measuring amount of phospho-AKT, an effector of PI-3-kinase. However, I could not see any decrease of amount of phospho-AKT (Fig. 7C). In contrast, I could see small increase of phospho-AKT. This result implied that KRIBB3 did inhibit cell migration not through PI-3-kinase signaling.

In order to study the effect of PKC activation on KRIBB3-dependent inhibition of cell migration, cells were treated with either PMA or KRIBB3 or both. As shown in Fig. 12A, treatment of MDA-MB-231 cells with PMA increased cell migration. In addition, KRIBB3-dependent inhibition of cell migration was significantly relieved by treatment of PMA. Therefore, I concluded that KRIBB3 inhibited cell migration by blocking PKC-dependent signaling.

The major technical challenge during phenotype-based screening is identification of target protein of bioactive molecule. Affinity chromatography can be a powerful method for target identification. However, this approach has its limits when chemical modification of the compound is not compatible with its biological activity. The synthesized biotinyl-KRIBB3 retained comparable anti-migratory activity (IC_{50} is 0.2 μM). Using bioactive biotinyl-KRIBB3, I identified Hsp27 as a direct target protein of KRIBB3 (Fig. 8). To exclude the possibility that Hsp27 is

non-specific binding partner, I synthesized biotinyl-KRIBB2, structural analogue of biotinyl-KRIBB3, and used it as a negative control. In addition, I carried out competition assay with free KRIBB3. As shown in Fig. 8D, a large molar excess amount of free KRIBB3 inhibited binding of Hsp27 to immobilized KRIBB3. Furthermore, I proved functional role of Hsp27 during the cell invasion and migration both by overexpressing Hsp27 and by knockdown of Hsp27 protein. As shown in Fig. 9, overexpression of Hsp27 antagonized KRIBB3-dependent inhibition of cell invasion and knockdown of Hsp27 protein by Hsp27 siRNA mimicked the KRIBB3 effect, inhibition of cell migration.

Hsp27 has been recognized as a potent regulator of cytoskeleton dynamics, actin microfilaments. Actin cytoskeleton is modulated by both the spatial arrangement as well as the polymerization dynamics of its different elements (Liang and MacRae, 1997). Hsp27 stabilizes actin filaments in a yet undefined manner resulting in increased resistance to stresses and this function is regulated by the phosphorylation of Hsp27. Phosphorylation of Hsp27 is catalyzed by MAKPAP kinase 2 and 3 (Landry et al., 1992; Ludwig et al., 1996; Stokoe et al., 1992), PKC (Maizels et al., 1998), PKD (Doppler et al., 2005), and cGMP-dependent protein kinase (Butt et al., 2001). Because KRIBB3 binds to Hsp27 (Fig. 8C) and PKC is important kinase for migration of MDA-MB-231 cell (Fig. 11) and activation of PKC by PMA antagonizes KRIBB3-dependent inhibition of cell migration (Fig. 12A), and KRIBB3 inhibits PKC-dependent phosphorylation of Hsp27 (Fig. 12C), it is highly likely that KRIBB3 specifically binds to Hsp27 and blocks PKC-dependent HSP27 phosphorylation and PKC-dependent migration. The specificity of KRIBB3

on HSP27 was further supported by the fact that KRIBB3 could not block PMA-induced phosphorylation of PLCβ3, another PKC substrate (Fig. 12C). To my knowledge, the KRIBB3 is the first inhibitor of Hsp27 and it will be useful to analyze Hsp27 functions in cell.

Higher levels of Hsp27 expression are reported in variety different cancers including breast (Love and King, 1994; Oesterreich et al., 1993) prostate (Cornford et al., 2000) gastric (Chen et al., 2004; Ehrenfried et al., 1995) and ovarian (Langdon et al., 1995) cancer. In addition, several studies point to the ability of Hsp27 to increase the metastatic potential of tumor cells in nude mice as well as enhancing their resistance to therapy (Blackburn et al., 1997) (Katoh et al., 2000). Interestingly, Blackburn and his colleagues reported that murine Hsp25 but not human Hsp27 enhanced tumor growth in nude mice. I do not know why murine Hsp27 and human Hsp27 showed such a difference. One possible explanation is cell type difference. Blackburn and his colleagues used murine L929 fibrosarcoma cells and I used human MDA-MB-231 epithelial carcinoma cells.

Recently, Yarrow and his colleagues reported inhibitor of cell migration from screening of library using wound healing assay (Yarrow et al., 2005). Using automated microscopy, they screened library of 16,000 chemicals and found one, 3-(4-pyridyl) indole. This inhibitor blocked cell migration via blocking Rho-kinase. However, my screening system could not identify 3-(4-pyridyl) indole-like compounds because migration of MDA-MB-231 cells is not inhibited by Rho kinase inhibitor, Y27632, in my assay system (Fig. 11). Similarly, natural product (migrastatin) from *Streptomyces* was shown to inhibit cell migration (Nakae et al.,

2000). In addition, more potent analogs of migrastatin were reported (Njardarson et al., 2004; Shan et al., 2005). Migrastatin was reported to exert its effect by inhibiting Rac activation. However, it is not known whether migrastatin binds directly to Rac or its upstream molecule(s) and target identification remains to be solved.

Currently, I do not know the binding constant of KRIBB3 to the Hsp27 or binding pocket in the Hsp27. The IC_{50} of KRIBB3 for migration was 50 nM, suggesting that KRIBB3 has high specific affinity to the target protein, Hsp27. This high affinity and relatively high abundance of Hsp27 may contribute this success of affinity chromatography for target identification. In addition, it will be very important to identify binding pocket of Hsp27 for KRIBB3 in order to optimize KRIBB3 structure for drug development in the future.

Overall, I identified Hsp27 and KRIBB3 as a migratory gene and its inhibitor, respectively, by using chemical genomic approach. The cellular basis for this effect rests on the inhibition of Hsp27 phosphorylation which regulates cell migration.

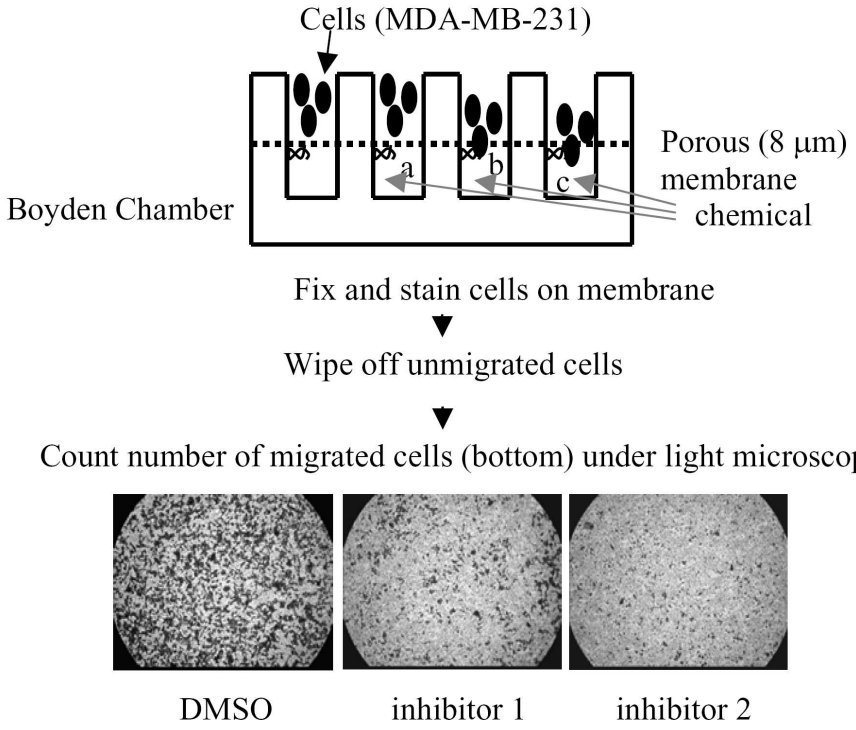

Fig. 2. Schematic diagram of method for screening of small molecules that affect cell migration. Chemical library compounds were added into bottom chamber with 10% of fetal bovine serum. Cancer cells were loaded into top chamber and incubated for 18 h. Migrated cells were stained and counted under the light microscope.

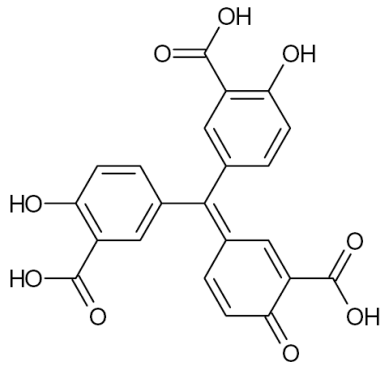

CAC-1098

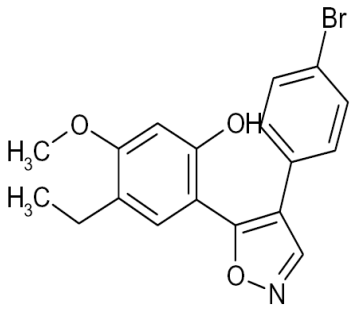

CBI-0997

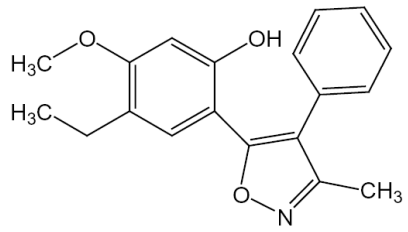

KRIBB2

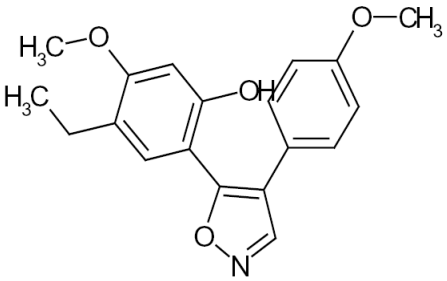

KRIBB3

Fig. 3. Structure of small molecules shown are the structure of compounds CAC-1098 (aurintricarboxylic acid), CBI-0997 (5-(2, 4-dimethoxy-5-ethylphenyl)-4-(4-Bromophenyl) isoxazole), and KRIBB3 (5-(5-ethyl-2-hydroxy-4-methoxyphenyl)-4-(4-methoxyphenyl) isoxazole) that inhibit cell migration. KRIBB2 (4-ethyl-5-methoxy-2(3-methyl-4-phenylisoxazole-5-yl) phenol) is an analogue of KRIBB3

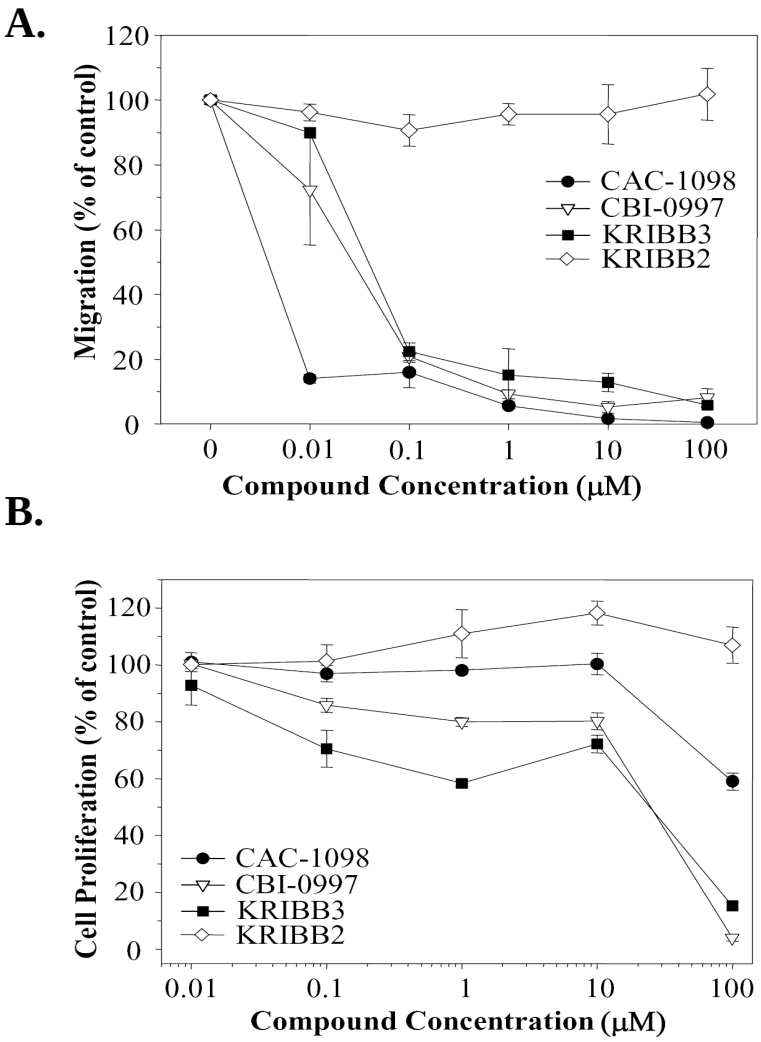

Fig. 4. The effects of identified inhibitors on migration and proliferation of tumor cells. A, MDA-MB-231 cells were treated with different concentrations of inhibitors or with vehicle solvent (1% DMSO), and the cell migration assays were performed as described under "Materials and Methods." The mean and standard deviation of relative migration rate (normalized to vehicle treated cell as 100) from three independent experiments are shown. B, MDA-MB-231 cells were treated with different concentrations of inhibitors or with vehicle solvent (0.1% DMSO) and viability were determined by using WST-1 at 48 h after treatment. The results are expressed as relative value to the vehicle treated cells

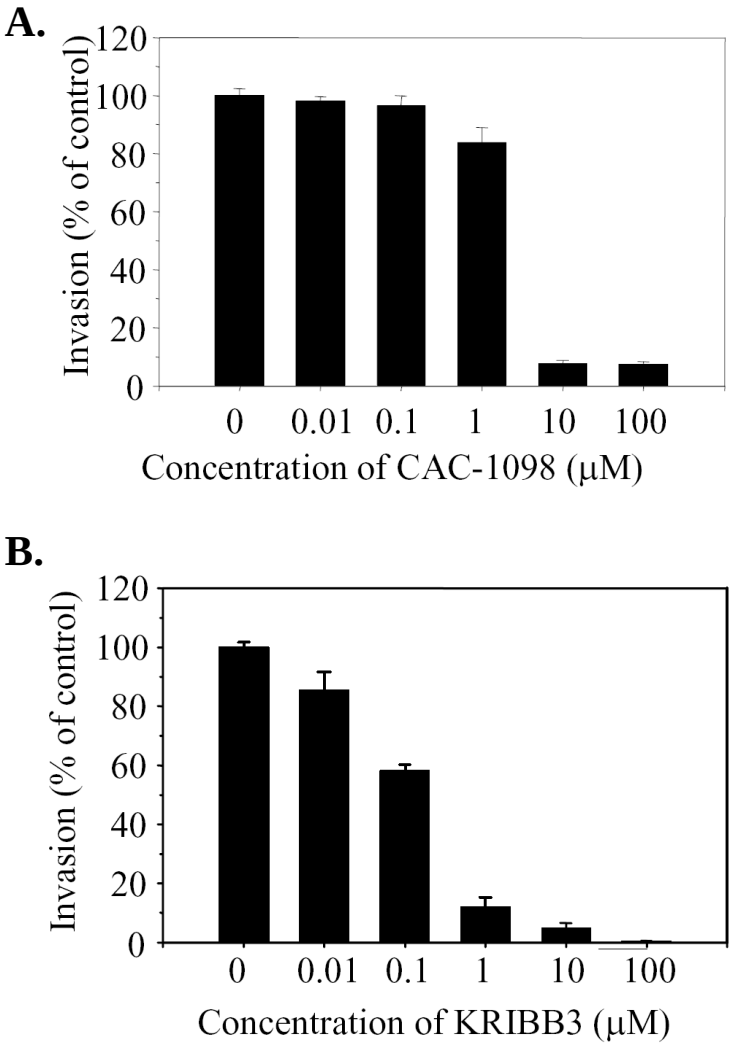

Fig. 5. The effects of identified inhibitors on invasion of tumor cells. A and B, MDA-MB-231 cells were treated with different concentrations of CAC-1098 and KRIBB3 or with vehicle solvent (1% DMSO), and the cell invasion assays were performed as described under "Materials and Methods." The mean and standard deviation of relative invasion rate (normalized to vehicle treated cell as 100) from three different fields are shown.

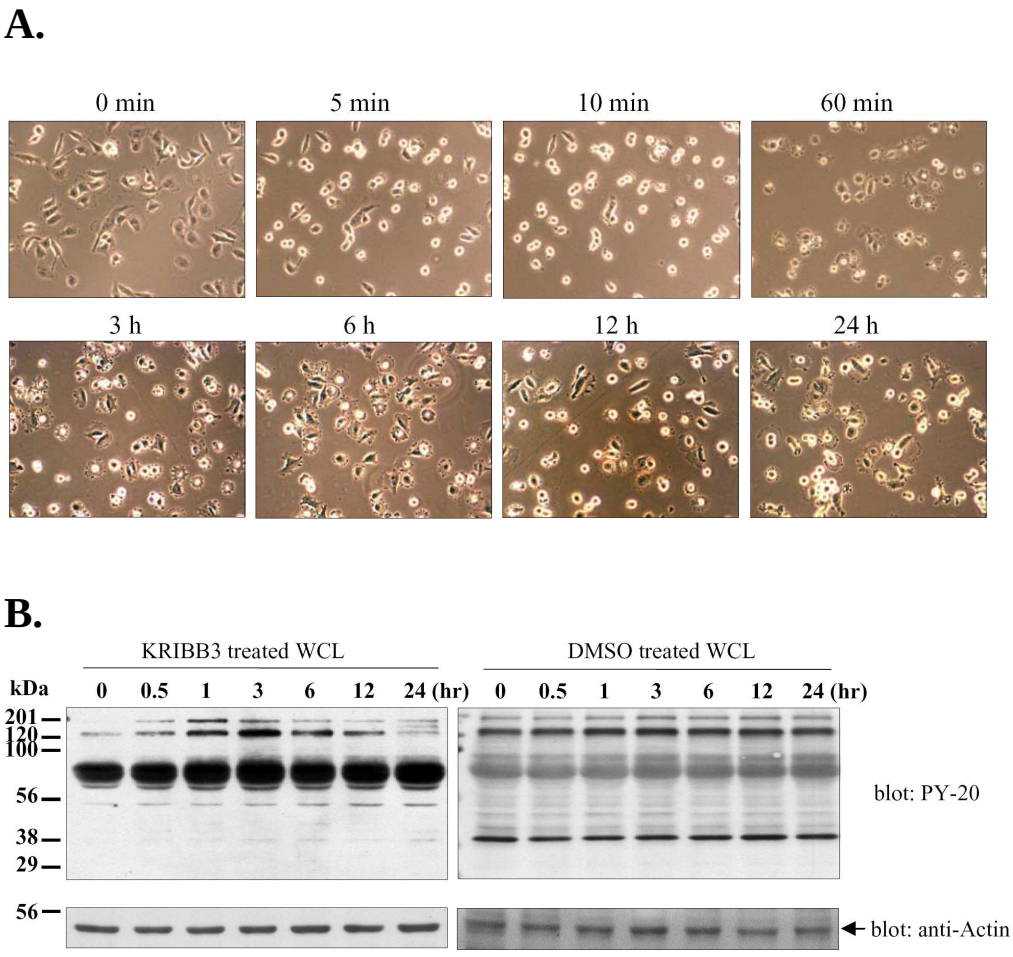

Fig. 6. Time course analysis of cell morphology and phosphorylation of after KRIBB3 treatment A, MDA-MB-231 cells were treated with 10 μM KRIBB3 or 0.1% of DMSO and incubated for different times as indicated. Cell morphology was imaged by Nikon microscope. B, MDA-MB-231 cells were treated with 10 μM KRIBB3 or 0.1% of DMSO and the lysates were prepared with RIPA buffer. 40 μg of lysate were resolved by SDS-PAGE and immunoblotted with PY-20 antibody

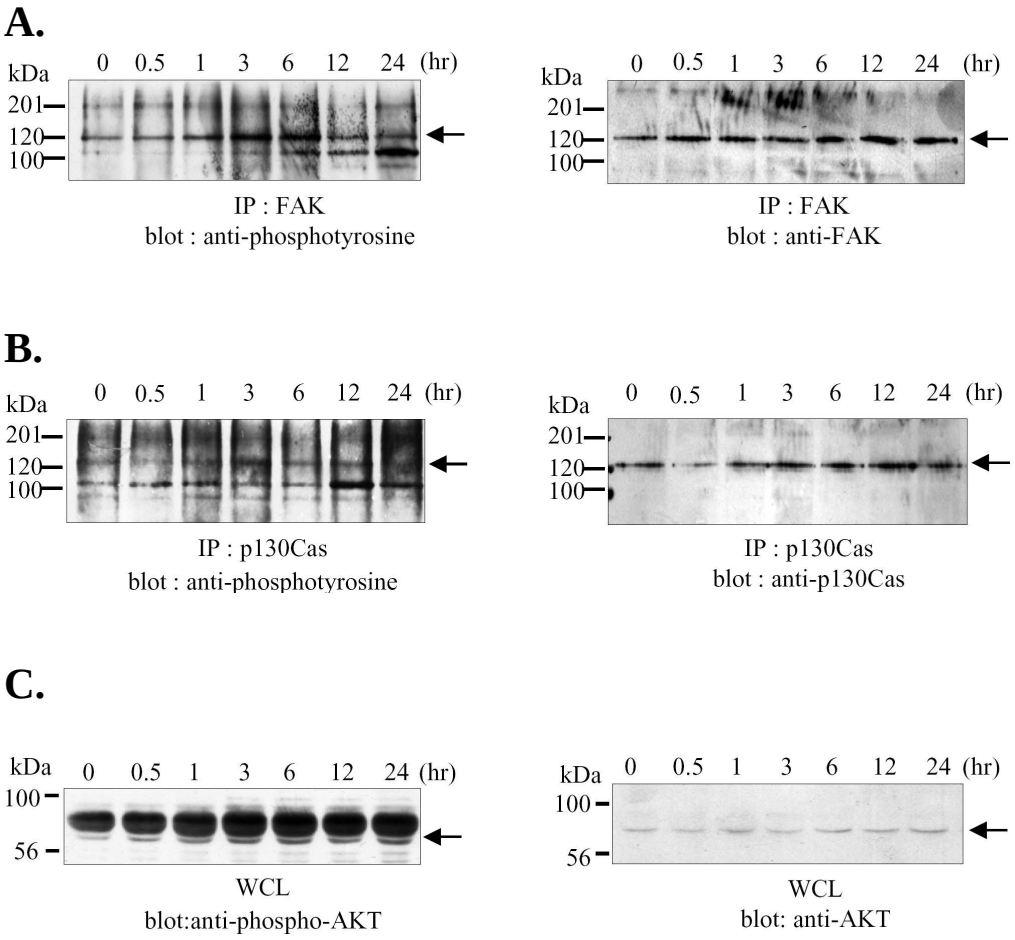

Fig. 7. Time course analysis of phosphorylation of FAK, p130^{cas}, and AKT after KRIBB3 treatment A and B, 400 μg of lysate treated with 10 μM KRIBB3 were immunoprecipitated with FAK antibody or p130^{Cas} antibody, respectively, and protein G-agarose beads, and precipitants were resolved by SDS-PAGE after washing three times and immunoblotted with PY-20 antibody (A and B, left panels), anti-FAK (A, right panels) antibody or anti-p130^{Cas} antibody (B right panels). C, the same whole cell lysates (WCL) were resolved by SDS-PAGE and immunoblotted with anti-phospho-AKT (left panels) or anti-AKT (right panels) antibody.

A.

Amino acid sequences	Protein	Accession no.
DGVVEITGK QDEHGYISR + Pyro-glu (N-term Q) LFDQAFGLPR VSLDVNHFAPDELTVK LATQSNEITIPVTFESR	Heat shock 27kDa protein 1 [Homo sapiens]	NP_001531

B.

1 MTERRVPFSLLRGPSWDPFRDWYPHSR**LFDQAFGLPR**LPEEWSQWLGGSS 50

51 WPGYVRPLPPAAIESPAVAAPAYSRALSRQLSSGVSEIRHTADRWR**VSLD** 100

101 **VNHFAPDELTVK**TK**DGVVEITGK**HEER**QDEHGYISR**CFTRKYTLPPGVDP 150

151 TQVSSSLSPEGTLTVEAPMPK**LATQSNEITIPVTFESR**AQ LGGPEAAKSD 200

201 ETAAK 205

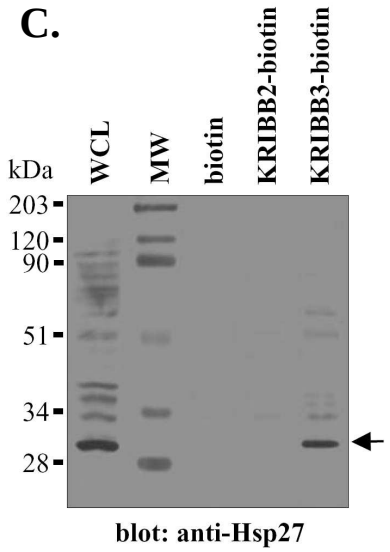

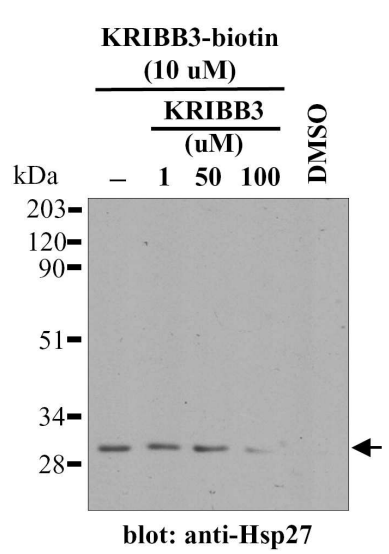

Fig. 8. Identification of KRIBB3 binding proteins. 10 mg of total protein was incubated with 10 μM of biotin or biotinyl-KRIBB3 and bound proteins were applied top column with NeutrAvidin beads. The proteins were eluted with biotin and analyzed by 10% SDS-PAE. Compared with biotin-treated sample, biotinyl-KRIBB3-treated sample has one unique band of 30-kDa. The 30-kDa protein was eluted and sent for sequencing. A, Peptides were sequenced by electrospray ionization quadrupole time-of-flight tandem mass spectrometry, and internal sequences were searched using the Mascot database. B, The Hsp27 has 205 amino acids. Peptides matching the Hsp27 protein are *underlined* and in *boldface*. C, 10 mg of total protein was incubated with 10 μM of biotin, biotinyl-KRIBB2, or biotinyl-KRIBB3, and bound proteins were applied to a column with NeutrAvidin beads. The eluted proteins were resolved with by 10% SDS-PAGE and immunoblotted with anti-Hsp27 specific antibody. D, shown is the competition of KRIBB3 with biotinyl-KRIBB3 for binding to the Hsp27 protein. DMSO, dimethyl sulfoxide.

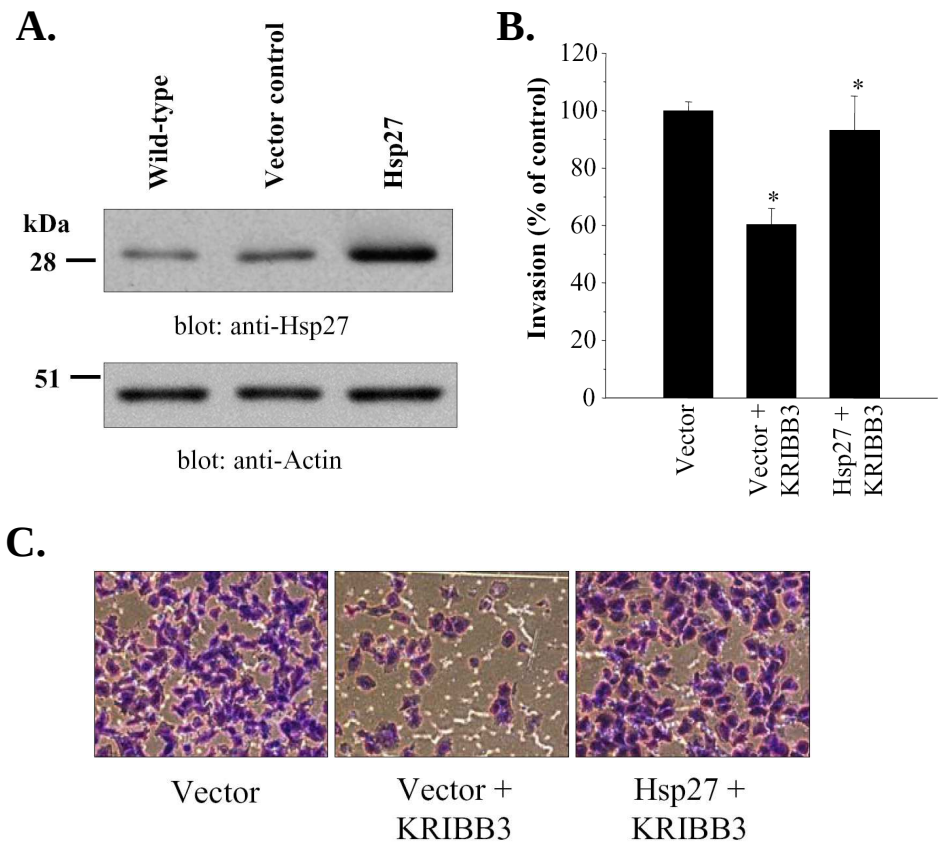

Fig. 9. Overexpression of Hsp27 can antagonize KRIBB3-induced inhibition of invasion A, shown are the results from Westen blot analysis of Hsp27 expressions in MDA-MB-231 (Wild-type), pcDNA3-transfected, and pcDNA3-Hsp27-transfected (Hsp27) cells. Whole cell lysates (10 μg) were separated by 12.5% SDS-PAGE and blotted with anti-Hsp27 antibody. B, Vector- or Hsp27-overexpressing MDA-MB-231 cells were treated with 0.1 μM of KRIBB3 or with vehicle solvent (1% DMSO), and the cell invasion assays were performed as described under "Materials and Methods." The mean ± S.D. of the relative invasion rate (normalized to vehicle-treated cell as 100%) from three different fields are shown. *, $P<0.01$ (Vector treated cells with KRIBB3 versus Hsp27-treated cells with KRIBB3). C, invading cells were imaged using a Nikon microscope after staining.

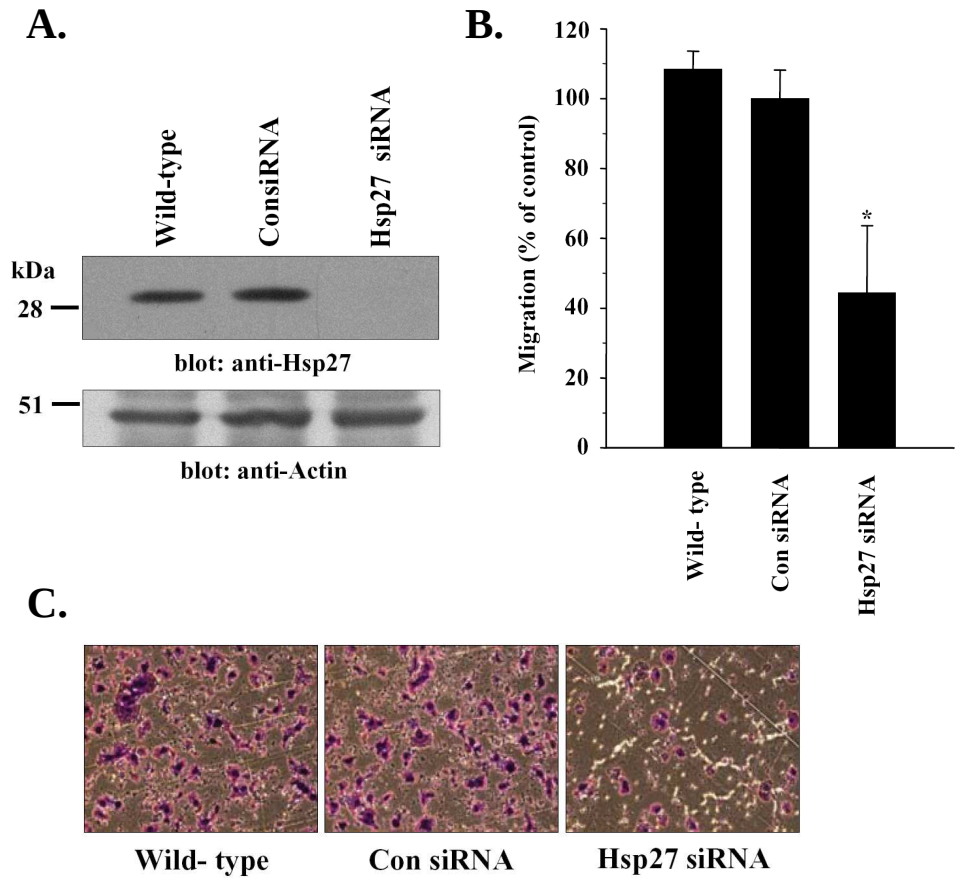

Fig. 10. Knockdown of Hsp27 protein can mimic KRIBB3 effect. A, shown are the results from Western blot analysis of Hsp27 expressions in MDA-MB-231(Wild-type), or control siRNA-transfected (Con siRNA), and Hsp27 siRNA-transfected (Hsp27 siRNA) cells. Whole cell lysates (30 μg) were separated by 12.5% SDS-PAGE and blotted with anti-Hsp27 antibody. B, MDA-MB-231 cells were transfected with control (con) siRNA or Hsp27 siRNA, and the migration assay was performed as described under "Materials and Methods." The mean ± S.D. of the relative migration rate (normalized to control siRNA as 100%) from three different fields are shown. *, $P<0.01$ (control siRNA versus Hsp27 siRNA as 100%). C, migrated cells were imaged using a Nikon microscope after staining.

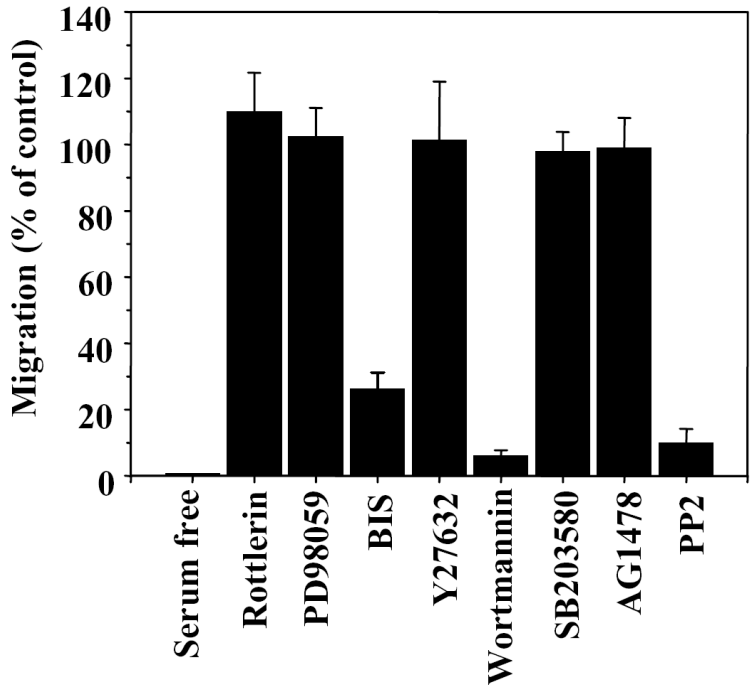

Fig. 11. Migration of MDA-MB-231 is decreased by inhibitor of PKC, PI3K, and Src kinase. MDA-MB-231 cells were treated with rottlerin (5 μM), PD98059 (40 μM), bisindolymaeimide I (BIS; 5 μM), Y27632 (10 μM), wortmanin (10 μM), SB203580 (10 μM), AG1478 (10 μM), or PP2 (50 μM) and cell migration assays were performed as described under "Materials and Methods." The means The mean ± S.D. of the relative migration rate (normalized to vehicle-treated cells as 100) from three independent experiments are shown.

A.

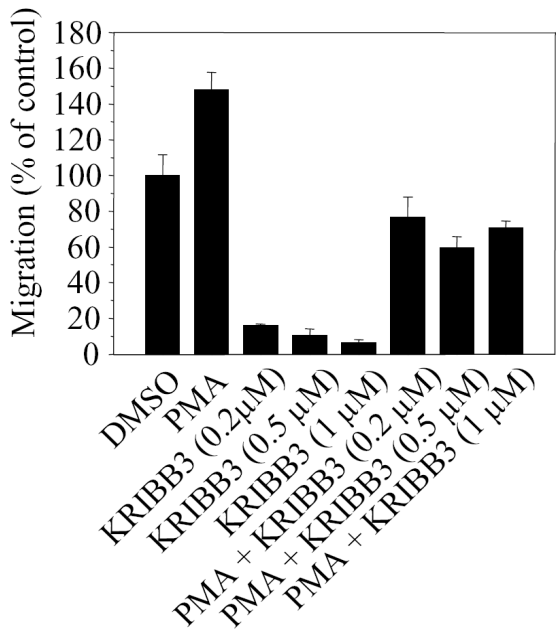
Migration (% of control)
180
160
140
120
100
80
60
40
20
0
DMSO
PMA
KRIBB3 (0.2μM)
KRIBB3 (0.5 μM)
KRIBB3 (1 μM)
PMA + KRIBB3 (0.2 μM)
PMA + KRIBB3 (0.5 μM)
PMA + KRIBB3 (1 μM)

B.

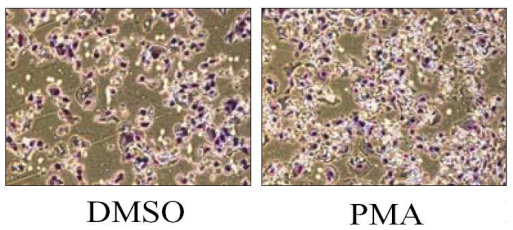
DMSO
PMA

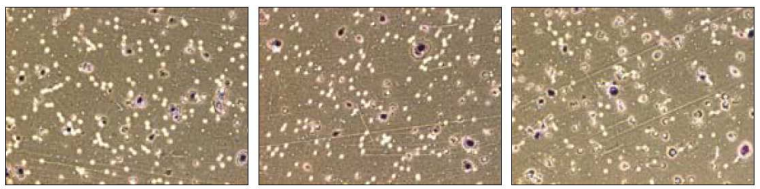
KRIBB3 (0.2 μM)
KRIBB3 (0.5 μM)
KRIBB3 (1 μM)

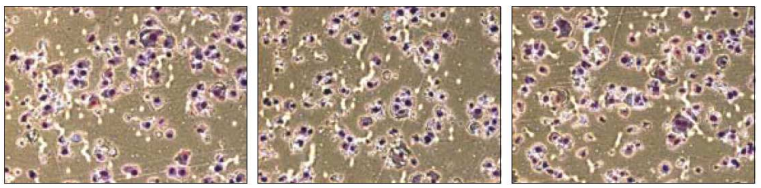
PMA + KRIBB3 (0.2 μM)
PMA + KRIBB3 (0.5 μM)
PMA + KRIBB3 (1 μM)

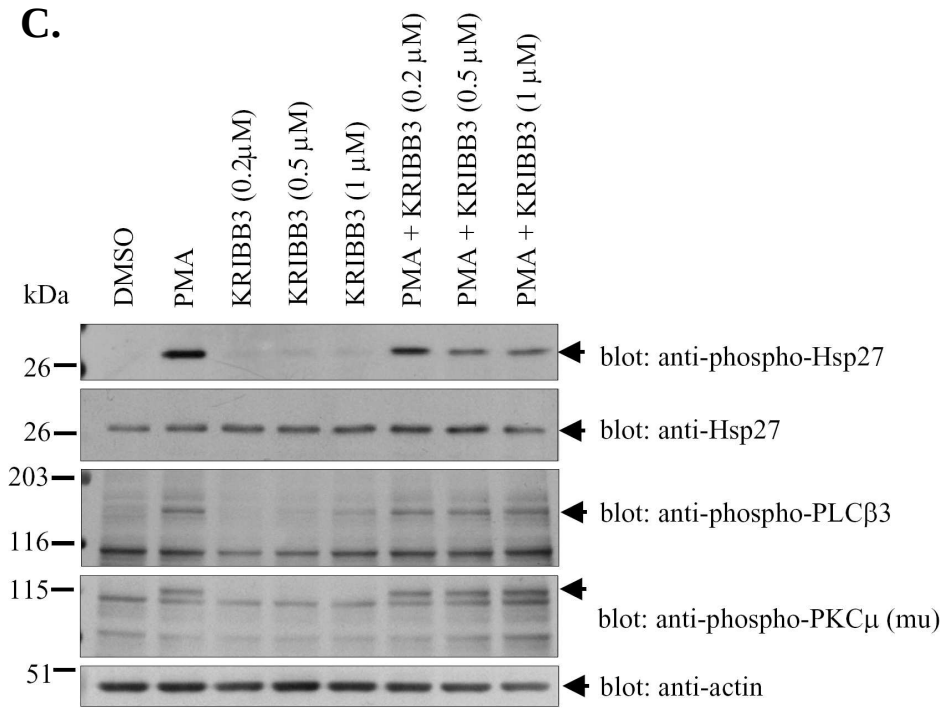

Fig. 12. KRIBB3-dependent inhibition of cell migration is antagonized by PKC activation. A, MDA-MB-231 cells were serum-starved overnight and then subjected to the cell migration assay using Transwells at different concentrations of KRIBB3 as indicated and/or PMA (0.1 μM). The means The mean ± S.D. of the relative migration rate (normalized to vehicle-treated cells as 100) from three independent experiments are shown. B, the cells were treated with KRIBB3 at the indicated concentration and/or PMA (0.1 μM) and incubated for 4 h, and the migrated cells were fixed, counted, and photographed. C, MDA-MB-231 cells were treated for 4 h with different concentrations of KRIBB3 and/or PMA (0.1 μM) or with vehicle solvent (0.1% DMSO), and lysates were prepared with RIPA buffer. 40 μg of lysates were resolved by SDS-PAGE and blotted with anti-phospho-Hsp27, anti-Hsp27, anti-phosphorylated phospholipase Cβ3 (anti-phospho-PLCβ3), anti-phospho-PKC μ, or anti-actin antibody.

Part Ⅱ

KRIBB3, a Novel Microtubule Inhibitor, Induces Mitotic Arrest and Apoptosis in Human Cancer Cells

Abstract

KRIBB3, (5-(5-ethyl-2-hydroxy-4-methoxyphenyl)-4-(4-methoxyphenyl) isoxazole) inhibited cancer cell growth *in vitro* and *in vivo*. Flow cytometry study showed that KRIBB3 caused cell cycle arrest at G_2/M phase and apoptosis. This was confirmed by detecting accumulation of Cyclin B1 and cleavage of poly (ADP-ribose) polymerase (PARP). While transient inhibition by KRIBB3 leaded to reversible mitotic arrest, prolonged exposure to the KRIBB3 induced apoptosis. Co-immunoprecipitation assay showed that KRIBB3 initially induced association of inhibitory Mad2 with p55CDC (mammalian homologue of CDC20), activator of APC/C (anaphase-promoting complex/cyclosome), suggesting that mitotic spindle checkpoint was activated by KRIBB3. However, this inhibitory complex of Mad2 with p55CDC was gradually decreased 24 h after KRIBB3 treatment and was hardly detectable after 48 h, indicating slippage of mitotic checkpoint. Consistent with these observations, KRIBB3 activated the mitotic spindle checkpoint by disrupting microtubule cytoskeleton. KRIBB3 was proven to be a tubulin inhibitor using *in vitro* polymerization assays and *in vivo* indirect immunofluorescence staining. The temporal pattern of Bax activation by KRIBB3 was similar to PARP cleavage, suggesting that Bax is a mediator of KRIBB3-dependent apoptosis. Furthermore, when KRIBB3 was administered intraperitoneally into nude mice at 50 mg/kg or 100 mg/kg, it inhibited 49.5% or 70.3% of tumor growth, respectively. These results suggest that KRIBB3 is a good drug candidate for cancer therapy.

Keywords: isoxazole, microtubule inhibitor, mitotic arrest, apoptosis, Bax activation, aurora kinase, and cancer therapy

Introduction

Chemicals that interfere with cell cycle progress have attracted much attention in cancer research because they can inhibit the proliferation of cancer cells. Among various anticancer drug targets known to date, microtubules are one of the most successful targets for cancer therapy (Zhou and Giannakakou, 2005). Microtubules are the principal components of the cytoskeletal system that takes part in intracellular transport, motility, architecture, and alignment and separation of chromosomes in meiosis and mitosis (Jordan and Wilson, 2004). Microtubules are polymeric structures composed of two structurally similar protein subunits, namely α– and β–tubulin, arranged head-to-tail to form a linear protofilament. During mitosis, microtubules undergo rapid polymerization and depolymerization to enable movement of the chromosomes. Mitotic checkpoint proteins monitor lack of tension or attachment between the kinetochores and microtubules.

Traditional antimitotic drugs produce “unattached” kinetochores in mitosis by altering microtubule dynamics and cause long-term mitotic arrest (Jordan and Wilson, 2004; Mollinedo and Gajate, 2003). Vinca alkaloids, inhibiting microtubule polymerization, have been used in the treatment of cancer over 30 years (Jordan et al., 1991). Unlike vinca alkaloids, taxanes promote tubulin polymerization, stabilize microtubules, and thereby inhibit microtubule dynamics, causing abnormal mitotic spindle and mitotic arrest (Manfredi and Horwitz, 1984; Schiff et al., 1979). Although the Vinca alkaloids and the taxanes are effective in the treatment of cancer,

their potential is limited by the appearance of drug resistant cancer cells during the cancer treatment (Dumontet and Sikic, 1999). One mechanism leading to drug resistance is mediated by overexpression of efflux pump, namely the p-gp170 (Fardel et al., 1996) and the MRP (Cole and Deeley, 1998). These efflux pumps are able to reduce the intracellular concentration of taxanes or Vinca alkaloids to a less toxic level. The link between prolonged mitotic checkpoint activation and cell death has not been well studied.

The mitotic spindle checkpoint is the major cell cycle control mechanism in mitosis (for review, (Bharadwaj and Yu, 2004; Jordan and Wilson, 2004; Weaver and Cleveland, 2005)). Mitotic progression is controlled by APC/C (anaphase-promoting complex/cyclosome), a multi-subunit E3 ubiquitin ligase (Peters, 2006). In order to recognize and interact with mitotic substrates, APC/C requires a specific factor CDC20 (cell-division-cycle 20 homologue). Genetic and biochemical studies have suggested that the most downstream event in checkpoint regulation is the inhibition of CDC20. Inhibition of CDC20 is accomplished by the mitotic checkpoint complex which is composed of Mad2, BubR1, Bub3, and CDC20 (Sudakin et al., 2001; Tang et al., 2001). Substrates that are targeted for degradation by APC/C include the master regulator of mitosis, Cyclin B1, as well as securin. These proteolytic events are controlled by mitotic checkpoint, the primary cell-cycle control mechanism in mitosis.

The signal generators of the mitotic checkpoint are unattached kinetochores which recruit mitotic checkpoint components and convert these in a form that

inhibits the CDC20-dependent APC/C activity (Weaver and Cleveland, 2005). The first checkpoint components were identified by genetic screening in yeast and were named Bub (budding uninhibited by benzimidazole) 1-3, Mad (mitotic arrest deficient) 1-3, and Mps 1 (monopolar spindle 1) (Hoyt et al., 1991; Li and Murray, 1991; Weiss and Winey, 1996). The vertebrate mitotic checkpoint requires the kinase BubR1 (a hybrid of Mad3 and Bub1), the ZW10-ROD-zwilch complex, CENPE (centromere protein E), and MAPK (mitogen activated protein kinase) (Abrieu et al., 2000; Chan et al., 2000; Chan et al., 1999; Mao et al., 2003). Following nuclear envelop breakdown, the checkpoint proteins are recruited to unattached kinetochore, protein-rich structures of chromosomes. Unoccupied kinetochores generate a "wait signal" to inhibit the anaphase promoting complex (Kops et al., 2005; Mao et al., 2003). Direct binding of CENPE to BubR1 activates the BubR1 kinase activity required for the recruitment of a stable Mad1-Mad2 heterodimer, which, in combination with other checkpoint proteins, modifies Mad2 into an active conformation. Activated Mad2 and/or BubR1 tightly associate with CDC20, preventing it from activating the APC/C, inhibiting degradation of Cyclin B1. For release of mitotic checkpoint, microtubule capture by CENPE is the most important signal transduction event because it shutdown production of the inhibitory complexes.

Although the capacity to carry out apoptosis is inherited to all cells, their susceptibility varies markedly and is influenced by external and internal events (Raff, 1992). Members of the Bcl-2 family of proteins play crucial roles in the regulation of apoptosis through controlling mitochondria function and releasing proapoptotic

proteins from mitochondria. Because mitochondria interact with microtubules, it is likely that mitochondria may connect microtubule damage to the apoptotic machinery, acting as appropriate and timing switches for the onset of apoptosis. In mammals, Bcl-2 has over 20 relatives, all of which share at least one of four conserved motifs known as the Bcl-2 homology (BH) domain, termed BH1, BH2, BH3, and BH4 (Adams and Cory, 1998). Bcl-2 overexpression suppresses the apoptotic response induced by distinct microtubule-active drugs, without affecting their actions on microtubules and on cell cycle arrest at G2/M (Gajate et al., 2000; Tang et al., 1994). Bim (Bcl-2 interacting mediator of cell death) (Puthalakath et al., 1999) and Bmf (Bcl-2 modifying factor) (Puthalakath et al., 2001) are important linkers of cytoskeleton and apoptotic machinery since they are indirectly sequestered by microtubule (Bim) or actin (Bmf) cytoskeleton. Apoptotic stimuli lead to the release of Bim from microtubules, and Bim is therefore freed to translocate to mitochondria where it binds Bcl-2 and Bcl-X_L and promote apoptosis through neutralization of the antiapoptotic activity of Bcl-2 and Bcl-X_L by forming Bim/Bcl-2 or Bim/Bcl-X_L heterodimers (Puthalakath et al., 1999), or through additional mechanisms, including Bax activation (Marani et al., 2002).

In previously part I, KRIBB3 was reported to inhibit tumor cell migration and invasion at 0.1-1 μM. However, it inhibited proliferation of MDA-MB-231 with a GI_{50} of > 25 μM, where GI_{50} is the concentration of an inhibition at which 50% inhibition of the cell growth is seen. This indicates that KRIBB3 significantly inhibits cell migration without cytotoxic problem. Using affinity chromatography, Hsp27 was identified as a molecular target of KRIBB3. Several other studies point

to the ability of Hsp27 to increase the metastatic potential of tumor cells in nude mice as well as enhancing their resistance to therapy (Blackburn et al., 1997; Katoh et al., 2000). Higher levels of Hsp27 expression are commonly detected in variety different cancers including breast (Love and King, 1994; Oesterreich et al., 1993), prostate (Cornford et al., 2000), gastric (Ehrenfried et al., 1995), and ovarian (Arts et al., 1999; Langdon et al., 1995) cancer.

Here we report the biological properties of KRIBB3 that displayed strong antimitotic activity against cancer cells. KRIBB3 exerted its antiproliferative activity through inhibition of tubulin polymerization and activating mitotic spindle checkpoint. In addition, KRIBB3 is not a substrate of p-gp170 and retains its activity in cell lines with MDR. When KRIBB3 was administered into nude mice, it significantly inhibited tumor growth compared with control mice, supporting its anticancer activity *in vivo*.

2. Materials and Methods

2.1. Materials

Rabbit polyclonal anti-phospho-Histone-H3 (Ser 10) antibody was purchased from Upstate Biotechnology. Antibodies against Hsp27 and PARP were purchased from Cell Signaling. Antibodies against Bax, Mad2, and BubR1 were purchased from BD biosciences (San Jose, CA). Antibodies of Cyclin B1, p55CDC, and actin were purchased from Santa Cruz Biotechnology, Inc. (Santa Cruz, CA). Monoclonal anti-Bax 6A7 antibody was purchased from Sigma (St. Louis, MO). Chemicals used in these experiments were purchased from Sigma Chemical (St. Louis, MO) and Calbiochem (San Diego, CA). Monoclonal anti-α-tubulin was purchased from Molecular Probes (Invitrogen; Carlsbad, CA). KRIBB2 (4-ethyl-5-methoxy-2(3-methyl-4-phenylisoxazole-5-yl) phenol) and KRIBB3 (5-(5-ethyl-2-hydroxy-4-methoxyphenyl)-4-(4-methoxyphenyl) isoxazole) were synthesized in my laboratory.

2.2. Cell culture

The cancer cell lines were obtained originally from ATCC. HCT-116 (human colon cancer cell line), HCA-7 (human breast cancer cell line), and SK-OV-3 (human ovarian cancer cell line) were maintained in McCoy's 5A (Invitogen) medium supplement with penicillin (50 units/ml)/streptomycin (50 μg/ml). MDA-

MB-231 (human breast cancer cell line), HT-29, HCT-15, SW620 (human colon cancer cell line), NCI-H23 (human non small lung cancer cell line), DU-145, and PC-3 (human prostate cancer cell line) were maintained in RPMI 1640 (Gibco/BRL). A549 (human non small lung cancer cell line) and HeLa (human cervical adenocarcinoma cell line) were maintained in Dulbecco's modified Eagle medium (Gibco/BRL). All culture media were supplemented with 10% heat-inactivated fetal bovine serum (Gibco/BRL). Cell cultures were maintained at 37℃ under a humidified atmosphere of 5% CO_2 in an incubator.

2.3. Cell proliferation assays

Proliferation assay was done, as described previously (Han et al., 2004). Briefly, cells (6,000 cells) were seeded into 96 well plates in McCoy's 5A media containing 10% FBS. After 20-24 h, cells were replenished with fresh complete medium containing either a test compound or 0.1% DMSO. After incubation for 48 h, cell proliferation reagent WST-1 (Roche Applied Science) was added to each well. The amount of WST-1 formazan produced was measured at 450 nm using an ELISA Reader (Bio-Rad, CA).

2.4. Western Blotting and immunoprecipitation

Lysates were prepared using RIPA buffer (50 mM Tris HCl, pH 7.4, 150 mM NaCl, 1% Triton X-100, 0.1% SDS, 5mM EDTA, 30 mM Na_2HPO_4, 50 mM NaF,

0.5 mM $NaVO_4$, 2mM PMSF, and 1% aprotinin), as described previously (Han et al., 2004). A 20~40 μg protein was resolved by SDS-PAGE and transferred to PVDF membrane (Roche, Germany). Membrane was blocked with 1% Western Blocking Reagent (Roche, Germany) in TBS-T (50 mM Tris-HCl, pH 7.4, 150 mM NaCl, 0.05% Tween 20). The primary antibodies were used as recommended by the manufactures. The secondary antibodies used were horseradish peroxidase-conjugated goat anti-rabbit or anti-mouse IgG from Jackson immunology. Membrane was incubated with primary antibody for 2 h at room temperature, washed 3 times with TBS-T, and visualized with chemiluminescent β-peroxidase reagents (Roche, Germany). For immunoprecipitation, 400 μg of lysates were incubated with primary antibody for 2 h at 4℃ in rotary shaker and then, 40 μl of protein G-agarose beads were added. After 1 hr, beads containing lysates were centrifuged and washed 3 times with lysis buffer. Beads-bound proteins were resolved by SDS-PAGE and immunoblotted using specific antibody.

2.5. siRNA Transfection

The human Hsp27 small interfering RNA (siRNA) duplex (5'-GUCUCAUCGGAUUUUGCAGC-3') was purchased from Bioneer, Inc. (Daejeon, KOREA). Cells plated at a density of 1.5×10^5 cells per well in six-well plates were transfected with 50 nM or 100 nM of Hsp27 specific and control siRNA oligoduplexes after a preincubation for 20 min with Oligofectamine in serum free OPTI-MEM (Invitrogen). Four hours after the beginning of the incubation, the

medium was added with the McCoy's 5A containing 30% of serum (without antibiotics), making final concentration of 10% of serum**.** 48 hours after transfection, cells were collected and used for cell cycle analysis or for preparation of whole cell lysates.

2.6. Cell synchronization

For synchronization at metaphase, cells were treated with nocodazole (1 μM) at 37℃ for 15 h. After treatment, metaphase cells were collected by gentle shake-off method, centrifuged at 300 × g for 5 min at room temperature, and washed twice with fresh medium. To relieve cells from the mitotic phase arrest, they were replated in a 100-mm cell culture dish (1×10^6 cells/dish) and incubated at 37℃ in fresh medium for various time periods.

2.7. Cell cycle analysis

Cell cycle was analyzed, as described previously (Han et al., 2004). Briefly, cells were trypsinized from the culture dish. After centrifugation at 300 × g for 5 min at room temperature, the supernatant was removed. The cells were then washed twice with phosphate-buffered saline (PBS; 8 g of NaCl, 0.2 g of KCl, 1.44 g of $Na_2HPO_4\cdot7H_2O$, 0.24 g of $KH_2PO_4\cdot H_2O$/liter, adjusted to pH 7.2) solution and fixed with 5 ml of ice-cold 70% ethanol overnight. Fixed cells were harvested by centrifugation at 300 × g for 5 min at room temperature and washed twice with PBS.

Collected cells were suspended in PBS (100 μl/1 × 10^5 cells) and treated with 100 μg/ml RNase A at 37℃ for 30 min. Propidium iodide was then added to final concentration of 50 μg/ml for DNA staining, and 20,000 fixed cells were analyzed on FACScalibur (BD Biosciences). Cell cycle distribution was analyzed using the Modifit's program (BD Biosciences).

2.8. Tubulin polymerization assay

For the detection of polymerization of tubulin/microtubule, The CytoDYNAMIX Screen 01 kits were purchased form Cytoskeleton Inc. (Denver, CO). Tubulin proteins (>97% purity) were suspended (300 μg/sample) with 100 μl of G-PEM buffer (80 mM PIPES, 2 mg $MgCl_2$, 0.5 mM EGTA, 1.0 mM GTP, pH 6.9) plus 5% glycerol in the 0.1% DMSO or test compounds at 4℃. Then the sample mixture was transferred to the prewarmed 96-well plate, and polymerization of tubulin was measured by the change in absorbance at 340 nm every 1 min for 70 min (Wallac victor2; PerkinElmer, Inc., Wellesley, MA) at 37℃.

2.9. Immunofluorescence Microscopy

HCT-116 cells were plated on 18 mm coverslip that was coated with 50 mg/ml of Poly-L-Lysine. Cells were incubated in a 37℃ incubator to allow cells to attach and spread. At the end of incubation, the cells were fixed with 3% formaldehyde for 10 min, washed three times with PBS for 5 min, permeabilized

with 0.5% Triton X-100 for 5 min, washed three times, and stained with primary antibodies (α-tubulin (1: 50)) for 1 hr at room temperature. After washing three times with PBS, the bound mouse IgG was detected with Texas Red-conjugated anti-mouse (1: 100) and counterstained with 1 μg/ml of DAPI (4', 6-diamidino-2-phenylindole) in PBS for 1 hr at room temperature. Image of stained cells was examined under a Zeiss LSM 510 META confocal microscope (Carl Zeiss, Inc., Thornwood, NY)

2.10. Detection of Bax conformational change (activation)

Metaphase synchronized cells were treated with 0.1% DMSO or 1 μM of KRIBB3. The method was modified from the previous description (Tao et al., 2005). In brief, cells were collected and lysed with Chaps lysis buffer (10 mM Hepes (pH 7.4), 150 mM NaCl, and 1% Chaps). Cell lysates containing 500 μg proteins were incubated with anti-Bax 6A7 monoclonal antibody for 3 h at 4℃ in rotary shaker and then, 40 μl of protein G-agarose beads were added. After 2 h, beads containing lysates were centrifuged and washed 3 times with Chaps lysis buffer. Beads-bound proteins were resolved by SDS-PAGE and immunoblotted using anti-Bax monoclonal antibody (BD bioscience).

2.11. Nude mouse xenograft assay.

Female inbred specific-pathogen-free (SPF) BALB/c nude mice, 7 weeks old, were obtained from Charles River Co. (Japan), and housed in sterile conditions under 12 h light/dark cycles, and fed food and water *ad libitum*. For the evaluation of *in vivo* anti-tumor activity of KRIBB3, HCT-116 cells (0.3 ml of 3×10^6 cells/ml) were implanted subcutaneously into the right flank of the mice on day 0. KRIBB3 or doxorubicin was dissolved in 0.5% Tween 80 and was daily administered intraperitoneally for 16 days at a concentration 50 or 100 mg/kg for KRIBB3 or 2 mg/kg for doxorubicin. The amount of dosage was 0.2 ml per 20 g body weight of animals. Tumor volumes were estimated as; length (mm) ×width (mm) ×height (mm)/2. To determine the toxicity of the compound, the body weight of tumor-bearing animals was measured. On day 16, the mice were sacrificed and the tumors were weighed.

3. Results

3.1. Inhibition of tumor cell growth by KRIBB3

To determine the effect of isoxazoles on growth of cancer cells, HCT-116 colon cancer cells were treated with compounds at different concentrations (0-100 μM) for 48 h (Fig 13). KRIBB2 is an inactive structural analogue of KRIBB3. KRIBB3 exhibited a dose dependent inhibition of cell growth in a broad range of concentrations and the GI_{50} value of KRIBB3 for *in vitro* growth inhibition was approximately 0.35 μM, where GI50 is the inhibitor concentration at which 50% inhibition of cell growth is seen.

Failure in cancer chemotherapy is often related to multidrug resistance (MDR). Therefore, I tested whether MDR1 overexpression confers resistance to KRIBB3. Paclitaxel and vinblastin are the most widely used antimitotic cancer drugs, and are substrates of P-glycoprotein (MDR1). Therefore, I used these chemicals as positive compounds for MDR1. HCT-15 is an MDR1 overexpressing colorectal carcinoma. As expected, HCT-15 has profound resistance to paclitaxel (53-fold), vinblastin (11-fold), and colchicines (4-fold) compared with HCT-116. In contrast, KRIBB3 is equally potent toward HCT-116 and HCT-15 (Fig. 14 A and B), suggesting that KRIBB3 can be effective against MDR1-overexpressing drug-resistant cells.

Similarly, the effect of KRIBB3 on the proliferation of various tumor cell lines was analyzed (Table 1). Because more than 50% of human cancers have mutated p53, which is known to be an important regulator of cell cycle progression and apoptosis, I chose to study both p53 wild type and p53-deficient cancer cell lines. Fortunately, KRIBB3 was able to exert its inhibitory activity in a p53-independent pathway, as shown by its similar effects on the p53 expressing and deficient cell lines.

3.2. Inhibition of Hsp27 does not block tumor cell growth

Previously, I reported that KRIBB3 inhibited tumor cell migration by blocking PKC-dependent phosphorylation of Hsp27 through its direct binding to Hsp27. To determine whether inhibition of Hsp27 affect cell proliferation, I introduced Hsp27 siRNA into HCT-116 cells. As shown in Fig. 15A, expression of Hsp27 was largely eliminated from HCT-116 cells after transfection of Hsp27 siRNA, indicating that siRNA can target Hsp27 mRNA efficiently in HCT-116 cells. Next, I analyzed the proliferation of HCT-116 cells after the cells were treated with control siRNA, Hsp27 siRNA, or H_2O. Surprisingly, there was no detectable inhibition of proliferation by Hsp27 siRNA transfection (Fig. 15B). This result implies that KRIBB3 inhibits the proliferation of HCT-116 cells in a Hsp27-independent manner. In addition, knockdown of Hsp27 using siRNA did not affect the HCT-116 cell cycle (Fig. 15C).

3.3. KRIBB3 arrests cells in the G_2/M phase

Because KRIBB3 inhibited cancer cell growth, I analyzed the effect of KRIBB3 on the cell cycle profile. HCT-116 cells were treated with 1 μM of KRIBB3 and harvested at 0, 1, 3, 6, 12, 24, and 48 h after treatment and analyzed with a FACScalibur. When HCT-116 cells were treated with KRIBB3, an increase in the proportion of G_2/M phase cells could be detected (Fig 16A and B). Seventy percent of cells were arrested at the G2/M phase checkpoint 12 h after treatment. Because KRIBB3 arrested the cell cycle in the G2/M phase, we used the well known antimitotic compound nocodazole as a control for further study. Treatment with nocodazole showed a similar effect on the cell cycle profile of HCT-116 cells. In addition, when DU-145 cells were treated with KRIBB3, cell cycle arrest could be detected at the G2/M phase (Fig. 23). Interestingly, treatment of asynchronous HCT-116 cells with KRIBB3 resulted in the accumulation of cells with a hyperploid DNA content (>4 N) (Fig. 16C). Thirty-seven percent of cells became hyperploid (>4 N) 48 h after KRIBB3 treatment. Similarly, 36% of nocodazole-treated cells were hyperploid. This result suggests that KRIBB3 first arrested cell cycle and then underwent mitosis to become hyperploid. Cell cycle arrest in the G2/M phase was confirmed by detecting G2/M phase-specific accumulation of Cyclin B1 and phosphorylation of Histone H3 (Ser10) (Fig. 16D). The Cyclin B1 protein levels increased after KRIBB3 treatment and remained elevated for 48 h. Similarly, phosphorylation of Histone H3 (Ser10) increased after KRIBB3 treatment and

remained elevated for 24 h. However, phosphorylation of Histone H3 (Ser 10) decreased to its basal level after 48 h. The temporal patterns of Cyclin B1 accumulation and Histone H3 phosphorylation are consistent with cell cycle arrest at the G2/M phase as shown in Fig. 16.

In order to determine whether KRIBB3-treated cells were blocked at the G2 phase or at the mitotic phase, cells were analyzed for progression from mitotic arrest. To synchronize cells in mitosis, HCT-116 cells were treated with 1 μM nocodazole for 15 h. After collection, synchronized mitotic cells were replated in medium containing DMSO or KRIBB3. Cells were collected at the time indicated, and the profile of the cell cycle was analyzed by FACS. As shown in Fig. 17A, HCT-116 cells were released from a nocodazole induced mitotic phase arrest after replating cells in the medium with DMSO. However, addition of KRIBB3 (Fig. 17A) into replating medium did not result in the release of mitotic phase arrested cells. These results suggest that KRIBB3 arrested the cell cycle at the same mitotic phase as nocodazole.

By treating with 1 μM of KRIBB3 for 15 h, HCT-116 cells were synchronized to mitotic phase. After collection, synchronized mitotic cells were replated in the medium with DMSO or nocodazole. As shown in Fig. 17B, addition of nocodazole in replating medium could not release KRIBB3-induced mitotic arrest of cells. This result confirmed that KRIBB3 arrested cell cycle at the same phase as nocodazole did. In addition, I tested whether detachment of cells by KRIBB3 is responsible for cell cycle arrest. For this, cells were replated into cell culture dish or

Petri dish on which cells could not attach. Cells could maintain cell cycle progression even in the absence of adhesion (Fig. 17C). This result suggest that de-adhesion by KRIBB3 is not involved in cell cycle arrest at mitotic phase.

3.4. Time-dependent effect of KRIBB3 in spindle checkpoint-competent cells

KRIBB3 arrested the cell cycle at the G_2/M phase (Fig. 16). Mitotic progression is controlled by APC/C, a multi-subunit E3 ubiquitin ligase (Peters, 2006). In order to recognize and interact with mitotic substrates, APC/C requires a specific factor p55CDC (mammalian homologue of CDC20). The most downstream event in checkpoint regulation is the inhibition of p55CDC. Therefore, I decided to test whether KRIBB3 exerts its activity through APC/C inhibition. APC/C inhibition is accomplished by recruiting checkpoint proteins, including Bub1, BubR1, Bub3, Mad1, and Mad2 to unattached kinetochores (Weaver and Cleveland, 2005). p55CDC forms a complex with inhibitory Mad2, BubR1, and Bub3. Therefore, I examined whether inhibitory complex of Mad2/p55CDC was formed by KRIBB3 or not. For this, p55CDC was immunoprecipitated with antibody specific to p55CDC and immunoblotted with antibody specific to Mad2 (Fig. 18A). Inhibitory association of p55CDC with Mad2 was induced and reached its maximum 12 h after KRIBB3 treatment. Then, this inhibitory complex was decreased 24 h after the KRIBB3 treatment and disappeared 48 h after the treatment. However, expression of Mad2 and p55CDC was not altered by the KRIBB3 treatment. These results

suggested that KRIBB3 caused cell cycle arrest at mitotic phase through the formation of inhibitory checkpoint complex of Mad2/p55CDC. Furthermore, this is consistent with the observation that a decrease of the inhibitory complex resulted in a slippage of the mitotic arrest 48 h after KRIBB3 treatment.

Substrates that are targeted for degradation by APC/C include the master regulator of mitosis, Cyclin B1. Therefore, if KRIBB3 could induce formation of inhibitory complex (Mad2/p55CDC) to inhibit APC/C activity, it should block Cyclin B1 degradation. To confirm this possibility, I accumulated Cyclin B1 by using nocodazole treatment and then analyzed whether accumulated Cyclin B1 was degraded in the absence or presence of KRIBB3. As shown Fig. 18B, when cells were arrested at G_2/M phase by nocodazole (time 0), Cyclin B1 was highly accumulated. However, accumulated Cyclin B1 was disappeared within 3 h when replated in the medium with DMSO control. In contrast, accumulated Cyclin B1 was significantly maintained for 9 h when replated in the medium with KRIBB3. This result confirmed that KRIBB3 inhibited Cyclin B1 degradation by blocking APC/C activity.

3.5. Induction of apoptosis by KRIBB3 is coupled with Bax activation.

Cell cycle arrest at G_2/M phase was begun 3 h after KRIBB3 treatment and more than 97% of cells were G_2/M phase after 6 h (Fig. 19). This temporal pattern is very similar to formation of inhibitory complex (p55CDC/Mad2) (Fig. 18A).

However, amount of inhibitory complex was decreased 24 h after KRIBB3 treatment and hardly detectable after 48 h. In addition, population of hypoploid (sub-G_0/G_1) and PARP degradation were detected 24 h after the KRIBB3 treatment (Fig. 16). These results suggested that slippage of cell cycle after arrest at mitotic phase could be important for induction of apoptosis. Therefore, I collected synchronized mitotic cells and analyzed cellular response for apoptosis in the presence or absence of KRIBB3. As shown in Fig. 19A, PARP cleavage was detected only from KRIBB3-treated cells. Bax is a proapoptotic protein of Bcl-2 family. In normal condition, Bax is mainly located in the cytosol as an inactive monomer. Upon stimulation by death signal, Bax is activated, resulting in a conformation change that targets it to the outer membrane of the mitochondria. Cells were collected at the indicated time and lysates were prepared with Chaps lysis buffer. Then, Bax activation was monitored by an immunoprecipitation-coupled western blot analysis. Monoclonal antibody Bax 6A7 can specifically precipitate the active conformers of Bax (Hsu and Youle, 1998; Tao et al., 2005). Fig. 18B showed that activation of Bax was detected only from lysates prepared from cells treated with KRIBB3. In addition, temporal pattern of Bax activation is very similar to that of PARP cleavage. These results supported that KRIBB3 induced apoptosis through activation of Bax.

3.6. KRIBB3 inhibits microtubule polymerization *in vivo* and *in vitro*.

It has been very well documented that microtubule inhibitors, including nocodazole, arrest cells at the G_2/M phase and induce apoptosis. In addition, microtubules play crucial roles in maintaining cell morphology and shape. Interestingly, when cells were treated with KRIBB3, cells become round, arrested cell cycle at G_2/M phase and underwent apoptosis. In the light of these observations, I speculated that microtubule and/or its function could be a potential target of KRIBB3. Therefore, immunofluorescence confocal microscopy was used to examine the effect of KRIBB3 on the microtubule cytoskeleton. The normal distribution of microtubules in untreated HCT-116 cells is shown in Fig. 20A. Paclitaxel treatment resulted in maintenance of microtubule polymerization with an increase in the density of microtubules. In contrast, treatment with KRIBB3 resulted in inhibition of microtubule polymerization and the appearance of short microtubule fragments in the cytoplasm. Similarly, treatment with nocodazole resulted in a diffuse stain visible throughout the cytoplasm, similar to staining for KRIBB3-induced microtubule changes.

Because KRIBB3 disrupted the microtubule organization *in vivo*, I further tested whether KRIBB3 directly inhibits tubulin polymerization *in vitro*. As shown in Fig. 20B, purified tubulins were polymerized to steady state in the presence of GTP at 37℃ in a control sample. As expected, treatment with KRIBB3 inhibited tubulin polymerization compared with DMSO. However, KRIBB2, an inactive structural analogue compound, did not inhibit tubulin polymerization. This result supports a structurally specific activity of KRIBB3 in microtubule polymerization.

In the presence of paclitaxel or nocodazole as a positive or a negative control, tubulin polymerization was enhanced or inhibited, respectively.

3.7. KRIBB3 inhibits growth of HCT-116 colon cancer cells in BALB/c nude mice.

A HCT-116 tumor xenograft model of nude mice was used to investigate inhibitory activity of KRIBB3 on tumor growth. HCT-116 cells were implanted subcutaneously into the right flank of nude mice on day 0, and the compound was administered intraperitoneally daily from day 1 at a concentration of 50 or 100 mg/kg for KRIBB3 or 2 mg/kg for doxorubicin per day. To determine the toxicity of the compound, the body weight of tumor-bearing animals was measured. On day 16 the mice were sacrificed and the tumors were removed and weighed. Sixteen days after implantation, tumor volume had decreased by 49.5% (50 mg/kg) and 70.3% (100 mg/kg) in mice treated with KRIBB3 compared to control mice (Fig. 21). There was no change in body weight when KRIBB3 was used at 50 mg/kg. However, when KRIBB3 was used at 100 mg/kg, there was 10.3% loss of body weight. Similarly, when doxorubicin was used as a positive control at 2 mg/kg, a 20% loss of body weight was observed.

4. Discussion

An unexpected finding of this study is that KRIBB3 inhibits tumor cell growth. KRIBB3 was initially discovered from chemical screening to identify inhibitors of migration (but not proliferation) of MDA-MB-231 breast cancer cells. However, it inhibited proliferation of a variety of other malignancies at sub-μM concentration except MDA-MB-231 and HT-29 (Table 1). KRIBB3 inhibits tumor cell migration and invasion by blocking PKC-dependent phosphorylation of Hsp27 through its direct binding to Hsp27. Several other studies point to the ability of Hsp27 to increase the metastatic potential of tumor cells in nude mice as well as enhancing their resistance to therapy (Blackburn et al., 1997; Katoh et al., 2000). Higher levels of Hsp27 expression are commonly detected in variety different cancers including breast (Love and King, 1994; Oesterreich et al., 1993), prostate (Cornford et al., 2000), gastric (Ehrenfried et al., 1995), and ovarian (Arts et al., 1999; Langdon et al., 1995) cancer.

Initially, I believed that KRIBB3 blocked cancer cell growth through inhibition of Hsp27. In order to test this possibility, I used Hsp27 siRNA to knockdown of Hsp27 expression and examined its effect on cell proliferation (Fig. 15). Surprisingly, knockdown of Hsp27 did not inhibit proliferation of HCT-116 and DU-145 cells. Therefore, I concluded that the effect of KRIBB3 on proliferation and cell cycle progression was not through Hsp27, but rather through another as yet unidentified KRIBB3 target.

In order to determine the molecular mechanism of KRIBB3-dependent growth inhibition, I analyzed cell cycle progression in a time-dependent manner. Seventy percent of cells were arrested at the G2/M phase 12 h after KRIBB3 treatment (Fig. 16A). Cell cycle arrest at G_2/M phase was further confirmed by detecting G_2/M phase-specific protein, Cyclin B1 and phosphorylation of Histone H-3 (Ser 10) (Fig. 16D). There are many possible KRIBB3 targets responsible for KRIBB3-dependent G_2/M phase arrest. Accumulation of Cyclin B1 implied that its degradation pathway could be blocked by KRIBB3. Cyclin B1 is degraded by proteasome in a cell cycle dependent manner after APC/C dependent-ubiquitination. APC/C activity is strictly controlled by mitotic spindle checkpoint machinery.

Therefore, I decided to test whether KRIBB3 activate mitotic spindle checkpoint. APC/C-dependent ubiquitination is dependent on CDC20 (p55CDC, mammalian homologue) to recognize substrate. This substrate recognition protein is associated with its inhibitory protein Mad2. Therefore, I examined the formation of the inhibitory complex p55CDC/Mad2 in a time-dependent manner after KRIBB3 treatment (Fig. 18A). As expected, KRIBB3 treatment induced association of p55CDC with the inhibitory protein Mad2. This inhibitory complex may block APC/C-dependent Cyclin B1 degradation.

This leads to the question of how KRIBB3 induces the inhibitory complex of p55CDC/Mad2. Because microtubule poisons such as vinca alkaloids cause all kinetochores to become unattached, thereby generating a mitotic-checkpoint signal, I decided to test whether KRIBB3 could inhibit microtubule structure. I carried out indirect immunofluorescence microscopy to check microtubule cytoskeleton *in vivo*.

Cells treated with KRIBB3 showed short microtubule fragments in the cytoplasm (Fig. 20A). This structure is similar to microtubules in cells treated with nocodazole. Furthermore, *in vitro*, purified tubulin polymerization was inhibited in the presence of KRIBB3 or nocodazole and enhanced in the presence of paclitaxel (Fig. 20B). The inhibitory activity of KRIBB3 on tubulin polymerization is similar to that of nocodazole. However, KRIBB2, an inactive structural analogue of KRIBB3, did not show any inhibitory effect on tubulin polymerization (Fig. 20B). Consistent with this, KRIBB2 did not inhibit proliferation of HCT-116 cells (Fig. 13). These results support my conclusion that inhibition of tubulin polymerization by KRIBB3 caused mitotic phase arrest and growth inhibition.

Because p53 has been shown to be involved in apoptosis and more than 50% of human cancers have mutated p53, it is important for drugs to be able to induce apoptosis in a p53-independent manner. Therefore, we tested whether KRIBB3 could inhibit the growth of p53 null cancer cell lines. Fortunately, KRIBB3 was able to induce cell cycle arrest at the mitotic phase, and apoptosis of both HCT-116 (p53+/+) and DU-145 (p53-/-) cells. This suggests that induction of apoptosis following slippage of the mitotic checkpoint may not depend on the p53-mediated tetraploid checkpoint.

Among 12 cancer cell lines, only MDA-MB-231 and HT-29 are relatively resistant to KRIBB3-induced growth inhibition (Table 1). Currently, I do not know the reason why these cells are refractory to KRIBB3. Currently, I do not know why these cells are refractory to KRIBB3, Recently, Tao et al. reported that cells that can sustain a long-term (48 h) arrest in mitosis (e.g., HT-29 colorectal adenocarcinoma

cells) are less susceptible to taxol-mediated killing than cells that more rapidly adapt into G1 after less than 24 h of drug exposure (e.g., HCT-116 colorectal carcinoma cells) (Tao et al., 2005). Therefore, it is likely that difference(s) in checkpoint response determine the sensitivity to inhibitors of microtubule dynamics.

Normal cells have a robust mitotic checkpoint in which one unattached kinetochore can generate a signal strong enough to inhibit all cellular APC/C activity and therefore block progress to anaphase. However, when checkpoint components are mutated or their expression is low, they cannot produce strong enough signal to arrest cell cycle. When HCT-116 cells were treated with 1 μM KRIBB3 for 48 h, 43% of the cells were in the sub-G1 phase, indicating apoptosis (Fig. 16). However, when Human Foreskin Fibroblast (HFF) cells (normal cell line) were treated with 1 μM KRRIBB3 for 48 h, only 10% of cells were sub-G1 phase (Fig. 22). This result supports the hypothesis that HCT-116 cells are more sensitive to KRIBB3 than HFF cells. In addition many cancer cells divide *in vivo* more frequently than normal cells, and therefore frequently pass through a stage of vulnerability to mitotic poisons. Therefore, cancer cells may be relatively sensitive to KRIBB3 compared with normal cells.

Failure in cancer chemotherapy is often related to multidrug resistance (MDR). Many microtubule-interacting drugs, such as the taxanes and vinblastine, are well-known substrates of P-glycoprotein (MDR1). This means that tumor cells can easily acquire drug resistance by overexpressing the MDR1 pump. The development of new compounds that are effective against drug-resistant cells is therefore important for cancer therapy. These results show that KRIBB3 exhibits a

similar potency regardless of the P-glycoprotein status (HCT-15 vs. HCT-116), indicating that KRIBB3 is not a substrate of P-glycoprotein, thereby suggesting that KRIBB3 is superior to other antimitotic agents in this regard.

This study reports the biological properties of the low-molecular-weight compound KRIBB3, which displays strong antimitotic activity against cancer cells. *In vitro*, KRIBB3 exerts significant antitumoral activity against a variety of malignancies (colon, prostate, breast, and lung). The mode of action of the KRIBB3 as a tubulin inhibitor was shown by *in vitro* tubulin polymerization assay and indirect immunofluorescence microscopy. The KRIBB3 selectively arrested cell cycle progression at the mitotic phase by activating mitotic spindle checkpoint. When KRIBB3 was administered, tumor volume decreased by 49.5% (50 mg/kg) and 70.3% (100 mg/kg) compared to control mice. The unique structural and biological properties of KRIBB3 make it an attractive candidate for further development toward potential clinical applications.

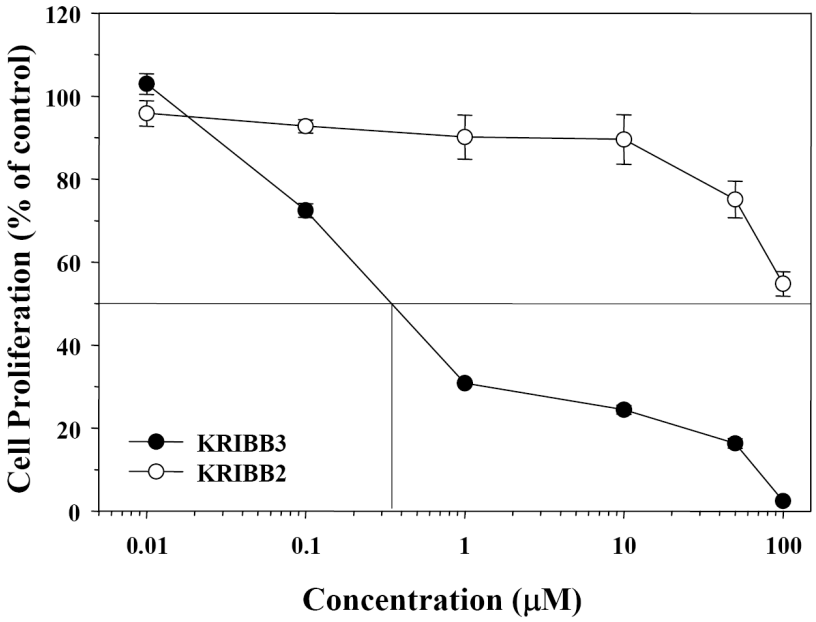

Fig. 13. Activity of isoxazole compounds on the proliferation of HCT-116 tumor cells. HCT-116 cells were treated with different concentrations of compounds or with vehicle solvent (0.1% DMSO) and viability were determined by using WST-1 at 48 h after treatment. The results were expressed relative value to the vehicle treated cells.

A.

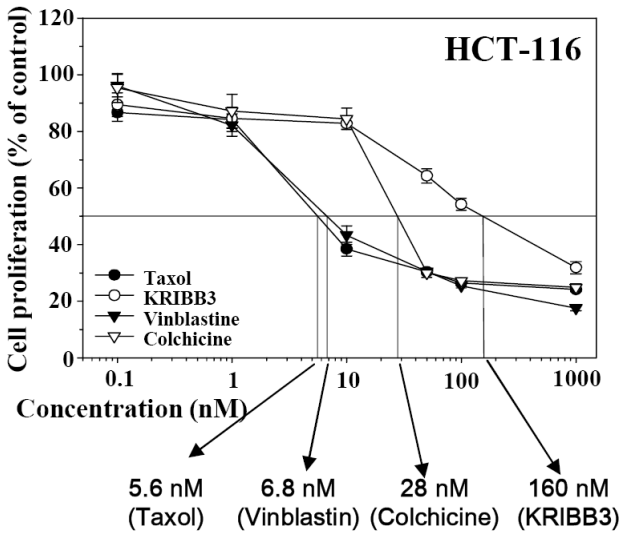

B.

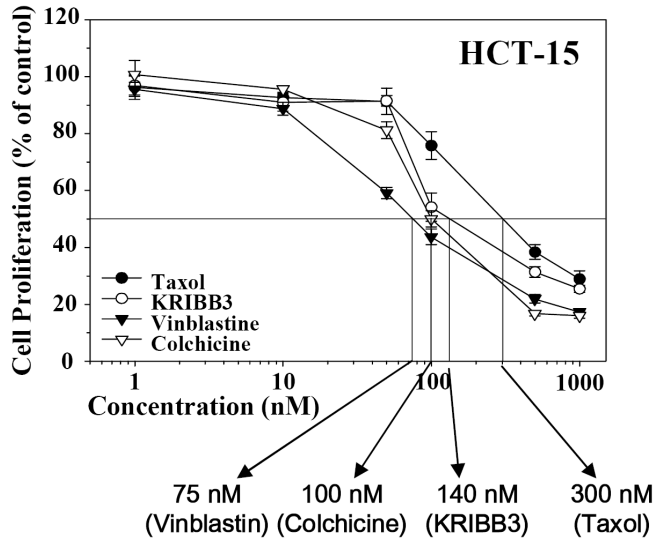

Fig. 14. Activity of isoxazole compounds, paclitaxel, vinblastin, and colchicines on the proliferation of HCT-116 or HCT15 tumor cells. HCT-116 or HCT-15 cells were treated with different concentrations of compounds or with vehicle solvent (0.1% DMSO) and viability were determined by using WST-1 at 48 h after treatment. The results were expressed as relative value to the vehicle treated cells.

A.

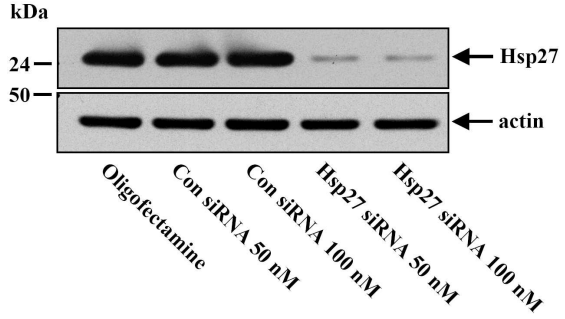
kDa
24
50
Hsp27
actin
Oligofectamine
Con siRNA 50 nM
Con siRNA 100 nM
Hsp27 siRNA 50 nM
Hsp27 siRNA 100 nM

B.

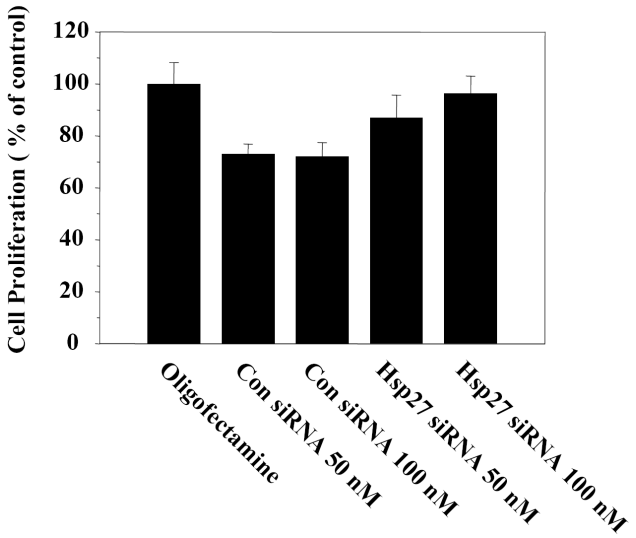
Cell Proliferation (% of control)
120
100
80
60
40
20
0
Oligofectamine
Con siRNA 50 nM
Con siRNA 100 nM
Hsp27 siRNA 50 nM
Hsp27 siRNA 100 nM

C.

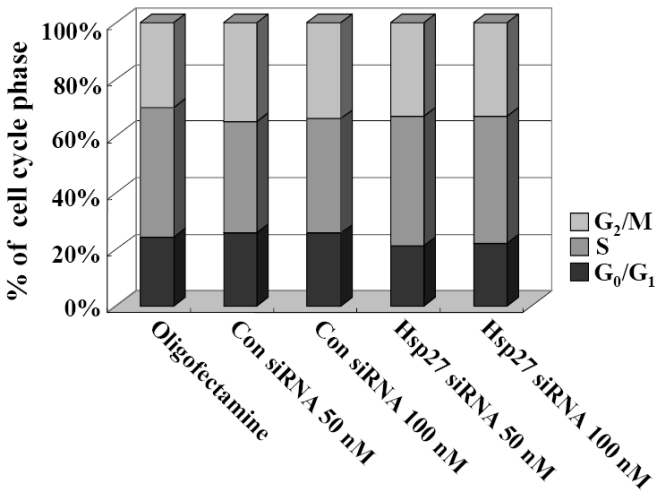
% of cell cycle phase
100%
80%
60%
40%
20%
0%
G2/M
S
G0/G1
Oligofectamine
Con siRNA 50 nM
Con siRNA 100 nM
Hsp27 siRNA 50 nM
Hsp27 siRNA 100 nM

Fig. 15. Knockdown of Hsp27 protein does not affect proliferation and cell cycle distribution. A, HCT-116 cells were transfected with siRNA as described in Materials and Methods, and then lysates were prepared with RIPA buffer. The whole cell lysates (30 μg) were separated using 12.5% SDS-PAGE, and blotted with anti-Hsp27 antibody or anti-Actin antibody. B, Proliferation of transfected HCT-116 cells was determined by using WST-1 48 h post-treatment. The results were expressed relative to the vehicle-treated cells. C, HCT-116 cells were transfected with control (Con) siRNA or Hsp27 siRNA for 48 h and harvested, fixed, and stained with propidium iodide. 20,000 stained cells were then subjected to FACScalibur analysis.

A.

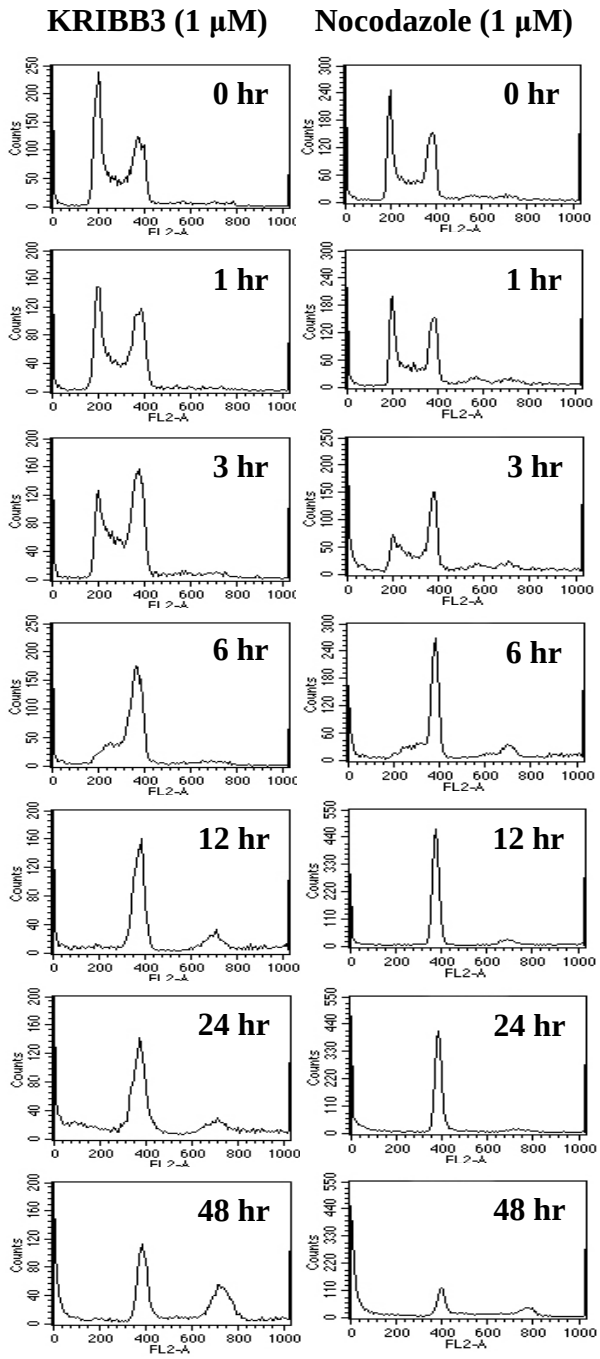
KRIBB3 (1 μM)
Nocodazole (1 μM)
0 hr
1 hr
3 hr
6 hr
12 hr
24 hr
48 hr
Counts
FL2-A

B.

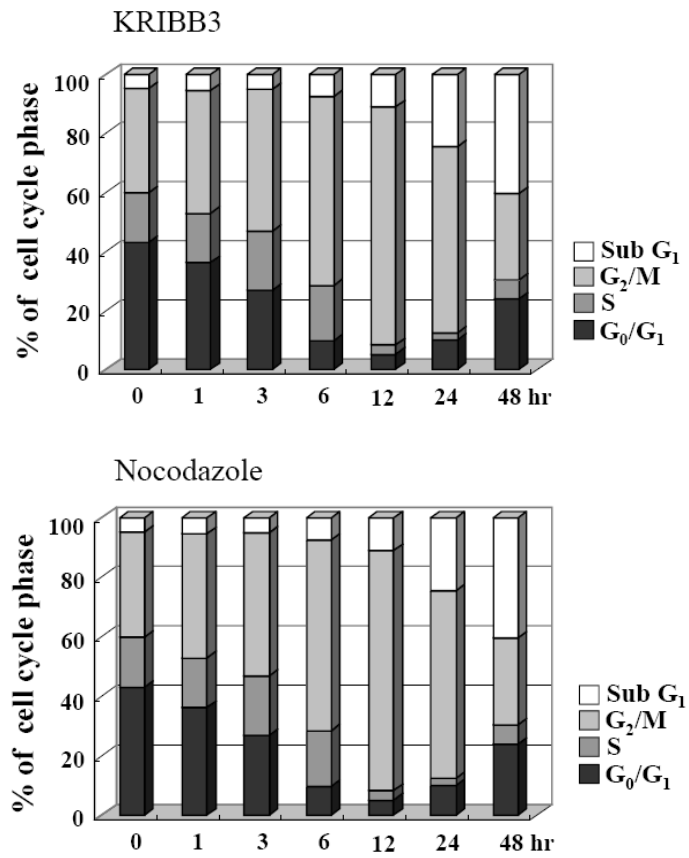
KRIBB3
% of cell cycle phase
100
80
60
40
20
0
0 1 3 6 12 24 48 hr
Sub G1
G2/M
S
G0/G1
Nocodazole
% of cell cycle phase
100
80
60
40
20
0
0 1 3 6 12 24 48 hr
Sub G1
G2/M
S
G0/G1

C.

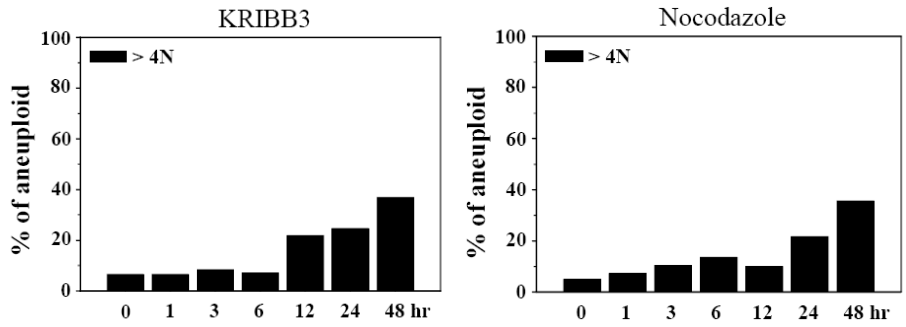
KRIBB3
> 4N
% of aneuploid
100
80
60
40
20
0
0 1 3 6 12 24 48 hr
Nocodazole
> 4N
% of aneuploid
100
80
60
40
20
0
0 1 3 6 12 24 48 hr

D.

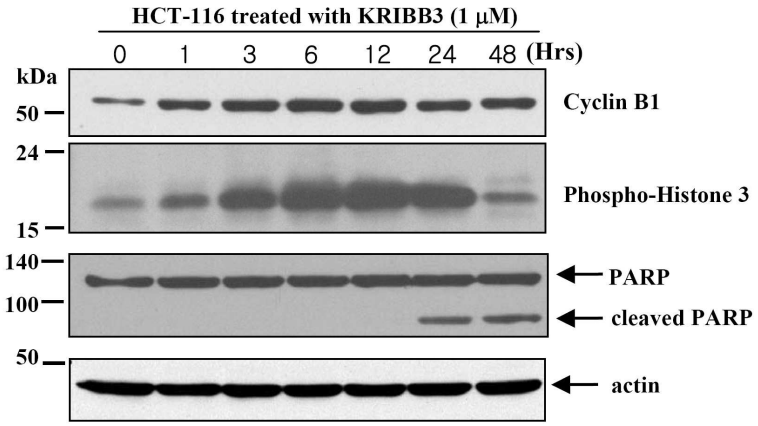

Fig. 16. KRIBB3 induces cell cycle arrest at G_2/M phase and causes apoptosis. A. HCT-116 cells were treated with 1 μM of KRIBB3 for 0, 1, 3, 6, 12, 24, and 48 h and harvested, fixed, and stained with propidium iodide. 20,000 stained cells were then subjected to FACScalibur analysis. B**.** Relative percentages of cells in the Sub-G1 (<2N), G_2/M, S, and G_0/G_1 stages. C. Relative percentages of hyperploid (>4N). Populations were derived from the flow cytometric analysis in A. D. HCT-116 cells were treated with 1 μM of KRIBB3 for different times as indicated, and lysates were prepared with RIPA buffer. 20 μg of lysate were resolved by SDS-PAGE and immunoblotted with anti-Cyclin B1, anti-phospho-histone H3 (Ser 10), anti-PARP, or anti-Actin antibody.

A.

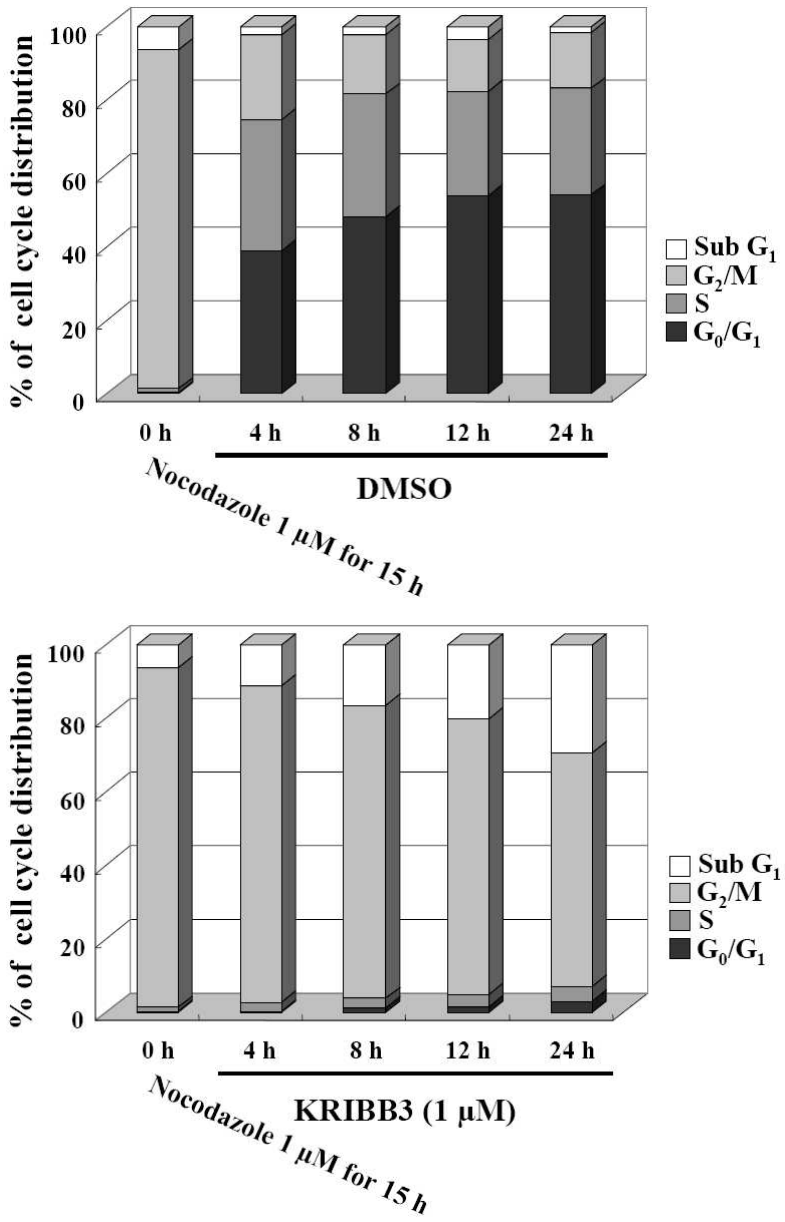
% of cell cycle distribution
100
80
60
40
20
0
0 h
4 h
8 h
12 h
24 h
DMSO
Nocodazole 1 μM for 15 h
Sub G1
G2/M
S
G0/G1
% of cell cycle distribution
100
80
60
40
20
0
0 h
4 h
8 h
12 h
24 h
KRIBB3 (1 μM)
Nocodazole 1 μM for 15 h
Sub G1
G2/M
S
G0/G1

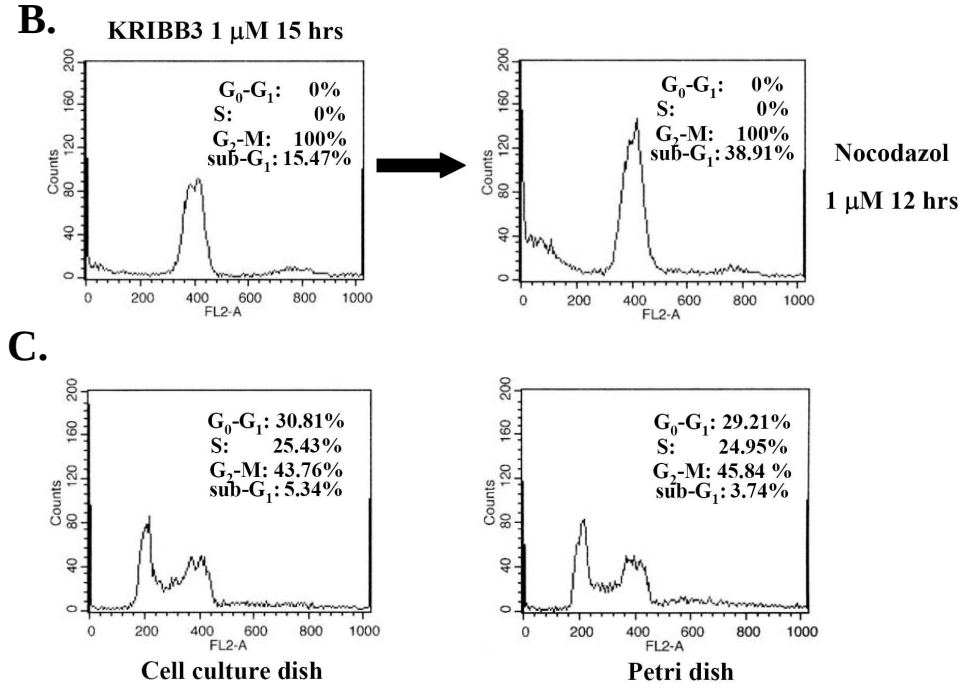

Fig. 17. KRIBB3 arrests cell cycle at the same mitotic phase as nocodazole does. A. HCT-116 cells were treated with 1 μM of nocodazole for 15 h in order to synchronizing at mitosis, as described in "Materials and Methods" The collected mitotic cells were replated at 100 mm culture dishes in medium containing 0.1% Me_2SO (DMSO) or KRIBB3 (1 μM). At the indicated time points after nocodazole release, cells were harvested, fixed, and stained with propidium iodide. 20,000 stained cells then were subjected to FACScalibur analysis. B. HCT-116 cells were treated with 1 μM of KRIBB3 for 15 h in order to synchronizing at mitosis. The collected cells were replated at 100 mm culture dishes in medium containing nocodazole (1 μM) for 12 h. Then, cells were harvested, fixed, and stained with propidium iodide. 20,000 stained cells then were subjected to FACScalibur analysis. C. HCT-116 cells were trypsinized and collected. Then cells were replated in 100 mm cell culture dish or Petri dish. After 24 h, cells were harvested, fixed, and stained with propidium iodide. 20,000 stained cells were then subjected to FACScalibur analysis.

A.

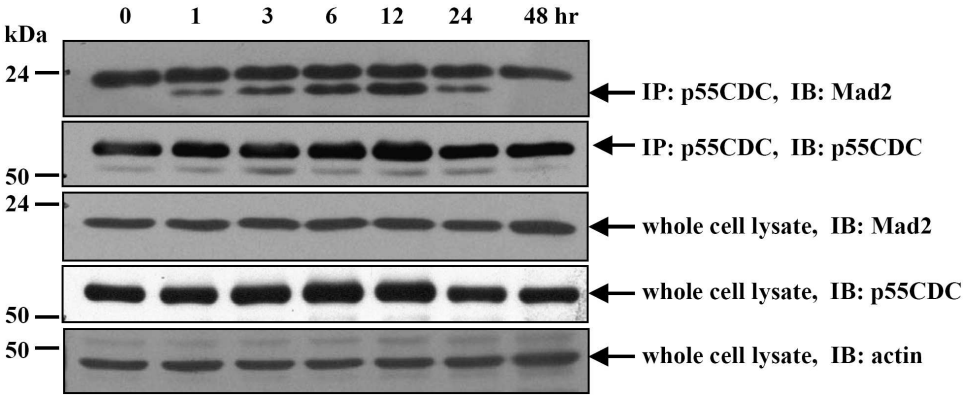
0 1 3 6 12 24 48 hr
kDa
24
50
24
50
50
IP: p55CDC, IB: Mad2
IP: p55CDC, IB: p55CDC
whole cell lysate, IB: Mad2
whole cell lysate, IB: p55CDC
whole cell lysate, IB: actin

B.

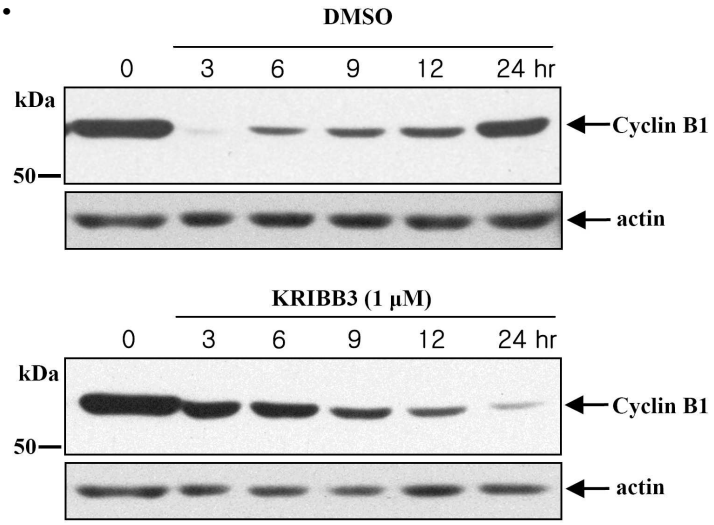
DMSO
0 3 6 9 12 24 hr
kDa
50
Cyclin B1
actin
KRIBB3 (1 μM)
0 3 6 9 12 24 hr
kDa
50
Cyclin B1
actin

Fig. 18. KRIBB3 induces formation of inhibitory complex of Mad2/p55CDC for APC/C blocking degradation of Cyclin B1. A, HCT-116 cells were treated with 1 μM of KRIBB3 and incubated for different times as indicated. 400 μg of lysate was immunoprecipitated (IP) with anti-p55CDC antibody and protein G-agarose beads, and precipitants were resolved by SDS-PAGE after washing three times and immunoblotted with anti-Mad2 antibody or anti-p55CDC antibody. The same whole cell lysates (WCL) were resolved by SDS-PAGE and immunoblotted with anti-Mad2 antibody, anti-p55CDC antibody, or anti-actin antibody. B, In order to accumulate Cyclin B1, HCT-116 cells were treated with 1 μM of nocodazole for 15 h. The mitotic cells were replated at 100 mm culture dishes in medium containing 0.1% Me_2SO (DMSO) or KRIBB3 (1 μM). At the indicated time points after nocodazole release, cell lysates were prepared with RIPA buffer. 20 μg of lysate was resolved by SDS-PAGE and immunoblotted with anti-Cyclin B1 antibody or anti-actin antibody.

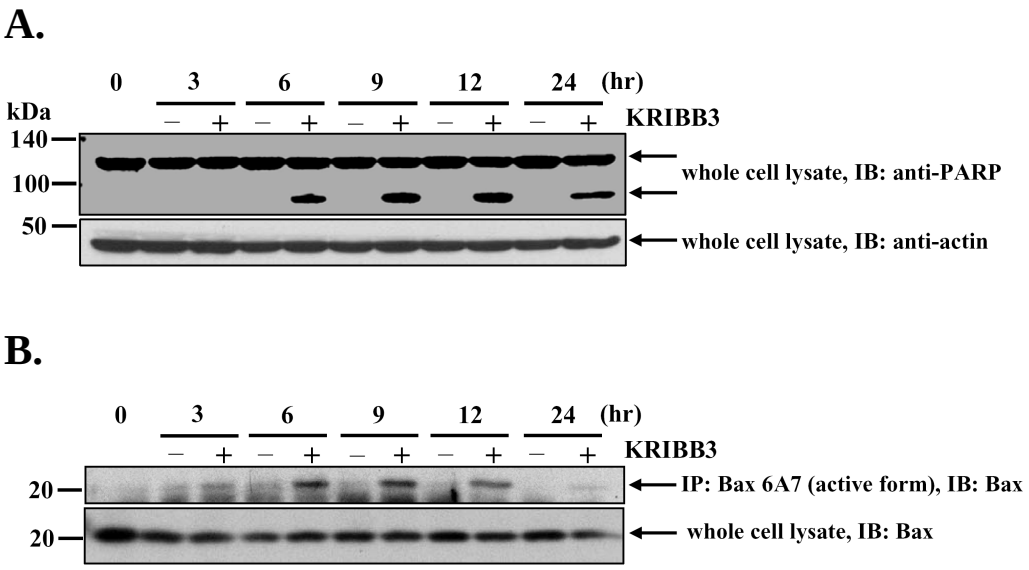

Fig. 19. KRIBB3 activates Bax and induces apoptosis of HCT-116 cells. A, HCT-116 cells were treated with 1 μM of nocodazole for 15 h. The mitotic cells were replated at 100 mm culture dishes in medium containing 0.1% Me_2SO (DMSO) or KRIBB3 (1 μM). At the indicated time points after nocodazole release, cells lysates were prepared with RIPA buffer or with 1% Chaps lysis buffer for active Bax 6A7 detection. 30 μg of lysate was resolved by SDS-PAGE and immunoblotted with anti-PARP antibody or anti-Actin antibody. B, 500 μg of Chaps buffer lysate was immunoprecipitated (IP) with anti-Bax 6A7 monoclonal antibody and protein G-agarose beads, and precipitants were resolved by SDS-PAGE after washing three times with Chaps lysis buffer and immunoblotted with anti-Bax monoclonal antibody. 30 μg of lysate was resolved by SDS-PAGE and immunoblotted with anti-Bax antibody.

A.

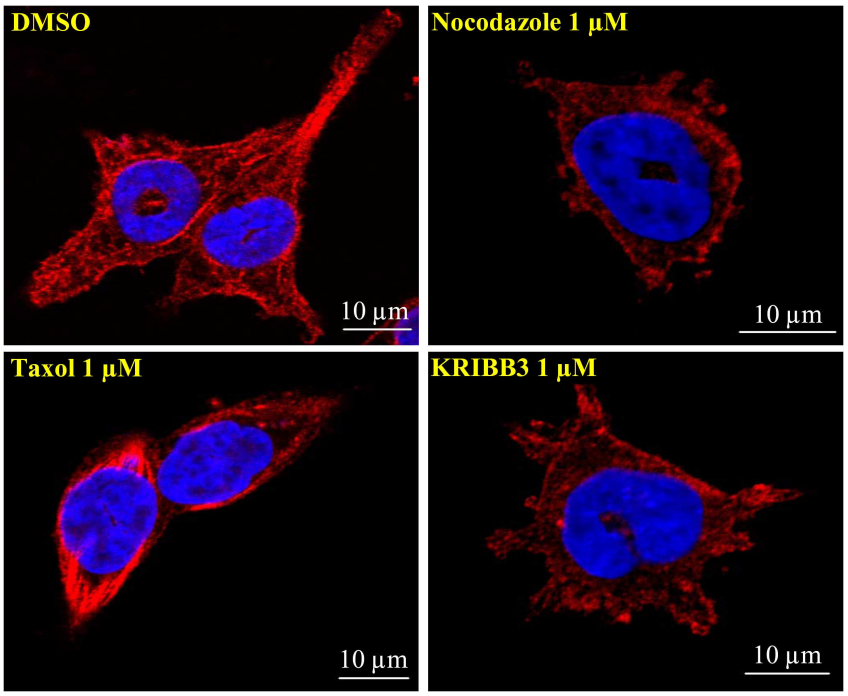
DMSO
10 µm
Nocodazole 1 µM
10 µm
Taxol 1 µM
10 µm
KRIBB3 1 µM
10 µm

B.

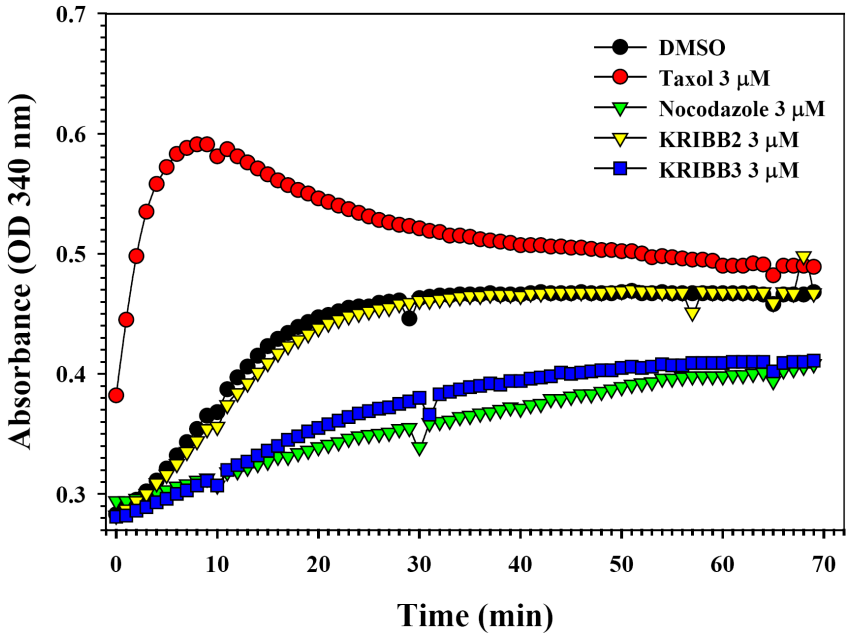
DMSO
Taxol 3 µM
Nocodazole 3 µM
KRIBB2 3 µM
KRIBB3 3 µM
Absorbance (OD 340 nm)
0.7
0.6
0.5
0.4
0.3
0
10
20
30
40
50
60
70
Time (min)

Fig. 20. Effect of KRIBB3 on the organization of microtubule cytoskeleton *in vivo* and *in vitro*. A, HCT-116 cells were incubated with 0.1% Me_2SO, 1 μM of nocodazole, 1 μM of taxol, or 1 μM of KRIBB3 for 6 h. The cellular microtubule network was analyzed by Carl Zeiss confocal system using monoclonal anti-α-Tubilin antibody, fluorescein Texas Red-conjugated goat anti-mouse antibody, and 4,6-diamidino-2-phenylindole. Scale bar, 10 μm. B, This assay was done using purified tubulins *in vitro*. The tubulins were incubated at 37℃ in the presence of vehicle (Me_2SO), 3 μM of Taxol, 3 μM of nocodazole, 3 μM of KRIBB2, or 3 μM of KRIBB3 and microtubule formation was measured by spectrophotometer.

A.

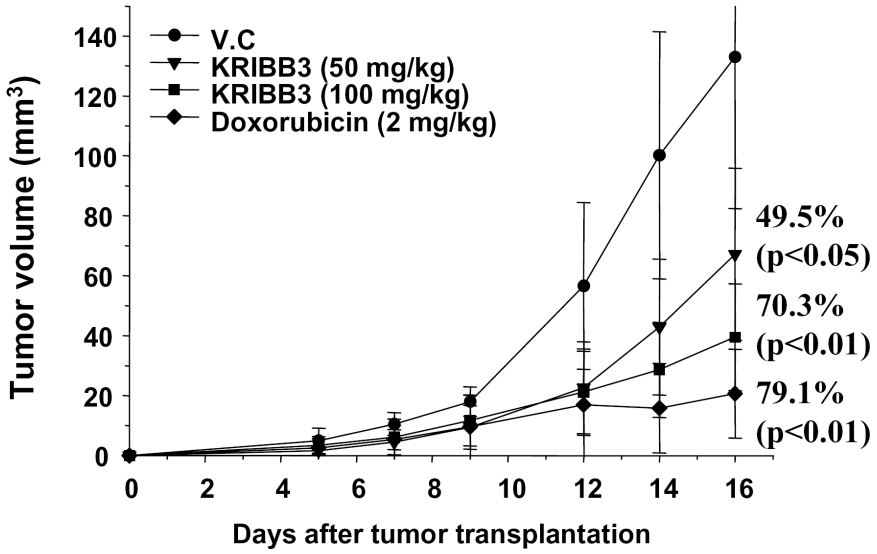
V.C
KRIBB3 (50 mg/kg)
KRIBB3 (100 mg/kg)
Doxorubicin (2 mg/kg)
Tumor volume (mm3)
Days after tumor transplantation
49.5%
(p<0.05)
70.3%
(p<0.01)
79.1%
(p<0.01)

B.

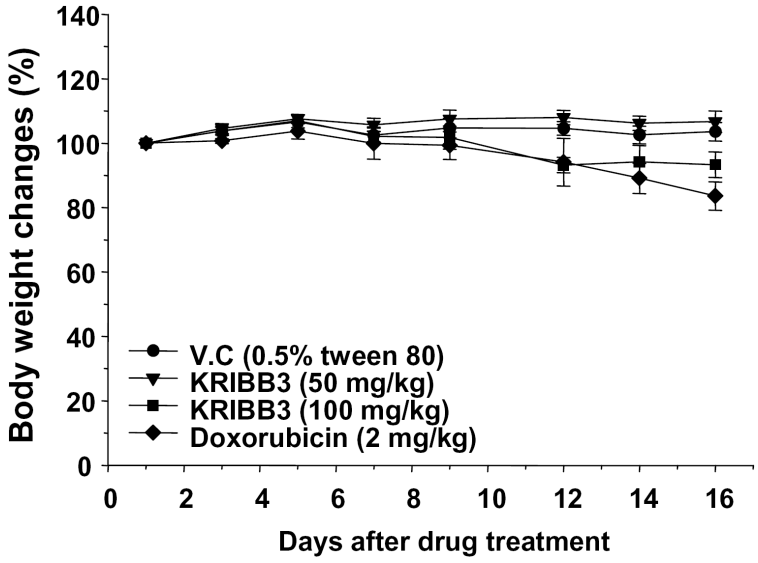
V.C (0.5% tween 80)
KRIBB3 (50 mg/kg)
KRIBB3 (100 mg/kg)
Doxorubicin (2 mg/kg)
Body weight changes (%)
Days after drug treatment

Fig. 21. KRIBB3 inhibits growth of HCT-116 colon cancers in nude mice. A. For the evaluation of *in vivo* anti-tumor activity of KRIBB3, HCT-116 cells (0.3 ml of 3×10^6 cells/ml) were implanted subcutaneously into the right flank of nude mice on day 0. Compound was dissolved 0.5% Tween 80 and was daily administered intraperitoneally for 16 days at a concentration 50 or 100 mg/kg for KRIBB3 or 2 mg/kg for doxorubicin. The dosage was 0.2 ml per 20 g body weight. These results were obtained from one assay using 24 mice (6 mice for each compound). Tumor volumes were estimated by the formula length (mm) × width (mm) × height (mm)/2, and the results were expressed relative value to the vehicle-treated mice. B, Body weight was measured on each indicated day using a balance.

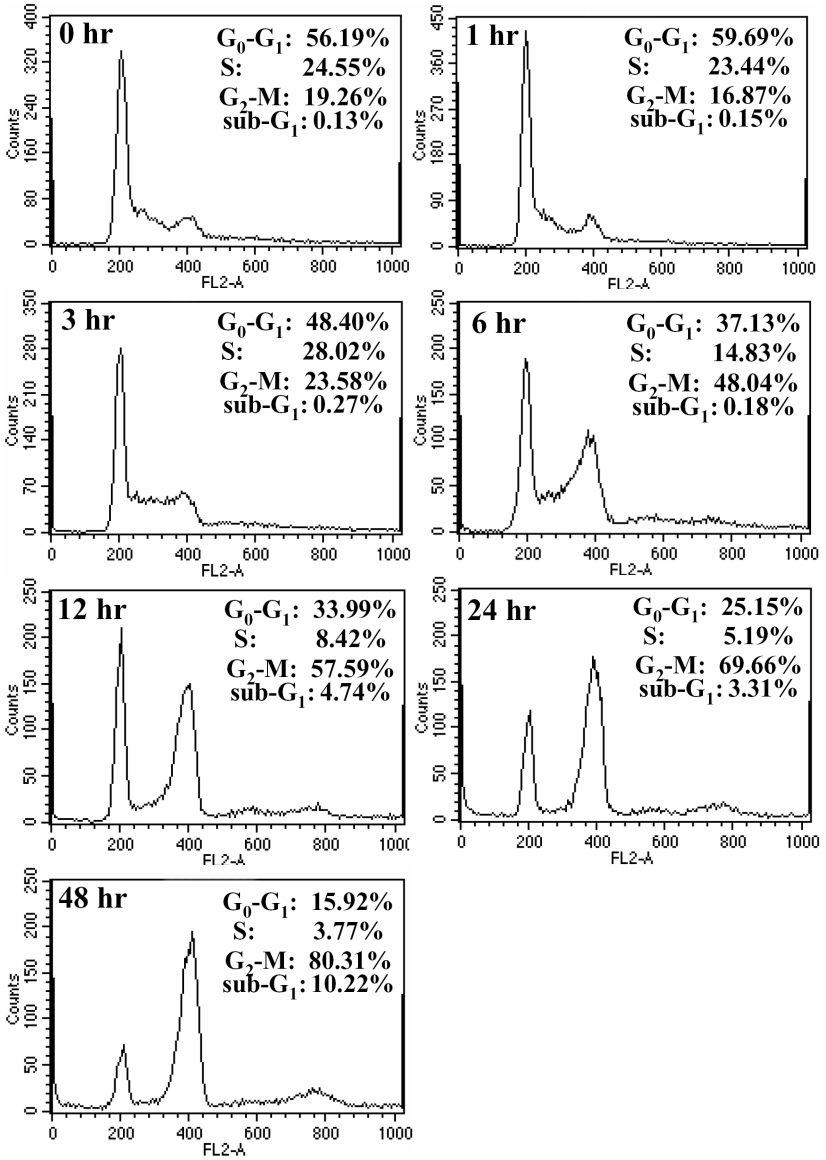

Fig. 22. Temporal analysis of cell cycle distribution of HFF cells. HFF cells were treated with 1 μM of KRIBB3 for 0, 1, 3, 6, 12, 24, and 48 h and harvested, fixed, and stained with propidium iodide. 20,000 stained cells were then subjected to FACScalibur analysis.

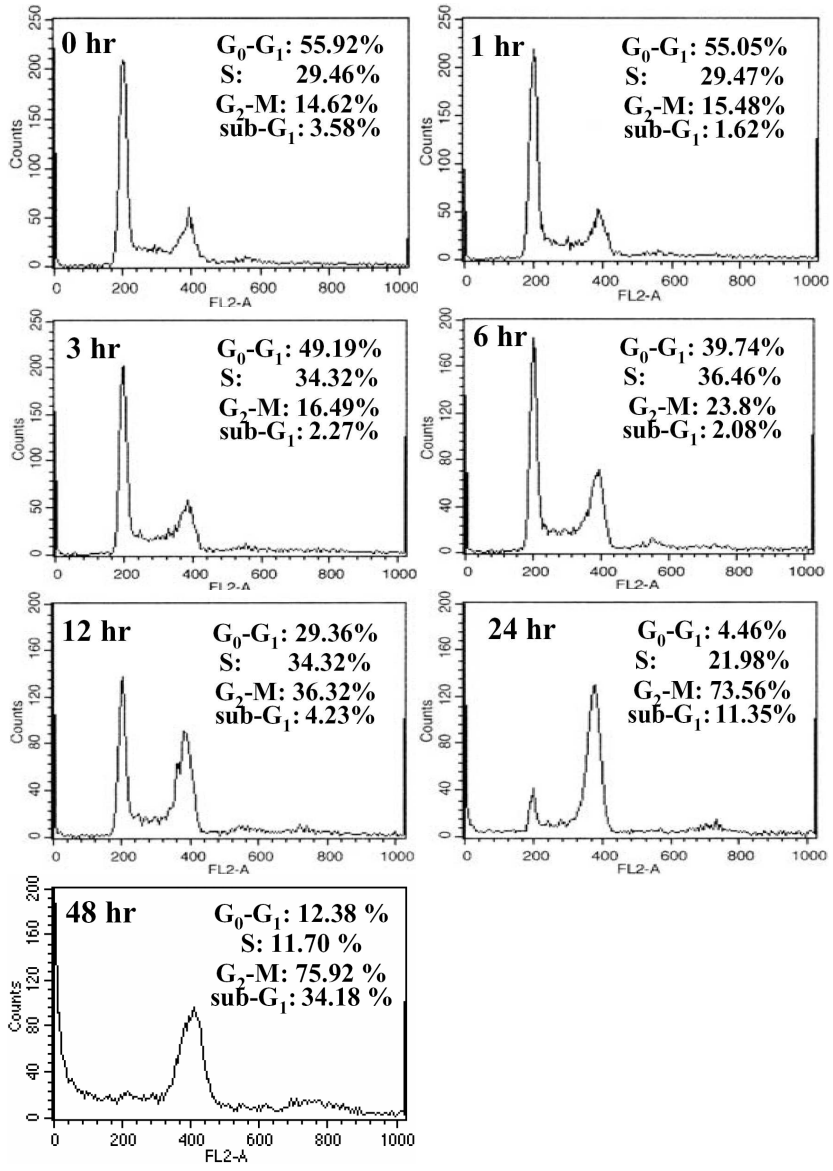

Fig. 23. Temporal analysis of cell cycle distribution of DU-145 cells. DU-145 cells were treated with 1 μM of KRIBB3 for 0, 1, 3, 6, 12, 24, and 48 h and harvested, fixed, and stained with propidium iodide. 20,000 stained cells were then subjected to FACScalibur analysis.

Table 2. Inhibitory effect of KRIBB3 on the proliferation of human tumor cells.

Tumor cell line	p53	GI_{50} (μM)
HCT-116	**Wild- type**	**0.35**
HCT-15	**Deficient**	**0.3**
SW620	**Deficient**	**0.8**
HT-29	**Deficient**	**23**
HCA-7	**Deficient**	**0.38**
MDA-MB-231	**Deficient**	**25**
NCI-H23	**Wild- type**	**0.64**
A549	**Wild- type**	**1.2**
DU-145	**Deficient**	**0.28**
PC-3	**Deficient**	**0.48**
SK-OV-3	**Deficient**	**0.6**
HeLa	**Wild- type**	**0.75**

Cells were treated with different concentrations of KRIBB3 or vehicle solvent (0.1% DMSO), and proliferation was determined using WST1 at 48 h after the treatment. This data is from one of two independent experiments with similar results.

Ⅲ. Reference

Abrieu, A., Kahana, J.A., Wood, K.W., and Cleveland, D.W. (2000). CENP-E as an essential component of the mitotic checkpoint in vitro. Cell *102*, 817-826.

Adams, J.M., and Cory, S. (1998). The Bcl-2 protein family: arbiters of cell survival. Science *281*, 1322-1326.

Alahari, S.K., Reddig, P.J., and Juliano, R.L. (2002). Biological aspects of signal transduction by cell adhesion receptors. Int Rev Cytol *220*, 145-184.

Arts, H.J., Hollema, H., Lemstra, W., Willemse, P.H., De Vries, E.G., Kampinga, H.H., and Van der Zee, A.G. (1999). Heat-shock-protein-27 (hsp27) expression in ovarian carcinoma: relation in response to chemotherapy and prognosis. Int J Cancer *84*, 234-238.

Benezra, M., Ben-Sasson, S.A., Regan, J., Chang, M., Bar-Shavit, R., and Vlodavsky, I. (1994). Antiproliferative activity to vascular smooth muscle cells and receptor binding of heparin-mimicking polyaromatic anionic compounds. Arterioscler Thromb *14*, 1992-1999.

Bharadwaj, R., and Yu, H. (2004). The spindle checkpoint, aneuploidy, and cancer. Oncogene *23*, 2016-2027.

Blackburn, R.V., Galoforo, S.S., Berns, C.M., Armour, E.P., McEachern, D., Corry, P.M., and Lee, Y.J. (1997). Comparison of tumor growth between hsp25- and hsp27-transfected murine L929 cells in nude mice. Int J Cancer *72*, 871-877.

Butt, E., Immler, D., Meyer, H.E., Kotlyarov, A., Laass, K., and Gaestel, M. (2001). Heat shock protein 27 is a substrate of cGMP-dependent protein kinase in intact human platelets: phosphorylation-induced actin polymerization caused by HSP27 mutants. J Biol Chem *276*, 7108-7113.

Camps, M., Ruckle, T., Ji, H., Ardissone, V., Rintelen, F., Shaw, J., Ferrandi, C., Chabert, C., Gillieron, C., Francon, B., *et al.* (2005). Blockade of PI3Kgamma suppresses joint inflammation and damage in mouse models of rheumatoid arthritis. Nature medicine *11*, 936-943.

Carragher, N.O., Westhoff, M.A., Fincham, V.J., Schaller, M.D., and Frame, M.C. (2003). A novel role for FAK as a protease-targeting adaptor protein: regulation by p42 ERK and Src. Curr Biol *13*, 1442-1450.

Chambers, A.F., Groom, A.C., and MacDonald, I.C. (2002). Dissemination and growth of cancer cells in metastatic sites. Nat Rev Cancer *2*, 563-572.

Chan, G.K., Jablonski, S.A., Starr, D.A., Goldberg, M.L., and Yen, T.J. (2000). Human Zw10 and ROD are mitotic checkpoint proteins that bind to kinetochores. Nat Cell Biol *2*, 944-947.

Chan, G.K., Jablonski, S.A., Sudakin, V., Hittle, J.C., and Yen, T.J. (1999). Human BUBR1 is a mitotic checkpoint kinase that monitors CENP-E functions at kinetochores and binds the cyclosome/APC. J Cell Biol *146*, 941-954.

Charest, P.G., and Firtel, R.A. (2007). Big roles for small GTPases in the control of directed cell movement. The Biochemical journal *401*, 377-390.

Chen, J., Kahne, T., Rocken, C., Gotze, T., Yu, J., Sung, J.J., Chen, M., Hu, P., Malfertheiner, P., and Ebert, M.P. (2004). Proteome analysis of gastric cancer metastasis by two-dimensional gel electrophoresis and matrix assisted laser desorption/ionization-mass spectrometry for identification of metastasis-related proteins. J Proteome Res *3*, 1009-1016.

Chhabra, E.S., and Higgs, H.N. (2007). The many faces of actin: matching assembly factors with cellular structures. Nature cell biology *9*, 1110-1121.

Clark, E.A., Golub, T.R., Lander, E.S., and Hynes, R.O. (2000). Genomic analysis of metastasis reveals an essential role for RhoC. Nature *406*, 532-535.

Clark, K., Langeslag, M., Figdor, C.G., and van Leeuwen, F.N. (2007). Myosin II and mechanotransduction: a balancing act. Trends in cell biology *17*, 178-186.

Cole, S.P., and Deeley, R.G. (1998). Multidrug resistance mediated by the ATP-binding cassette transporter protein MRP. Bioessays *20*, 931-940.

Concannon, C.G., Gorman, A.M., and Samali, A. (2003). On the role of Hsp27 in regulating apoptosis. Apoptosis *8*, 61-70.

Condliffe, A.M., Davidson, K., Anderson, K.E., Ellson, C.D., Crabbe, T., Okkenhaug, K., Vanhaesebroeck, B., Turner, M., Webb, L., Wymann, M.P., *et al.* (2005). Sequential activation of class IB and class IA PI3K is important for the primed respiratory burst of human but not murine neutrophils. Blood *106*, 1432-1440.

Cornford, P.A., Dodson, A.R., Parsons, K.F., Desmond, A.D., Woolfenden, A., Fordham, M., Neoptolemos, J.P., Ke, Y., and Foster, C.S. (2000). Heat shock protein expression independently predicts clinical outcome in prostate cancer. Cancer Res *60*, 7099-7105.

Doppler, H., Storz, P., Li, J., Comb, M.J., and Toker, A. (2005). A Phosphorylation State-specific Antibody Recognizes Hsp27, a Novel Substrate of Protein Kinase D. J Biol Chem *280*, 15013-15019.

Dumontet, C., and Sikic, B.I. (1999). Mechanisms of action of and resistance to antitubulin agents: microtubule dynamics, drug transport, and cell death. J Clin Oncol *17*, 1061-1070.

Ehrenfried, J.A., Herron, B.E., Townsend, C.M., Jr., and Evers, B.M. (1995). Heat shock proteins are differentially expressed in human gastrointestinal cancers. Surg Oncol *4*, 197-203.

Etienne-Manneville, S., and Hall, A. (2003). Cell polarity: Par6, aPKC and cytoskeletal crosstalk. Current opinion in cell biology *15*, 67-72.

Fardel, O., Lecureur, V., and Guillouzo, A. (1996). The P-glycoprotein multidrug transporter. Gen Pharmacol *27*, 1283-1291.

Firtel, R.A., and Chung, C.Y. (2000). The molecular genetics of chemotaxis: sensing and responding to chemoattractant gradients. Bioessays *22*, 603-615.

Franco, S.J., Rodgers, M.A., Perrin, B.J., Han, J., Bennin, D.A., Critchley, D.R., and Huttenlocher, A. (2004). Calpain-mediated proteolysis of talin regulates adhesion dynamics. Nature cell biology *6*, 977-983.

Franz, C.M., Jones, G.E., and Ridley, A.J. (2002). Cell migration in development and disease. Dev Cell *2*, 153-158.

Friedl, P., and Wolf, K. (2003). Tumour-cell invasion and migration: diversity and escape mechanisms. Nature reviews *3*, 362-374.

Funamoto, S., Meili, R., Lee, S., Parry, L., and Firtel, R.A. (2002). Spatial and temporal regulation of 3-phosphoinositides by PI 3-kinase and PTEN mediates chemotaxis. Cell *109*, 611-623.

Gagliardi, A., and Collins, D.C. (1993). Inhibition of angiogenesis by antiestrogens. Cancer Res *53*, 533-535.

Gajate, C., Barasoain, I., Andreu, J.M., and Mollinedo, F. (2000). Induction of apoptosis in leukemic cells by the reversible microtubule-disrupting agent 2-methoxy-5-(2',3',4'-trimethoxyphenyl)-2,4,6-cycloheptatrien-1 -one: protection by Bcl-2 and Bcl-X(L) and cell cycle arrest. Cancer Res *60*, 2651-2659.

Gottlieb, A.B., and Bos, J.D. (2002). Recombinantly engineered human proteins: transforming the treatment of psoriasis. Clinical immunology (Orlando, Fla *105*, 105-116.

Guan, J.L., and Shalloway, D. (1992). Regulation of focal adhesion-associated protein tyrosine kinase by both cellular adhesion and oncogenic transformation. Nature *358*, 690-692.

Guay, J., Lambert, H., Gingras-Breton, G., Lavoie, J.N., Huot, J., and Landry, J. (1997). Regulation of actin filament dynamics by p38 map kinase-mediated phosphorylation of heat shock protein 27. J Cell Sci *110 (Pt 3)*, 357-368.

Hall, A. (2005). Rho GTPases and the control of cell behaviour. Biochemical Society transactions *33*, 891-895.

Han, D.C., Lee, M.Y., Shin, K.D., Jeon, S.B., Kim, J.M., Son, K.H., Kim, H.C., Kim, H.M., and Kwon, B.M. (2004). 2'-benzoyloxycinnamaldehyde induces apoptosis in human carcinoma via reactive oxygen species. The Journal of biological chemistry *279*, 6911-6920.

Hino, M., Kurogi, K., Okubo, M.A., Murata-Hori, M., and Hosoya, H. (2000). Small heat shock protein 27 (HSP27) associates with tubulin/microtubules in HeLa cells. Biochem Biophys Res Commun *271*, 164-169.

Hirsch, E., Katanaev, V.L., Garlanda, C., Azzolino, O., Pirola, L., Silengo, L., Sozzani, S., Mantovani, A., Altruda, F., and Wymann, M.P. (2000). Central role for G protein-coupled phosphoinositide 3-kinase gamma in inflammation. Science (New York, NY *287*, 1049-1053.

Hoeflich, K.P., and Ikura, M. (2004). Radixin: cytoskeletal adopter and signaling protein. The international journal of biochemistry & cell biology *36*, 2131-2136.

Hood, J.D., and Cheresh, D.A. (2002). Role of integrins in cell invasion and migration. Nat Rev Cancer *2*, 91-100.

Hoyt, M.A., Totis, L., and Roberts, B.T. (1991). S. cerevisiae genes required for cell cycle arrest in response to loss of microtubule function. Cell *66*, 507-517.

Hsu, Y.T., and Youle, R.J. (1998). Bax in murine thymus is a soluble monomeric protein that displays differential detergent-induced conformations. J Biol Chem *273*, 10777-10783.

Huot, J., Lambert, H., Lavoie, J.N., Guimond, A., Houle, F., and Landry, J. (1995). Characterization of 45-kDa/54-kDa HSP27 kinase, a stress-sensitive kinase which may activate the phosphorylation-dependent protective function of mammalian 27-kDa heat-shock protein HSP27. Eur J Biochem *227*, 416-427.

Jordan, M.A., Thrower, D., and Wilson, L. (1991). Mechanism of inhibition of cell proliferation by Vinca alkaloids. Cancer Res *51*, 2212-2222.

Jordan, M.A., and Wilson, L. (2004). Microtubules as a target for anticancer drugs. Nat Rev Cancer *4*, 253-265.

Kahsai, A.W., Zhu, S., Wardrop, D.J., Lane, W.S., and Fenteany, G. (2006). Quinocarmycin analog DX-52-1 inhibits cell migration and targets radixin, disrupting interactions of radixin with actin and CD44. Chemistry & biology *13*, 973-983.

Katoh, M., Koninkx, J., and Schumacher, U. (2000). Heat shock protein expression in human tumours grown in severe combined immunodeficient mice. Cancer Lett *161*, 113-120.

Kedrin, D., van Rheenen, J., Hernandez, L., Condeelis, J., and Segall, J.E. (2007). Cell motility and cytoskeletal regulation in invasion and metastasis. Journal of mammary gland biology and neoplasia *12*, 143-152.

Kops, G.J., Weaver, B.A., and Cleveland, D.W. (2005). On the road to cancer: aneuploidy and the mitotic checkpoint. Nat Rev Cancer *5*, 773-785.

Landry, J., Chretien, P., Laszlo, A., and Lambert, H. (1991). Phosphorylation of HSP27 during development and decay of thermotolerance in Chinese hamster cells. J Cell Physiol *147*, 93-101.

Landry, J., Lambert, H., Zhou, M., Lavoie, J.N., Hickey, E., Weber, L.A., and Anderson, C.W. (1992). Human HSP27 is phosphorylated at serines 78 and 82 by heat shock and mitogen-activated kinases that recognize the same amino acid motif as S6 kinase II. J Biol Chem *267*, 794-803.

Langdon, S.P., Rabiasz, G.J., Hirst, G.L., King, R.J., Hawkins, R.A., Smyth, J.F., and Miller, W.R. (1995). Expression of the heat shock protein HSP27 in human ovarian cancer. Clin Cancer Res *1*, 1603-1609.

Lauffenburger, D.A., and Horwitz, A.F. (1996). Cell migration: a physically integrated molecular process. Cell *84*, 359-369.

Lavoie, J.N., Gingras-Breton, G., Tanguay, R.M., and Landry, J. (1993). Induction of Chinese hamster HSP27 gene expression in mouse cells confers resistance to heat shock. HSP27 stabilization of the microfilament organization. J Biol Chem *268*, 3420-3429.

Lavoie, J.N., Lambert, H., Hickey, E., Weber, L.A., and Landry, J. (1995). Modulation of cellular thermoresistance and actin filament stability accompanies

phosphorylation-induced changes in the oligomeric structure of heat shock protein 27. Mol Cell Biol *15*, 505-516.

Li, R., and Murray, A.W. (1991). Feedback control of mitosis in budding yeast. Cell *66*, 519-531.

Li, Z., Jiang, H., Xie, W., Zhang, Z., Smrcka, A.V., and Wu, D. (2000). Roles of PLC-beta2 and -beta3 and PI3Kgamma in chemoattractant-mediated signal transduction. Science (New York, NY *287*, 1046-1049.

Liang, P., and MacRae, T.H. (1997). Molecular chaperones and the cytoskeleton. J Cell Sci *110 (Pt 13)*, 1431-1440.

Love, S., and King, R.J. (1994). A 27 kDa heat shock protein that has anomalous prognostic powers in early and advanced breast cancer. British journal of cancer *69*, 743-748.

Ludwig, S., Engel, K., Hoffmeyer, A., Sithanandam, G., Neufeld, B., Palm, D., Gaestel, M., and Rapp, U.R. (1996). 3pK, a novel mitogen-activated protein (MAP) kinase-activated protein kinase, is targeted by three MAP kinase pathways. Mol Cell Biol *16*, 6687-6697.

Maizels, E.T., Peters, C.A., Kline, M., Cutler, R.E., Jr., Shanmugam, M., and Hunzicker-Dunn, M. (1998). Heat-shock protein-25/27 phosphorylation by the delta isoform of protein kinase C. Biochem J *332 (Pt 3)*, 703-712.

Manfredi, J.J., and Horwitz, S.B. (1984). Taxol: an antimitotic agent with a new mechanism of action. Pharmacol Ther *25*, 83-125.

Mao, Y., Abrieu, A., and Cleveland, D.W. (2003). Activating and silencing the mitotic checkpoint through CENP-E-dependent activation/inactivation of BubR1. Cell *114*, 87-98.

Marani, M., Tenev, T., Hancock, D., Downward, J., and Lemoine, N.R. (2002). Identification of novel isoforms of the BH3 domain protein Bim which directly activate Bax to trigger apoptosis. Mol Cell Biol *22*, 3577-3589.

Mayer, T.U. (2003). Chemical genetics: tailoring tools for cell biology. Trends Cell Biol *13*, 270-277.

Mc Henry, K.T., Ankala, S.V., Ghosh, A.K., and Fenteany, G. (2002). A non-antibacterial oxazolidinone derivative that inhibits epithelial cell sheet migration. Chembiochem *3*, 1105-1111.

Metaferia, B.B., Chen, L., Baker, H.L., Huang, X.Y., and Bewley, C.A. (2007). Synthetic macrolides that inhibit breast cancer cell migration in vitro. Journal of the American Chemical Society *129*, 2434-2435.

Moissoglu, K., and Schwartz, M.A. (2006). Integrin signalling in directed cell migration. Biology of the cell / under the auspices of the European Cell Biology Organization *98*, 547-555.

Mollinedo, F., and Gajate, C. (2003). Microtubules, microtubule-interfering agents and apoptosis. Apoptosis *8*, 413-450.

Mundy, G.R. (2002). Metastasis to bone: causes, consequences and therapeutic opportunities. Nature reviews *2*, 584-593.

Nakae, K., Yoshimoto, Y., Sawa, T., Homma, Y., Hamada, M., Takeuchi, T., and Imoto, M. (2000). Migrastatin, a new inhibitor of tumor cell migration from Streptomyces sp. MK929-43F1. Taxonomy, fermentation, isolation and biological activities. The Journal of antibiotics *53*, 1130-1136.

Nam, M.H., Heo, E.J., Kim, J.Y., Kim, S.I., Kwon, K.H., Seo, J.B., Kwon, O., Yoo, J.S., and Park, Y.M. (2003). Proteome analysis of the responses of Panax ginseng C. A. Meyer leaves to high light: use of electrospray ionization quadrupole-time of flight mass spectrometry and expressed sequence tag data. Proteomics *3*, 2351-2367.

Njardarson, J.T., Gaul, C., Shan, D., Huang, X.Y., and Danishefsky, S.J. (2004). Discovery of potent cell migration inhibitors through total synthesis: lessons from

structure-activity studies of (+)-migrastatin. Journal of the American Chemical Society *126*, 1038-1040.

Oesterreich, S., Weng, C.N., Qiu, M., Hilsenbeck, S.G., Osborne, C.K., and Fuqua, S.A. (1993). The small heat shock protein hsp27 is correlated with growth and drug resistance in human breast cancer cell lines. Cancer Res *53*, 4443-4448.

Pantel, K., and Brakenhoff, R.H. (2004). Dissecting the metastatic cascade. Nat Rev Cancer *4*, 448-456.

Parent, C.A., and Devreotes, P.N. (1999). A cell's sense of direction. Science *284*, 765-770.

Peters, J.M. (2006). The anaphase promoting complex/cyclosome: a machine designed to destroy. Nat Rev Mol Cell Biol *7*, 644-656.

Pomel, V., Klicic, J., Covini, D., Church, D.D., Shaw, J.P., Roulin, K., Burgat-Charvillon, F., Valognes, D., Camps, M., Chabert, C., *et al.* (2006). Furan-2-ylmethylene thiazolidinediones as novel, potent, and selective inhibitors of phosphoinositide 3-kinase gamma. Journal of medicinal chemistry *49*, 3857-3871.

Pullikuth, A.K., and Catling, A.D. (2007). Scaffold mediated regulation of MAPK signaling and cytoskeletal dynamics: a perspective. Cellular signalling *19*, 1621-1632.

Puthalakath, H., Huang, D.C., O'Reilly, L.A., King, S.M., and Strasser, A. (1999). The proapoptotic activity of the Bcl-2 family member Bim is regulated by interaction with the dynein motor complex. Mol Cell *3*, 287-296.

Puthalakath, H., Villunger, A., O'Reilly, L.A., Beaumont, J.G., Coultas, L., Cheney, R.E., Huang, D.C., and Strasser, A. (2001). Bmf: a proapoptotic BH3-only protein regulated by interaction with the myosin V actin motor complex, activated by anoikis. Science *293*, 1829-1832.

Raff, M.C. (1992). Social controls on cell survival and cell death. Nature *356*, 397-400.

Ridley, A.J., Schwartz, M.A., Burridge, K., Firtel, R.A., Ginsberg, M.H., Borisy, G., Parsons, J.T., and Horwitz, A.R. (2003). Cell migration: integrating signals from front to back. Science (New York, NY *302*, 1704-1709.

Sakai, R., Iwamatsu, A., Hirano, N., Ogawa, S., Tanaka, T., Mano, H., Yazaki, Y., and Hirai, H. (1994). A novel signaling molecule, p130, forms stable complexes in

vivo with v-Crk and v-Src in a tyrosine phosphorylation-dependent manner. Embo J *13*, 3748-3756.

Salas, A., Shimaoka, M., Kogan, A.N., Harwood, C., von Andrian, U.H., and Springer, T.A. (2004). Rolling adhesion through an extended conformation of integrin alphaLbeta2 and relation to alpha I and beta I-like domain interaction. Immunity *20*, 393-406.

Sasaki, A.T., and Firtel, R.A. (2006). Regulation of chemotaxis by the orchestrated activation of Ras, PI3K, and TOR. European journal of cell biology *85*, 873-895.

Sasaki, T., Irie-Sasaki, J., Jones, R.G., Oliveira-dos-Santos, A.J., Stanford, W.L., Bolon, B., Wakeham, A., Itie, A., Bouchard, D., Kozieradzki, I., *et al.* (2000). Function of PI3Kgamma in thymocyte development, T cell activation, and neutrophil migration. Science (New York, NY *287*, 1040-1046.

Schiff, P.B., Fant, J., and Horwitz, S.B. (1979). Promotion of microtubule assembly in vitro by taxol. Nature *277*, 665-667.

Schreiber, S.L. (1998). Chemical genetics resulting from a passion for synthetic organic chemistry. Bioorg Med Chem *6*, 1127-1152.

Shan, D., Chen, L., Njardarson, J.T., Gaul, C., Ma, X., Danishefsky, S.J., and Huang, X.Y. (2005). Synthetic analogues of migrastatin that inhibit mammary tumor metastasis in mice. Proceedings of the National Academy of Sciences of the United States of America *102*, 3772-3776.

Shimaoka, M., Salas, A., Yang, W., Weitz-Schmidt, G., and Springer, T.A. (2003). Small molecule integrin antagonists that bind to the beta2 subunit I-like domain and activate signals in one direction and block them in the other. Immunity *19*, 391-402.

Slack-Davis, J.K., Martin, K.H., Tilghman, R.W., Iwanicki, M., Ung, E.J., Autry, C., Luzzio, M.J., Cooper, B., Kath, J.C., Roberts, W.G., *et al.* (2007). Cellular characterization of a novel focal adhesion kinase inhibitor. The Journal of biological chemistry *282*, 14845-14852.

Stockwell, B.R. (2004). Exploring biology with small organic molecules. Nature *432*, 846-854.

Stokoe, D., Engel, K., Campbell, D.G., Cohen, P., and Gaestel, M. (1992). Identification of MAPKAP kinase 2 as a major enzyme responsible for the phosphorylation of the small mammalian heat shock proteins. FEBS Lett *313*, 307-313.

Strassheim, D., and Williams, C.L. (2000). P2Y2 purinergic and M3 muscarinic acetylcholine receptors activate different phospholipase C-beta isoforms that are uniquely susceptible to protein kinase C-dependent phosphorylation and inactivation. J Biol Chem *275*, 39767-39772.

Sudakin, V., Chan, G.K., and Yen, T.J. (2001). Checkpoint inhibition of the APC/C in HeLa cells is mediated by a complex of BUBR1, BUB3, CDC20, and MAD2. J Cell Biol *154*, 925-936.

Tang, C., Willingham, M.C., Reed, J.C., Miyashita, T., Ray, S., Ponnathpur, V., Huang, Y., Mahoney, M.E., Bullock, G., and Bhalla, K. (1994). High levels of p26BCL-2 oncoprotein retard taxol-induced apoptosis in human pre-B leukemia cells. Leukemia *8*, 1960-1969.

Tang, Z., Bharadwaj, R., Li, B., and Yu, H. (2001). Mad2-Independent inhibition of APCCdc20 by the mitotic checkpoint protein BubR1. Dev Cell *1*, 227-237.

Tao, W., South, V.J., Zhang, Y., Davide, J.P., Farrell, L., Kohl, N.E., Sepp-Lorenzino, L., and Lobell, R.B. (2005). Induction of apoptosis by an inhibitor of the mitotic kinesin KSP requires both activation of the spindle assembly checkpoint and mitotic slippage. Cancer Cell *8*, 49-59.

van der Valk, P., Lindeman, J., and Kamphorst, W. (1997). Growth factor profiles of human gliomas. Do non-tumour cells contribute to tumour growth in glioma? Ann Oncol *8*, 1023-1029.

Volk, T., Geiger, B., and Raz, A. (1984). Motility and adhesive properties of high- and low-metastatic murine neoplastic cells. Cancer Res *44*, 811-824.

Vuori, K., and Ruoslahti, E. (1995). Tyrosine phosphorylation of p130Cas and cortactin accompanies integrin-mediated cell adhesion to extracellular matrix. J Biol Chem *270*, 22259-22262.

Weaver, B.A., and Cleveland, D.W. (2005). Decoding the links between mitosis, cancer, and chemotherapy: The mitotic checkpoint, adaptation, and cell death. Cancer Cell *8*, 7-12.

Webb, D.J., Parsons, J.T., and Horwitz, A.F. (2002). Adhesion assembly, disassembly and turnover in migrating cells -- over and over and over again. Nat Cell Biol *4*, E97-100.

Weiss, E., and Winey, M. (1996). The Saccharomyces cerevisiae spindle pole body duplication gene MPS1 is part of a mitotic checkpoint. J Cell Biol *132*, 111-123.

Weitz-Schmidt, G., Welzenbach, K., Brinkmann, V., Kamata, T., Kallen, J., Bruns, C., Cottens, S., Takada, Y., and Hommel, U. (2001). Statins selectively inhibit leukocyte function antigen-1 by binding to a novel regulatory integrin site. Nature medicine *7*, 687-692.

Welzenbach, K., Hommel, U., and Weitz-Schmidt, G. (2002). Small molecule inhibitors induce conformational changes in the I domain and the I-like domain of lymphocyte function-associated antigen-1. Molecular insights into integrin inhibition. The Journal of biological chemistry *277*, 10590-10598.

Wu, J.P., Emeigh, J., Gao, D.A., Goldberg, D.R., Kuzmich, D., Miao, C., Potocki, I., Qian, K.C., Sorcek, R.J., Jeanfavre, D.D., *et al.* (2004). Second-generation lymphocyte function-associated antigen-1 inhibitors: 1H-imidazo[1,2-alpha]imidazol-2-one derivatives. Journal of medicinal chemistry *47*, 5356-5366.

Wymann, M.P., Bjorklof, K., Calvez, R., Finan, P., Thomast, M., Trifilieff, A., Barbier, M., Altruda, F., Hirsch, E., and Laffargue, M. (2003). Phosphoinositide 3-kinase gamma: a key modulator in inflammation and allergy. Biochemical Society transactions *31*, 275-280.

Yang, W., Carman, C.V., Kim, M., Salas, A., Shimaoka, M., and Springer, T.A. (2006). A small molecule agonist of an integrin, alphaLbeta2. The Journal of biological chemistry *281*, 37904-37912.

Yarrow, J.C., Totsukawa, G., Charras, G.T., and Mitchison, T.J. (2005). Screening for cell migration inhibitors via automated microscopy reveals a Rho-kinase inhibitor. Chemistry & biology *12*, 385-395.

Yusuf-Makagiansar, H., Anderson, M.E., Yakovleva, T.V., Murray, J.S., and Siahaan, T.J. (2002). Inhibition of LFA-1/ICAM-1 and VLA-4/VCAM-1 as a therapeutic approach to inflammation and autoimmune diseases. Medicinal research reviews *22*, 146-167.

Zantema, A., Verlaan-De Vries, M., Maasdam, D., Bol, S., and van der Eb, A. (1992). Heat shock protein 27 and alpha B-crystallin can form a complex, which dissociates by heat shock. J Biol Chem *267*, 12936-12941.

Zhou, J., and Giannakakou, P. (2005). Targeting microtubules for cancer chemotherapy. Curr Med Chem Anticancer Agents *5*, 65-71.

Zhu, S., Mc Henry, K.T., Lane, W.S., and Fenteany, G. (2005). A chemical inhibitor reveals the role of Raf kinase inhibitor protein in cell migration. Chemistry & biology *12*, 981-991.

Ⅳ. Abstract in Korean

암이 생명에 위협이 되는 가장 큰 원인은 암세포의 전이성에 있으며, 암으로 인한 사망의 대부분은 암 전이로 설명된다. 따라서, 암세포의 침윤과 전이에 필수적인 세포이동이 암 치료에 있어서 좋은 치료 표적이 될 수 있다. 암세포이동을 억제하는 화합물을 찾기 위해서 화합물은행으로부터 분양 받은 합성화합물을 대상으로 탐색한 결과 CAC-1098 (aurintricarboxylic acid) 및 CBI-0997 (5-(2,4-dimethoxy-5-ethyphenyl)-4-(4-Bromophenyl) isoxazole) 두 개의 화합물이 유방암 세포주인 MDA-MB-231 의 암세포이동을 IC_{50} 값 5 및 50 nM 농도에서 각각 저해하였다. 특히, CBI-0997 의 브롬 위치를 메톡시로 치환한 KRIBB3 (5-(5-ethyl-2-hydroxy-4-methoxyphenyl)-4-(4-methoxyphenyl) 화합물도 MDA-MB-231 세포에서 세포이동과 세포침윤 억제 활성을 나타내었으며, KRIBB3 화합물은 CBI-0997 보다 좋은 drug-like 구조이기 때문에 세포이동억제 메커니즘을 규명하는 일에 이 화합물을 사용하였다. KRIBB3 화합물에 결합하는 단백질을 동정하기 위해 바이오틴(biotin)을 결합한 KRIBB3 를 합성하였으며, 친화성 크로마토그래피(affinity chromatography) 방법을 이용해서 KRIBB3 의 타깃 단백질이 Hsp27 단백질이라는 것을 동정하였다. MDA-MB-231 세포주에 PKC 활성물질인 PMA 를 처리하였을 때 PKC 에 의존적으로 Hsp27 을 인산화 시켰으며, 세포 이동 또한 유도하였다.

대조적으로, KRIBB3 를 처리한 세포주에서는 PMA 에 의한 Hsp27 의 인산화와 세포이동을 저해 시켰다. 또한, Hsp27 을 과발현 시켰을 때 KRIBB3 에 의한 세포침윤의 억제효과가 상쇄되는 것을 알 수 있었고, siRNA 로 Hsp27 의 발현 양을 감소시켰을 때 세포이동을 감소시키는 것을 알 수 있었다. 이 모든 결과를 종합해 볼 때 KRIBB3 가 직접적으로 Hsp27 단백질과의 결합을 통해서 PKC 에 의한 Hsp27 단백질의 인산화를 저해하고 그에 따라 암 세포의 이동과 침윤을 억제한다는 것을 보여주고 있다.

KRIBB3 의 여러 항암활성을 관찰하는 동안 KRIBB3 가 여러 암세포에서 세포 성장을 억제 시킨다는 것을 관찰하였다. 특히, 인간 결장암 세포주인 HCT-116 에서 GI_{50} 값이 0.35 μM 농도에서 세포 성장을 억제하였다. Flow cytometry 연구에서 KRIBB3 가 세포주기중 G_2/M 기에서 세포주기를 정지시키고 세포사멸을 유도한다는 것을 관찰 하였고, 이 사실은 Cyclin B1 의 축적과 세포사멸 마커인 poly (ADP-ribose) polymerase (PARP) 절편(cleavage)의 형태를 western blot 으로 증명하였다. 면역침강법으로 관찰한 결과, KRIBB3 를 처리한 초기에 APC/C 의 활성인자인 p55CDC 와 억제단백질인 매드 2(Mad2)와의 결합이 유도된다는 것을 확인하였으며, 이는 KRIBB3 에 의해서 유사분열 검사점(mitotic checkpoint)이 활성화 되었다는 것을 보여주고 있다. 그러나, 매드 2 와 p55CDC 의 억제결합은 KRIBB3 처리 후 24 시간 때에 점차 감소하기

시작해 48 시간 때에는 관찰되지 않았으며, 이는 유사분열 검사점에서 세포가 빠져 나왔다는 것을 의미한다. 이러한 실험결과들을 볼 때 KRIBB3 가 미세소관(microtubule)을 망가뜨려서 유사분열 검사점을 활성화 시켰다는 것을 보여준다. 이에 따라, 인 비트로*(in vitro)*와 인 비보*(in vivo)* 실험인 튜뷸린 중합반응(tubulin polymerization)과 면역형광 염색 실험을 통해서 관찰한 결과 KRIBB3 가 튜뷸린 억제제라는 것을 증명하였다. KRIBB3 에 의한 일시적인 백스(Bax)의 활성은 PARP 절편과 유사하게 관찰되었는데 이는 KRIBB3 에 의한 세포사멸이 백스를 통해서 일어난다는 것을 보여주었다. KRIBB3 50 mg/kg 또는 100 mg/kg 를 누드마우스의 복강에 투여했을 때, 49.5% 또는 70.3%의 종양성장 억제활성을 나타내었다. 따라서, KRIBB3 가 항암치료에 좋은 항암제 후보물질이라는 것을 보여주고 있다.